

8-1-2015

INFLUENCE OF TIO₂ ENGINEERED NANOPARTICLES ON PHOTOSYNTHETIC EFFICIENCY AND CONTAMINANT UPTAKE

Scott Jared Bradfield

Southern Illinois University Carbondale, sbradfield@siu.edu

Follow this and additional works at: <http://opensiuc.lib.siu.edu/theses>

Recommended Citation

Bradfield, Scott Jared, "INFLUENCE OF TIO₂ ENGINEERED NANOPARTICLES ON PHOTOSYNTHETIC EFFICIENCY AND CONTAMINANT UPTAKE" (2015). *Theses*. Paper 1758.

This Open Access Thesis is brought to you for free and open access by the Theses and Dissertations at OpenSIUC. It has been accepted for inclusion in Theses by an authorized administrator of OpenSIUC. For more information, please contact opensiuc@lib.siu.edu.

**INFLUENCE OF TiO₂ ENGINEERED NANOPARTICLES ON
PHOTOSYNTHETIC EFFICIENCY AND CONTAMINANT UPTAKE**

by

Scott J. Bradfield

B.S., Southern Illinois University Carbondale, 2012

A Thesis

Submitted in Partial Fulfillment of the Requirements for the
Master of Science

Department of Plant Biology

in the Graduate School

Southern Illinois University Carbondale

August 2015

THESIS APPROVAL

**INFLUENCE OF TiO₂ ENGINEERED NANOPARTICLES ON
PHOTOSYNTHETIC EFFICIENCY AND CONTAMINANT UPTAKE**

By

Scott J. Bradfield

B.S., Southern Illinois University Carbondale, 2012

A Thesis Submitted in Partial Fulfillment of the Requirements for the Degree of Masters of

Science in the field of Plant Biology

Approved by:

Dr. Stephen D. Ebbs, Chair

Dr. Xingmao Ma

Dr. Andrew Wood

Graduate School

Southern Illinois University Carbondale

April 14, 2015

AN ABSTRACT OF THE THESIS OF:

Scott Bradfield, for the Master of Science degree in Plant Biology, presented on April 14, 2015,
at Southern Illinois University Carbondale

**TITLE: INFLUENCE OF TiO₂ ENGINEERED NANOPARTICLES ON PHOTOSYNTHETIC
EFFICIENCY AND CONTAMINANT UPTAKE**

MAJOR PROFESSOR: Dr. Stephen D. Ebbs

The production of engineered nanoparticles (ENPs) is growing at an incredibly fast rate and will soon become a trillion dollar industry. At this rate of production, there is a great potential for engineered nanomaterials to be released into the environment, both intentionally and unintentionally. TiO₂ ENPs are one of the most widely produced nanoparticles with a broad range of applications in paints, inks, sunscreens, cosmetics, astronautics, and air/water purification.

TiO₂ ENPs have been proposed for their use in agricultural settings as a UV protectant, a defense against harmful bacteria and fungi, or a catalyst for the degradation of pesticides and herbicides. Furthermore, it has been shown to increase several aspects of photosynthesis in spinach including Rubisco and Rubisco activase activity, chlorophyll synthesis, and oxygen evolution. Foliar application of TiO₂ ENPs on spinach resulted in a significant increase in plant fresh weight, dry weight, chlorophyll content, net photosynthetic rate, and carboxylase activity of Rubisco. These findings have prompted investigations for the use of TiO₂ ENPs as a foliar spray to promote plant growth and yield.

The first main objective of this research was to determine if TiO₂ ENPs has the capabilities to increase photosynthetic production in *Zea mays* at concentrations similar to that of the experiments performed with spinach. Secondly, it was examined if the size of the TiO₂ was a factor in the increased photosynthetic response by comparing TiO₂ ENPs with bulk TiO₂. Finally, the determination of whether the boost in photosynthesis resulted in an increased seed quality/quantity.

Another aspect of this research was to determine how the interaction of TiO₂ ENPs with inorganic contaminants may affect the uptake and accumulation of the contaminants in plants. Cadmium and arsenic are two of the top ten most hazardous substances on the priority list of the Agency for Toxic Substances and Disease Registry. Sources for Cd and As contamination include atmospheric deposition resulting from mining, smelting, and fuel combustion, phosphate fertilizers, and sewage sludge. Both of these contaminants can be taken up by plant roots and translocated to the leaves and fruits, thus entering the food chain.

The release of TiO₂ ENPs into domestic and industrial wastewaters is expected to represent the largest release of these nanoparticles. There has been data showing that up to 99% of TiO₂ ENPs that enter wastewater treatment plants are retained in the sludge. In addition, TiO₂ ENPs are being used at some water treatment plants because of their strong adsorption strength for hazardous materials, such as cadmium, arsenic, and copper and also the photocatalytic breakdown of harmful organic compounds. Since sewage sludge from wastewater treatment plants is applied to agricultural lands as a soil conditioner and fertilizer, this has resulted in the introduction of an estimated 120 µg kg⁻³ per year of TiO₂ ENPs.

With sewer sludge being the common factor for contamination of agricultural fields, there is a high potential for the simultaneous introduction of TiO₂ ENPs and heavy metal

contaminants. To date, there has been very little research done for ENP and contaminant interactions. Of the research that has been performed on the subject, the majority of it was conducted using aquatic systems involving fish and daphnids. This research has shown that the interaction of TiO₂ ENPs and metal contaminants generally increases the concentration of the contaminant in the organism, however it is still unclear whether the contaminant is biologically available or if it is adsorbed to the surface of the TiO₂ ENPs.

This information gives rise to two alternative hypotheses on how TiO₂ ENPs may affect the fate of heavy metal contaminants in a single substrate growth media. The first is that the TiO₂ ENPs may sequester the heavy metals in the soil thus decreasing the amount of the heavy metals that can be taken up by the plant. The alternative is that the TiO₂ ENPs could act as a carrier of the metals i.e. if the plant is able to take up the intact TiO₂ ENP with heavy metals adsorbed to the surface, it could potentially increase the amount of the metals that enter the plants. The main objective of this study was to determine which of these scenarios is true for broccoli plants that were grown in cadmium and arsenate contaminated growth media.

DEDICATION

I would like to dedicate this research to all of those who have influenced me and helped motivate me to pursue my academic goals. Firstly, my parents for always believing in me even though they are never really sure about what it is that I am doing. They have always been there for me and pushed me to accomplish great things. Secondly, my girlfriend Kristin Allen, who stood by me throughout the endeavors of my research and who would always help me out when I needed her. Finally, my dogs, Makanda and Nieko, who always helped me to unwind after a stressful day and would never let me hold onto the frustrations from work once I returned home. To all of those mentioned I love you all more than words can describe and am forever grateful for everything that you have done for me.

ACKNOWLEDGEMENTS

I would like to formally acknowledge Dr. Stephen Ebbs for allowing me to work in his lab. I have learned so much over the past few years that I can't list it all and will be forever grateful for this opportunity. He has been ever supportive and always willing to help when I was completely stuck on a problem. I am also grateful for my other committee members, Dr. Samuel Ma and Dr. Andrew Wood, for their continued support and advice throughout my time here.

I would like to acknowledge the Plant Biology department for allowing me to be a part of their family during my time here. A special thanks goes out to Richard Cole and Karen Frailey from the greenhouse for everything they have done for me including advice on how to grow my research plants, allowing me to borrow equipment and space, and their friendship. Also I would like to thank Becky Yancey and Ashley Patterson from the main office for making sure all of my papers are in on time and trying their hardest to keep things running smoothly for this department.

I also would like to thank all of the members of the Ebbs Lab. Both graduate and undergraduates alike, have been very helpful at assisting me with designing and executing my experiments. The countless hours spent in the lab working will never be forgotten.

Last, but certainly not least, the United States Department of Agriculture for providing the funding which allowed me to conduct my research.

TABLE OF CONTENTS

AN ABSTRACT OF THE THESIS OF:	i
DEDICATION	iv
ACKNOWLEDGEMENTS	v
LIST OF TABLES	ix
LIST OF FIGURES	x
CHAPTER 1 INTRODUCTION	1
CHAPTER 2 LITERATURE REVIEW	4
2.1 TiO ₂ Engineered Nanoparticles.....	4
2.1.1 <i>Influence of TiO₂ ENPs on Photosynthesis</i>	6
2.1.2 <i>Influence of TiO₂ ENPs on Nitrogen Reduction</i>	13
2.1.3 <i>Effect of TiO₂ ENPs on Other Organisms</i>	15
2.1.4 <i>TiO₂ Sorption of Metal Ions</i>	17
2.1.5 <i>TiO₂ Disruption of Membranes</i>	20
2.2 Cadmium and Arsenic.....	21
2.2.1 <i>Cadmium uptake and translocation by plants</i>	21
2.2.2 <i>Arsenic uptake and translocation by plants</i>	27
2.3 Rationale.....	30
2.4 Objectives.....	32
2.4.1 <i>Influence of TiO₂ ENPS on photosynthetic efficacy</i>	32

2.4.2 <i>Influence of TiO₂ on the Toxicity of Cadmium and Arsenic</i>	32
CHAPTER 3 INFLUENCE OF TiO ₂ ENPS ON PHOTOSYNTHETIC EFFICACY	44
3.1 Introduction	44
3.2 Materials and Methods	45
3.2.1 <i>Reagents and Plants</i>	45
3.2.2 <i>Influence of TiO₂ ENPS on photosynthetic efficacy</i>	45
3.2.3 <i>Data Analysis</i>	48
3.3 Results	49
3.3.1 <i>Meteorological Data</i>	49
3.3.2 <i>Influence of TiO₂ on Photosynthetic Efficacy on Z. mays</i>	49
3.4 Discussion	54
CHAPTER 4 INFLUENCE OF TiO ₂ ENPS ON THE TOXICITY OF CADMIUM AND ARSENIC	80
4.1 Introduction	80
4.2 Materials and Methods	83
4.2.1 <i>Reagents and Plants</i>	83
4.2.2 <i>Experimental Design</i>	84
4.2.3 <i>Data Analysis</i>	85
4.3 Results	86
4.3.1 <i>Influence of the TiO₂ ENPs and Cd treatments</i>	86

4.3.2 Influence of the TiO_2 ENPs and As(V).....	88
4.4 Discussion	91
CHAPTER 5 CONCLUSIONS.....	108
LITERATURE CITED	110
VITA.....	120

LIST OF TABLES

Table 2.1	41
Table 3.1	61
Table 3.2	63
Table 3.3	64
Table 3.4	66
Table 3.5	67
Table 3.6	69
Table 3.7	70
Table 3.8	72
Table 3.9	73
Table 3.10.	75
Table 3.11.	76
Table 3.12.	78
Table 3.13	79
Table 4.1	95
Table 4.2	96
Table 4.3	102

LIST OF FIGURES

Figure 2.1	33
Figure 2.2	34
Figure 2.3	35
Figure 2.4	36
Figure 2.5	37
Figure 2.6	38
Figure 2.7	39
Figure 2.8	40
Figure 2.9	42
Figure 2.10	43
Figure 3.1	60
Figure 3.2	62
Figure 3.3	65
Figure 3.4	68
Figure 3.5	71
Figure 3.6	74
Figure 3.7	77
Figure 4.1	97
Figure 4.2	98
Figure 4.3	99
Figure 4.4	100
Figure 4.5	101

Figure 4.6	103
Figure 4.7	104
Figure 4.8	105
Figure 4.9	106
Figure 4.10	107

CHAPTER 1

INTRODUCTION

Nanotechnology is developing rapidly into a trillion-dollar industry (Nel et al., 2006). A nanoparticle is described as a material with at least two dimensions between 1 and 100nm (American Society for Testing and Materials, 2006; Scientific Committee on Emerging and Newly Identified Health Risk, 2007). Nanoparticles at this size often display properties different than their bulk (>100 nm in at least two dimensions) or ionic counterparts due to their composition, surface properties, and high surface to volume ratio. Metallic nanoparticles are one of the most common nanoparticles and have found numerous applications in society. Substantial amounts of engineered nanoparticles are expected to be released into the environment, both intentionally and unintentionally.

Nanoparticles are generally broken down into three categories: natural, incidental, and manufactured. Natural nanoparticles occur naturally and are generated from processes like chemical weathering and microbial processes. Incidental nanoparticles are formed as the byproduct of processes such as combustion. Manufactured nanoparticles are a recent discovery in which nanoparticles are intentionally created in laboratory and/or industrial settings (Dunphy Guzman et al. 2006a). Production of manufactured nanoparticles (also referred to as engineered nanoparticles) has increased rapidly because of the unique physiochemical properties of materials at the nanoscale. The use of engineered nanoparticles (ENPs) in electronics, energy, textiles, pharmaceuticals, and cosmetics (to name a few) has shown promise for increased performance with a decreased consumption of resources and generation of waste (Gogos et al.

2012). The increased production and use of ENPs greatly increases the likelihood of ENPs benign released into the environment.

To date, there are very few studies that have quantified the release of ENPs from products containing ENPs, furthermore there is nearly no information pertaining to the environmental concentrations of ENPs (Gottschalk et al. 2009). While this information is nearly undocumented, it is thought that the greatest efflux of ENPs into the environment will occur in aquatic systems. The release of ENPs from consumer products will likely end up in the sewage sludge of wastewater treatment plants, which is sometimes applied to agricultural fields as a soil conditioner and fertilizer. Approximately 40-60% of sewage sludge generated from wastewater treatment plants is applied to agricultural fields annually (Sablayrolles et al. 2010), indicating this may be the major source of ENPs for terrestrial systems (Tourinho et al. 2012). This practice yields the potential for ENPs to enter our food supply with unknown consequences to human health. However, ENPs are being investigated for their potential beneficial use in agricultural systems for fertilization systems and plant protection products (Gogos et al. 2012).

Recent research has shown that ENPs have the potential to be used as delivery systems for slow release pesticides/fertilizers and genetic material, UV protectants, dispersing agent, photocatalyst for degradation of pesticides/herbicides, nanosensors for plant pathogen and pesticide detection, and for soil conservation and remediation (Ghormade et al. 2011; Gogos et al. 2012). There have also been studies indicating that the use of TiO₂ ENPs as a foliar spray resulted in an increase in many aspects of photosynthesis in spinach (Hong et al., 2005a; Hong et al., 2005b; Gao et al., 2006; Linglan et al., 2008; Gao et al., 2008; Su et al., 2007; Zheng et al., 2007; Zheng et al., 2008). While it appears that the use of ENPs in agriculture has the potential

to be quite beneficial, research in nanotoxicology and ENP-contaminant interactions are showing signs that they have the potential to be harmful as well.

There have been several studies showing that ENPs have the potential to adsorb environmental contaminants (Mahdavi et al. 2013; Hartmann 2010; Engates and Shipley 2011; Yang et al. 2012; Jegadeesan et al., 2010; Sun et al., 2009; Xu and Meng, 2009). Since previous research has demonstrated that ENPs are capable of entering cells (Dunphy Guzman et al. 2006a), the potential for a “Trojan horse” scenario is possible, in which, the contaminants adsorb to the ENP and then the ENP enters the cell thus increasing the concentrations of the contaminants that enter the cell. In fact this has been shown to occur in carp (*Cyprinus carpio*) (Zhang et al., 2007; Sun et al., 2007;) and *Daphnia magna* (Fan et al., 2011; Tan and Wang, 2014). However it is still unclear whether the contaminants are biologically available or if they remain adsorbed to the ENP once inside the organism.

The overall goals for the foliar application of TiO₂ ENPs experiments were to monitor several aspects of photosynthesis of plants that will be exposed to TiO₂ ENPs in an effort to determine how TiO₂ ENPs may influence the efficiency of CO₂ assimilation. The general approach involved the foliar application of 5-15 nm TiO₂ ENPs at 500, 1,000, 2,500, and 5,000 mg L⁻¹ to corn (*Zea mays* L.) plants and then determine the resulting effect on various aspects of photosynthesis and plant metabolism.

The overall goals of the TiO₂ ENP and heavy metal(oid) interaction experiments were to determine how TiO₂ ENPs may effect on the uptake of the metal(oid)s. The general approach was to treat broccoli plants with three concentrations of TiO₂ ENPs (0, 333, and 3,333 mg kg⁻¹) and three concentrations of Cd (0, 2, and 20 mg kg⁻¹) or As(V) (0, 20, and 200 mg kg⁻¹) and determine if the TiO₂ ENPs increased or decreased the uptake of the contaminants.

CHAPTER 2

LITERATURE REVIEW

2.1 TiO₂ Engineered Nanoparticles

TiO₂ engineered nanoparticles (ENPs) are one of the most widely produced nanoparticles with a broad range of applications in paints, inks, sunscreens, cosmetics, astronautics, and air/water purification. It is because of their vast range of applications that concerns have been raised about the introduction of TiO₂ ENPs into the environment. The release of TiO₂ ENPs into domestic and industrial wastewaters is expected to represent the largest release of these nanoparticles. There has been data showing that up to 99% of TiO₂ ENPs that enter wastewater treatment plants are retained in the sludge (Tourinho et al., 2012). In addition, TiO₂ ENPs are being used at some water treatment plants because of their strong adsorption strength for hazardous materials, such as cadmium, arsenic, and copper (Zhang et al., 2007; Sun et al., 2007; Fan et al., 2011) and also the photocatalytic breakdown of harmful organic compounds. Since sewage sludge from wastewater treatment plants is applied to some agricultural lands as a soil conditioner and fertilizer, this has resulted in the introduction of an estimated 120 μg kg⁻³ per year of TiO₂ ENPs (Tourinho et al., 2012).

The reason TiO₂ is one of the most widely used nanoparticles is due to its UV absorption and photoactive properties. The term photoactive refers to the ability of TiO₂ ENPs to emit electrons in the presence of ultraviolet light. Of the different forms of TiO₂ ENPs, anatase TiO₂ exhibits the greatest amount of photoactivity. This photoactivity has been shown to make TiO₂ a photocatalyst, mediating oxidation-reduction reactions on the surface of the ENP (Dodd and Jha, 2011). This photocatalytic property has led to the use of TiO₂ in waste water treatment plants as

a means of killing harmful bacteria and in air purification to break down organic pollutants to increase air quality.

The properties of TiO₂ ENPs have also prompted investigation of potential uses in plant-based agricultural settings, including use of it as a UV protectant, a defense against harmful bacteria and fungi, or a catalyst for the degradation of pesticides and herbicides (Ghormade et al., 2011; Gogos et al., 2012). The underlying thought is that the photocatalytic properties of TiO₂ ENPs have the ability to produce reactive oxygen species (ROS) which would prove to be a strong defense against bacteria and fungi due to peroxidation of their cell membranes. TiO₂ ENPs generate ROS when exposed to UV light. When TiO₂ ENPs are exposed to UV light (<390 nm) it creates a charge separation by promoting an electron to the conductance band generating a positively charged hole in the valence band. The positively charged hole scavenges electrons from water and/or hydroxyl ions, which produces hydroxyl radicals. The electrons in the conductance band reduce O₂ to generate the superoxide anion. Singlet oxygen can also be created by TiO₂ ENPs but is usually formed indirectly by the superoxide anions (Brunet et al. 2009). The photocatalytic property would also prove to be effective at increasing the degradation of organic pesticides without decreasing the effectiveness of the pesticide. A previous study showed that TiO₂ ENPs were capable of reducing the half-life of the pesticide imidacloprid while also lowering the LC₅₀ of a storage pest beetle (*Martianus dermestoides*) when compared to the conventional imidacloprid (LC₅₀ TiO₂ ENP imidacloprid=9.86; LC₅₀ conventional imidacloprid=13.45) at an application rate of 25 mg L⁻¹ (Guan et al. 2008).

2.1.1 Influence of TiO₂ ENPs on Photosynthesis

There has been a recent interest in the use of TiO₂ ENPs to enhance photosynthesis. In recent studies, foliar application of TiO₂ ENP's have been shown to increase several aspects of the photosynthetic process in spinach (*Spinacia oleracea* L.), including Rubisco and Rubisco activase activity, chlorophyll synthesis, and oxygen evolution (Hong et al., 2005a; Hong et al., 2005b; Gao et al., 2006; Linglan et al., 2008). However, these are all descriptive studies and have not yet given rise to a more detailed mechanistic approach as to how the TiO₂ ENPs are eliciting these responses.

Foliar application of TiO₂ ENPs on spinach resulted in a significant increase in plant fresh weight, dry weight, chlorophyll content, net photosynthetic rate, and carboxylase activity of Rubisco (Linglan et al., 2008; Hong et al., 2005b; Gao et al., 2006; Gao et al., 2008; Su et al., 2007; Zheng et al., 2007; Zheng et al., 2008). Research has shown that foliar application of 0.25% TiO₂ (2,500 mg L⁻¹). ENPs significantly increased the biomass of spinach. A range from 1.69 – 2.36 fold increase in dry weight has been observed (Zheng et al., 2005; Linglan et al., 2008; Hong et al., 2005b; Gao et al., 2008; Gao et al., 2006). This increase in biomass is attributed to the increase in photosynthetic activity from the TiO₂ ENPs.

One of the hypotheses of how TiO₂ ENPs increase photosynthetic activity is from its capability to decrease ROS in the chloroplast of spinach (Zheng et al., 2008; Hong et al., 2005a). TiO₂ ENPs have been shown to significantly decrease O₂⁻ and H₂O₂ generation by isolated chloroplasts when exposed to a light intensity of 500 μmol m⁻² s⁻¹ (Hong et al., 2005a) and UV-B radiation (Zheng et al., 2008). Chloroplasts exposed to this light intensity showed an O₂⁻ and H₂O₂ production that was approximately 50 and 57% (Figure 2.1B; Figure 2.2B), respectively, less in plants treated with TiO₂ ENPs compared to controls (Figure 2.1B; Hong et al., 2005a).

Under UV-B radiation TiO₂ ENP treated chloroplasts generated up to 59.1% less O₂⁻ (Figure 2.1A) and up to 58.9% less H₂O₂ (Figure 2.2A) compared to that of the control. The decrease generation of O₂⁻ and H₂O₂ from application of TiO₂ ENPs was approximately 20% less than that of the bulk TiO₂ (Figure 2.1A and 2.2A; Zheng et al., 2008). The production of ROS is closely related to the stability of chloroplast membranes. Malondialdehyde (MDA) is frequently used as an indicator of lipid peroxidation because it is the product of decomposition of polyunsaturated fatty acids found in bio-membranes. Chloroplasts exposed to a light intensity of 500 μmol m⁻² s⁻¹ showed a decrease of up to 28% less MDA than that of the control (Figure 2.3B; Hong et al., 2005a). MDA content of chloroplasts under UV-B radiation treated with TiO₂ ENPs was 49.9% lower than that in the control chloroplasts while the bulk TiO₂ treatment reduced MDA by only 21.9% relative to the control (Figure 2.3A; Zheng et al., 2008). The reduction of ROS and MDA show that the application of TiO₂ ENPs could effectively alleviate stress from ROS and lipid peroxidation, allowing the chloroplast membranes to remain stable under UV-B radiation.

There are many enzymes involved in the processing of ROS within cells. Spinach chloroplasts treated with 2,500 mg L⁻¹ TiO₂ showed elevated activity levels of superoxide dismutase (SOD), catalase (CAT), and peroxidase (POD) compared to the controls ENPs under a light intensity of 500 μmol m⁻² s⁻¹ (Figure 2.4 E-G; Hong et al., 2005a). Isolated spinach chloroplasts exposed to UV-B radiation showed a higher activity level of SOD, CAT, ascorbate peroxidase (APX), and guaiacol peroxidase (GPX) when treated with TiO₂ ENPs compared to the controls (Zheng et al., 2008). SOD, CAT, APX, and GPX were found to increase their activity by as much as 2.2, 1.8, 1.5, and 1.5 times that of the control respectively (Figure 2.4 A-D; Zheng et al., 2008).

These data suggest that foliar application of TiO₂ ENPs could activate SOD, CAT, and POD in spinach chloroplasts; these enzymes in turn remove the free radicals which alleviate any stress that they may have caused to the chloroplast, mainly to the cell membrane. Zheng et al. (2008) proposed that TiO₂ ENPs could promote antioxidant defense in chloroplasts in two ways: 1) TiO₂ ENPs could activate antioxidant enzymes such as SOD, CAT, APX, and GPX. 2) TiO₂ ENPs could directly reduce O₂⁻ by the Ti⁴⁺ of TiO₂ oxidizing O₂⁻ to O₂ and reduce itself to Ti³⁺, which could reduce O₂⁻ to H₂O₂ and oxidize itself to Ti⁴⁺. The H₂O₂ could then be reduced to H₂O and O₂ by enzymes such as CAT, GPX, APX, and POD.

Chlorophyll is the pigment in plants that absorbs light energy and converts it into electronic and chemical energy. Numerous studies reported that foliar application of TiO₂ ENPs can significantly increase chlorophyll contents in spinach plants. Foliar application of 0.25% (2,500 mg L⁻¹) anatase TiO₂ ENPs resulted in an increase of chlorophyll contents from 18.96-20.71% (Gao et al., 2006; Linglan et al., 2008). Spinach plants treated with 300 mg L⁻¹ anatase TiO₂ ENPs showed a 17.23% increase in chlorophyll contents (Gao et al., 2008). Application of 2,500 mg L⁻¹ anatase TiO₂ ENPs showed an increase of chlorophyll-*a* and chlorophyll-*b* by 39.54 to 44.53% and 27.69 to 54.12% respectively (Hong et al., 2005b; Zheng et al., 2007). Spinach seed soaked in 2.5% rutile TiO₂ ENPs for 48 hours then transferred to two layers of moistened gauze in Petri dishes containing perlite with a Hoagland culture solution at 20°C, 80-86% humidity, and 450 μmol m⁻² s⁻¹ light intensity for 30 days also showed a 44.53% and 27.69% increase in chlorophyll-*a* and chlorophyll-*b* respectively (Zheng et al., 2005). However, foliar application of TiO₂ ENPs ≥4,000 mg L⁻¹ resulted in a decrease of chlorophyll contents in spinach (Hong et al., 2005b) and there were no significant changes in plants treated with bulk TiO₂ compared to the control (Linglan et al., 2008). An increase in chlorophyll contents would

be beneficial to plants by allowing them to synthesize more light harvesting complexes to capture a greater amount of light energy and enhance photosynthesis.

Light harvesting complexes are pigment-protein complexes that are associated with photosystem I and photosystem II. Foliar application of 2,500 mg L⁻¹ anatase TiO₂ ENPs on spinach leaves resulted in an increase in light harvesting complex II (LHCII) of 24.24% compared to the control while there was only a 9.19% increase for the bulk TiO₂ at the same concentration (Figure 2.5A; Zheng et al. 2007). Ze et al. (2011) performed the same experiment with *Arabidopsis thaliana* and found the contents of LHCII for the TiO₂ ENP treated plants was 3.83 times greater than the control, while the bulk TiO₂ only showed a 37.14% increase compared to the control (Figure 2.5B). This study also examined the mRNA transcript level of the LHCII b subunit of LHCII and found that *A. thaliana* plants that were sprayed with TiO₂ ENPs had 29.33 and 12.57 times more than the control and bulk TiO₂ treated plants, respectively (Ze et al. 2011).

Once light energy has been captured by the light harvesting complexes, it is transferred to the electron transport chain as electronic energy. An earlier study found that TiO₂ ENPs increased whole chain electron transport, enhancing the photoreduction activity of DCPIP by PSII. In contrast, treatment reduced the activity of PSI with the greatest effect being observed at a concentration of 5 μM anatase TiO₂ ENPs (Su et al., 2007). At this concentration, treatment with TiO₂ ENPs increased whole chain electron transport [H₂O to MV (methyl viologen)] by 86.81%, PSII reductive activity (H₂O to DCPIP) by 79.65%, PSII oxidative capacity [DPC (1,5-diphenylcarbazide) to DCPIP (2,6-dichlorophenol indophenol)] by 25.90% and decreased the PSI activity (DCPIP to MV) by 7.36% (Figure 2.6) (Su et al., 2007). These data suggest that TiO₂

ENPs have a much greater effect on the function of PSII than PSI, but still promoted increased flow overall through the electron transport chain.

Linolenic acid acts as an inhibitor to the electron transport chain in higher plants. It may accumulate in plants under various stresses, such as: drought, low temperature, heavy metals, ultraviolet radiation, or senescence (Su et al., 2008). It has been reported that the application of TiO₂ ENPs can reduce the inhibitory effects of linolenic acid on several parameters of the electron transport chain (Su et al., 2008). Adding 5 μM of TiO₂ ENPs reduced the inhibitory effects of 20 to 100 μM linolenic acid on whole chain electron transport by 31.82, 95.45, 86.36, and 59.09% respectively (Figure 2.7A). Chloroplasts treated with 20 to 100 μM linolenic acid had a 15.15, 29.41, 35.29, 76.47, and 94.18% decrease compared to the controls, respectively; while the ones treated with TiO₂ ENPs only decreased by 2.54, 11.06, 36.59, 43.26, and 61.43% respectively (Figure 2.7B). Similar results were seen on the reducing side of PSII with the plants treated with linolenic acid showing a decrease of 42.86, 49.29, 57.14, 64.29, and 71.43% compared to the controls, while the TiO₂ treated chloroplasts only decreased by 4.0, 18.29, 31.57, 44.86, and 58.14% respectively (Figure 2.7C). Finally, PSI photoreduction activity was decreased by 15.17, 53.62, 71.89, 78.31, and 85.43% compared the control, respectively. The addition of TiO₂ ENPs increased the photoreduction activity by 6.39 and 2.69% in the 0 to 20μM linolenic acid treatments and the decrease in activity for 40 to 100 μM linolenic acid was 27.18, 62.07, 65.52, and 79.31% compared to the control (Figure 2.7D) (Su et al., 2008).

Oxygen evolution is a byproduct of the electron transport chain, for when P680 transfers its excited electron to pheophytin, it must replace the lost electron. This is accomplished through the splitting of water molecules, in which the electron from the hydrogen is taken by P680 and the hydrogen proton is used to generate a chemiosmotic gradient. This being said, an increase

functioning of the electron transport chain should result in an increase in oxygen evolution by the chloroplasts. In fact, research has demonstrated that the application of TiO₂ ENPs to spinach chloroplasts resulted in increased evolution of oxygen (Hong et al., 2005a; Hong et al., 2005b; Zheng et al., 2007; Su et al., 2007; Zheng et al., 2008). Spinach chloroplasts treated with 2.5, 5, and 10 μM anatase TiO₂ ENPs showed an increase in oxygen evolution rates of 29.70, 57.23, and 23.20% compared to the controls, respectively (Figure 2.8A; Su et al., 2007). Chloroplasts treated with 2,500 mg L⁻¹ rutile TiO₂ ENPs at a light intensity of 500 μmol m⁻² s⁻¹ showed an increased oxygen evolution rate at 1, 5, 10, 20, 30, and 40 minutes after treatment of 10.82, 41.23, 79.16, 84.22, 116.31, and 131.41% compared to the control, respectively (Hong et al., 2005a). A similar study done at the same light intensity and varying concentrations of rutile TiO₂ ENPs found 2,500 mg L⁻¹ to have the greatest enhancement of oxygen evolution, 1.58 times that of the control (Figure 2.8C; Hong et al., 2005b). Chloroplasts treated with 2,500 mg L⁻¹ anatase TiO₂ ENPs showed an increased O₂ evolution rate 40.35% greater than the control (Figure 2.8B; Zheng et al., 2007). Under UV-B radiation, chloroplasts treated with 2,500 mg L⁻¹ anatase TiO₂ ENPs had an oxygen evolution rate that was 1.6, 1.8, 2.5, and 9 times that of the control from 6 to 15 minutes in 3 minute increments (Figure 2.8D; Zheng et al., 2008).

Spinach plants treated with 2,500 mg L⁻¹ anatase TiO₂ ENPs showed an increase in net photosynthetic rate (μmol CO₂ m⁻² s⁻¹) of 29.9% (Linglan et al., 2008) to 31.87% (Gao et al., 2006) that of the control. Similarly, foliar application with 300 mg L⁻¹ anatase TiO₂ ENPs resulted in a 28.82% increase in net photosynthetic rate compared to the control (Gao et al., 2008) but no significant changes were observed with application of bulk TiO₂ (Linglan et al., 2008; Gao et al., 2008). Spinach seeds soaked in 2,500 (Hong et al., 2005b) and 25,000 (Zheng et al., 2005) mg L⁻¹ rutile TiO₂ ENPs for 48 hours at 15°C under natural light, then planted in a

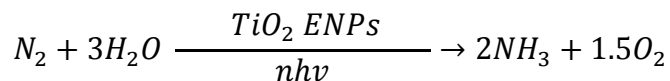
pot containing perlite with a Hoagland culture solution at 20⁰C, 80-86% humidity, and a light intensity of 500 and 450 $\mu\text{mol m}^{-2} \text{s}^{-1}$, respectively, for 30 days, increased the photosynthetic rate by 3.13 times that of the control, but at concentrations over 4,000 mg L^{-1} a decrease in photosynthetic rate was observed (Honget al., 2005b; Zheng et al., 2005). The major component in CO₂ assimilation is the Rubisco enzyme, so in order for there to be an increase in net photosynthetic rates, there must be an increase in Rubisco activity.

Spinach plants that were treated with foliar application of 2,500 mg L^{-1} anatase TiO₂ increased the carboxylase activity of Rubisco by 1.9 (Gao et al., 2008; Linglan et al., 2008) to 2.7 (Gao et al., 2006) times that of the control. Soaking spinach seeds in 25,000 mg L^{-1} rutile TiO₂ ENPs for 48 hours at 15⁰C under natural light, then transferred to were two layers of moistened gauze in Petri dishes containing perlite with a Hoagland culture solution at 20⁰C, 80-86% humidity, and 450 $\mu\text{mol m}^{-2} \text{s}^{-1}$ light intensity for 30 days resulted in an increase in Rubisco activity of 4.22 times that of the control (Zheng et al., 2005). The increase in the carboxylase activity is more so thought to be the result of an increased association of Rubisco activase rather than Rubisco itself. It was later shown that foliar application of 2,500 mg L^{-1} TiO₂ ENPs increased the concentration of Rubisco activase up to 42% (Gao et al., 2006; Gao et al., 2008; Linglan et al., 2008), as well as the activity of purified Rubisco activase was 2.5 times (Gao et al., 2008) to 2.75 times (Linglan et al., 2008) that of the control in spinach. Gao et al. (2008) proposed that the increased activity of Rubisco activase in plants treated with TiO₂ ENPs is due to the influence that the ENPs have on the conformation of the Rubisco activase enzyme. Their research showed that the Rubisco activase of TiO₂ treated spinach had a 12% α -helix increase, an 18% β -sheet increase, and a 13% β -turn; as well as a 57% decrease in random coil contents when compared to controls (Gao et al., 2008).

Interestingly, the above results of Gao (2008) and Linglan (2008) are very similar but the method for treatment was slightly different. The two studies used the same concentration of TiO₂ ENPs but their treatment regimens differed from one another. The former study germinated the spinach seeds in 2,500 mg L⁻¹ TiO₂ and then foliar applied 2,500 mg L⁻¹ TiO₂ suspension in the growth stage of two leaves, whereas the latter study used no exposure to seeds and foliar applied 2,500 mg L⁻¹ TiO₂ once a week between the growth stages of two leaves to eight leaves. This may indicate that weekly application of the TiO₂ ENPs is not necessary for the sustained increase in photosynthetic efficacy; though it must be noted that neither study stated the time period between the last treatment and the analysis of plant tissues.

2.1.2 Influence of TiO₂ ENPs on Nitrogen Reduction

Prior studies revealed that bulk TiO₂ (2 μm) with chemisorbed H₂O in the presence of N₂ gas at 1 atm pressure was capable of reducing N₂ to NH₃ or N₂H₄ (hydrazine) under near UV light in vitro (Schrauzer and Guth, 1977). The estimated amount of nitrogen fixation by rutile TiO₂ found in arid to semi-arid desert sands was estimated to be about one third of the amount of N₂ fixed by lightning and about 10% of N₂ that is fixed biologically (Schrauzer and Guth, 1983). It is thought that TiO₂ ENP's chemisorb N₂ and H₂O; when exposed to sunlight, the H₂O is converted to O₂ and the hydrogen atoms are transferred to N₂ to form NH₃ (Yang et al., 2007).



The phenomena of N₂ reduction to NH₃ via TiO₂ ENPs would provide an increased nitrogen source at the leaf level if the nanoparticles are foliar applied.

The reduction of N₂ via the TiO₂ photocatalytic activity is not the only means which TiO₂ ENPs affect nitrogen levels within plants. It has also been shown by Yang et al. (2006) to

increase the activities of nitrogen assimilation. Nitrate reductase (NR) is the enzyme that catalyzes the reaction of NO_3^- to NH_4^+ . Glutamate dehydrogenase (GDH) and glutamine synthetase (GS) are the key enzymes that assimilate NH_4^+ which consists of the synthesis of amino acids, proteins, and chlorophyll. Soaking spinach seeds in $2,500 \text{ mg L}^{-1}$ TiO_2 ENPs for 48 hr at 10°C under natural light, then planting seeds in a pot containing perlite and grown maintained at 20°C , 80–86% humidity, and $500 \mu\text{mol m}^{-2} \text{ s}^{-1}$ light intensity for 20–45 days, followed by a single foliar application of $2,500 \text{ mg L}^{-1}$ TiO_2 ENPs at the V2 growth stage on spinach resulted in an increase in NR activity which peaked with an activity that was 1.2 times greater than that of the control. This increase in activity resulted in an accelerated transformation of NO_3^- to NH_4^+ in vivo and improved the growth of the spinach. Additionally, this study showed soaking spinach seeds and followed by a single foliar application of $2,500 \text{ mg L}^{-1}$ TiO_2 ENPs promote the absorption of nitrate by spinach. The nitrate concentration within the plants treated with TiO_2 was found to be 2.34 times higher than that of the control after being cultured for 20 days (Table 2.1). This study also showed that the NH_4^+ concentration within the spinach was not significantly different from that of the control after being cultured for 30 days (Table 2.1). Furthermore, there was a decrease in NH_4^+ in spinach plants treated with TiO_2 ENPs for the times before and after 30 days. The authors speculated that this suggests the exposure of spinach to TiO_2 ENP enhanced the activity of enzymes that are involved in ammonia assimilation, which led to the transformation of NH_4^+ to organic nitrogen. This is corroborated by the fact that there was a significant increase in protein and chlorophyll content of spinach (Yang et al., 2006).

Glutamate dehydrogenase (GDH) activity was nearly doubled compared to that of the control from 20 days to 45 days culture time. The same trend was noticed with glutamine

synthetase (GS) and glutamic-pyruvate transaminase (GPT) for 20 days culture time but decreased after 25 days, but the activity levels still remained higher than that of the control (Table 2.1). The increase of these enzymes explains why NH_4^+ levels were reduced when exposed to TiO_2 , because as the NH_4^+ was produced, it was quickly assimilated which is confirmed by the increase in protein and chlorophyll content (Yang et al., 2006).

2.1.3 Effect of TiO_2 ENPs on Other Organisms

Earthworms were referred to as the intestines of the Earth by Aristotle because they ingest soil particles and process them resulting in an improvement in organic matter and the enhanced bioavailability of soil nutrients (Bystrzejewska-Piotrowska et al., 2012). A study to determine how earthworms affect the bioavailability of TiO_2 ENPs in soil reported that the presence of earthworms reduced the water soluble Ti by 80% and Ti extractability with EDTA was reduced by 49% after a ten day incubation period at a concentration of 32 g TiO_2 ENPs kg^{-1} soil DW (19 g Ti kg^{-1} soil DW) suggesting that earthworms may reduce the bioavailability of TiO_2 ENPs in the soil (Bystrzejewska-Piotrowska et al., 2012). They hypothesized that this could be the result of stable binding of titanium to proteins, which were mediated by the digestive track of the earthworms (*Dendrobaena veneta*). In fact, they showed the metal concentrations in the gut of *D. veneta* were about twenty-seven times higher than that of the concentrations in the rest of the earthworms' tissues (Bystrzejewska-Piotrowska et al., 2012). The low retention of titanium by *D. veneta* indicates that the ENPs were not toxic at the 32 g TiO_2 ENPs kg^{-1} soil DW concentration over a ten day period (Bystrzejewska-Piotrowska et al., 2012). However, it has been observed that TiO_2 ENPs caused reproductive toxicity to the

earthworm *Eisenia fetida* at 1,000 mg kg⁻¹ in a dry natural soil, but it was not affected by bulk TiO₂ (Tourinho et al., 2012).

TiO₂ ENPs in the 50 nm range have been found to be toxic to the nematode *Caenorhabditis elegans* with a 24 hour LC₅₀ of 80 mg L⁻¹ (Tourinho et al., 2012). It was found that toxicity increases with decreasing size of the nanoparticles, which is most likely due to the fact that the negatively charged cuticle of the nematode tends to attract nanoparticles more than it attracts bulk materials (Tourinho et al., 2012). Yet there was still a significant reduction in growth and reproduction in *C. elegans* when exposed to bulk TiO₂ (Tourinho et al., 2012).

Not surprisingly, TiO₂ ENPs have been shown to have a negative effect on soil bacterial communities (Ge et al., 2011). The reason this is not surprising because one of the proposed uses of TiO₂ ENPs is as an antimicrobial agent. Ge et al. (2011) observed that there is a significant negative dose-response between extractable DNA and TiO₂ concentration (Ge et al., 2011). The concentration of TiO₂ ENPs exhibited a fairly linear dose-response curve which appeared to have less of a negative effect on extractable DNA over time as there is a greater DNA pool on day 60 compared to day 15 with respect to the lower concentrations. Ge et al. (2011) also examined the effects of TiO₂ ENPs on microbial biomass using soil induced respiration as an indication of the biomass. The results of this experiment showed that there was a exposure of TiO₂ ENPs at concentrations of 0.5, 1, and 2 mg TiO₂ ENPs g⁻¹ soil resulted in a significant decrease in on microbial respiration but there was no significant difference within the concentrations of TiO₂ ENPs. Finally, Ge et al. (2011) used terminal restriction fragment length polymorphism (T-RFLP) to assess the microbial community composition and found that the high doses of TiO₂ resulted in a shift in the microbial community composition as well as a reduction in diversity.

Since TiO₂ ENPs have such a large surface to volume ratio, it holds the capability of having strong adsorption strength for hazardous materials, such as cadmium, arsenic, and copper (Zhang et al., 2007; Sun et al., 2007; Fan et al., 2011). TiO₂ has been shown to enhance the exposure of cadmium and arsenate in carp (Zhang et al., 2007; Sun et al., 2007). The accumulation of cadmium was much more accelerated in the gills and viscera of the carp than it was the skin and muscle tissue (Zhang et al., 2007). This same trend can be recognized in relation to carp exposure to arsenate (Sun et al., 2007). This distribution pattern leads researchers to believe that the majority of the heavy metal doped TiO₂ ENPs retained the majority metal ions on the surface of the nanoparticle. If the metals were released from the nanoparticle once ingested by the carp, either orally or through the gills, then there would have been a greater distribution of the metals throughout the carps' skin and muscle tissues.

As mention above, TiO₂ ENPs were also shown to adsorb copper, which lead to an increased accumulation of copper in *Daphnia magna*, but resulted in a decreased mortality rate (Fan et al., 2011). This was most likely due to the fact that the copper entering into the *Daphnia* weren't entering as free ions, but rather adsorbed to the TiO₂ ENPs. However, in the absence of copper, there has been evidence that TiO₂ ENPs still yield toxic effects to *D. Magna*. In fact, it is a rather acute toxicity, showing an LC₅₀ (Lethal Concentration to 50% of the population) at 1 mg L⁻¹ for 15 nm TiO₂ ENPs (Clement et al., 2013). As with most organisms, the toxicity of the ENPs decreases with increasing size.

2.1.4 TiO₂ Sorption of Metal Ions

As mentioned above, TiO₂ ENPs have a high surface area which gives them a high affinity for sorption of metal ions. Metal-oxide particles with terminal oxygen atoms on the

macro-scale are known to form a hydroxylated surface-functional group from the particles reaction with water (Ridley 2006; Mahdavi et al. 2013). This forms an electric double layer which acts as an electric potential gradient between the particle surface and the bulk solution and heavily influences the adsorption of ions from the solution (Ridley 2006). The sorption capacity of the TiO₂ ENPs is largely dictated by the surface charge of the TiO₂ ENPs which is dependent on the pH of the solution due to the electric double layer. TiO₂ ENPs have a point of zero charge (pzc) in which a pH level below this point results in a positive surface charge and a pH above this point results in a negative surface charge due to the hydroxylated surface functional groups ability to receive and release protons from the water (Dutta et al. 2004; Engates and Shipley 2011; Mahdavi et al. 2013). For TiO₂ ENPs the pH_{pzc} is generally in the range of 4.8-6.2 (Dunphy Guzman et al. 2006b).

The adsorption of Cd to TiO₂ ENPs is rather rapid and achieves equilibrium within 30-60 minutes (Hartmann 2010; Engates and Shipley 2011; Yang et al. 2012). When 100µg Cd L⁻¹ was mixed with 0.01 and 0.1 g TiO₂ ENPs L⁻¹ (pH=8.0), 84.3 and 99.8% of the Cd was adsorbed to the TiO₂ ENPs, respectively (Engates and Shipley 2011). This suggests that the adsorption capacity of the TiO₂ ENPs is highly influenced by the amount of available sorption sites on the surface of the TiO₂ ENPs. Mahdavi et al. (2013) performed a batch experiment with four metals (Cd²⁺, Cu²⁺, Ni²⁺, and Pb²⁺) at 100 mg L⁻¹ in combination with 2,000 mg L⁻¹ TiO₂ ENPs (17 nm) at a pH range from 2-7. The pH_{pzc} for the TiO₂ ENPs was relatively high at 7.4. This study showed that there was competition for binding sites on the TiO₂ ENPs and the binding sites were dominated by H⁺ ions at low pH. However, as the pH increased, the sorption capacity for the metals increased due to the release of H⁺ ions into the solution. TiO₂ ENPs displayed the greatest removal of metal ions from the solution at pH 4, removing 37.5, 14.9, 47.8, and 14.9%

of Cd^{2+} , Cu^{2+} , Ni^{2+} , and Pb^{2+} , respectively (Figure 2.9; Mahdavi et al. 2013). There was a large increase in sorption around pH 6, but this may have been the result of the formation of metal complexes and precipitation. When examining the differences in sorption of single metals vs. multiple metals in a solution at a native pH (not given) the single metal absorption of Cd to TiO_2 ENPs had a maximum absorption of $120.1 \text{ mg Cd g}^{-1} \text{ TiO}_2 \text{ ENP}$. However when multiple metals were in solution at the same time, the maximum absorption of Cd to TiO_2 ENPs was 14.7. This indicated that competition for binding sites on TiO_2 reduced the sorption of Cd by 87% (Mahdavi et al. 2013).

There have been many studies investigating the sorption capacity of arsenic to TiO_2 ENPs. Arsenate (As(V)) has a greater sorption strength to TiO_2 than As(III) at neutral pH and pH of 6.3 (Jegadeesan et al., 2010). However, it was discovered that As(III) had a greater surface coverage at a broader range of pH than As(V) . As(V) sorption was highest between pH 3 and 7 with surface coverage of 12 and $50 \mu\text{g m}^{-2}$ respectively, but the sorption decreased significantly in pH greater than 8. As(III) surface coverage increased from 24 to $46 \mu\text{g m}^{-2}$ with the pH increasing from 4 to 9 (Jegadeesan et al., 2010). Sun et al. (2009) stated that sorption of As(III) and As(V) onto TiO_2 ENPs took approximately 30 minutes to come to equilibrium in an aqueous solution in the dark (solution contained $200 \mu\text{g L}^{-1} \text{ As}$ and $10 \text{ mg L}^{-1} \text{ TiO}_2$). The adsorption equilibrium of this study showed that TiO_2 adsorbed 30% of the initial As(III) or 25% of the initial As(V) (Sun et al., 2009). A prior study revealed that the adsorption of As(V) to TiO_2 ENPs reduces as the size of the particle increases (Xu and Meng, 2009) most likely a result of the change in the surface to volume ratio. However, it should be noted that all of these experiments were conducted in an aqueous solution and there will be many substances competing for sorption sites on TiO_2 ENPs in a natural setting. Jegadeesan et al. (2010)

conducted a sorption study where they included phosphate and silicate ions in the solution to determine how this competition may affect the sorption of arsenic to TiO₂ ENPs. They found in the presence of phosphate and silicate, the surface coverage of As(V) and As(III) was reduced. This is because As(V), silicate, and phosphate have tetrahedral structures which form bidentate complexes with TiO₂ resulting in a competitive sorption which lowers the sorption capacity of As(V) (Jegadeesan et al., 2010).

2.1.5 TiO₂ Disruption of Membranes

It has been observed that TiO₂ is bactericidal at sizes less than 25 nm. It was originally thought that TiO₂ was toxic to bacteria because of its photocatalytic properties, however, Simon-Deckers et al. (2009) found that TiO₂ were still toxic to *E. coli* (*Escherichia coli*) when kept in the dark. They also found that TiO₂ is only toxic to the bacteria when it is adhered to the membrane of the cell or if it is found in the periplasm. Lin et al. (2012) observed nanoparticles adhering to algal cells at a treatment of 10 mg L⁻¹. They also observed the nanoparticles destroying the cell walls and entering into the cells.

Ghosh et al. reported that after 24 hours of exposure, 4 mM (319 mg L⁻¹) TiO₂ ENPs increased the levels of MDA in the roots of onion (*Allium cepa*) by ~4.5 times indicating that TiO₂ ENPs increase the generation of ROS which leads to increased lipid peroxidation and oxidative stress (Ghosh et al., 2010). A recent study has also shown MDA content of algae (*Chlorella sp.*) growing in contact with TiO₂ ENPs was significantly higher than the control showing that TiO₂ ENPs could impose oxidative stress on the algal cells causing lipid peroxidation, however, in the presence of humic acid, the MDA levels were decreased because the humic acid worked as a buffer preventing the formation of ROS at the surface of the

nanoparticle (Lin et al., 2012). While the humic acid may have reduced the generation of ROS from TiO₂ ENPs, it did not alleviate the damage done to the cell walls of the algae cells. Even the TiO₂ ENPs that were coated with humic acid were found to adhere to the cells which resulted in the destruction of the cell walls (Lin et al., 2012). These findings similar to that of Simon-Deckers et al. (2009), which stated that while the generation of ROS may be a contributing factor to TiO₂ toxicity, it is most likely not the main factor. They found that particle sizes up to 140 nm generated ROS in *E. coli*, but the bacteria were still viable. From the results of this experiment, the authors postulated that the contributing factor in TiO₂ toxicity to *E. coli* is the impairment/disruption of membrane integrity. This indicates that there may be a physical interaction with the membranes that is causing the toxicity rather than the generation of ROS (Simon-Deckers et al., 2009).

2.2 Cadmium and Arsenic

2.2.1 Cadmium uptake and translocation by plants

Cadmium is considered the seventh most hazardous substance on the priority list of Agency for Toxic Substances and Disease Registry. Cadmium is considered a non-essential heavy metal. Cd exists in rather high abundance in the earth's crust; with its content ranging in the range of 0.1-2 ppm for non-contaminated soil, but it is usually below 1 ppm (Clemens, 2006). Sources for Cd contamination include atmospheric deposition resulting from mining, smelting, fuel combustion, and sewage sludge (Clemens, 2006). Cd is a member of the divalent family of metals; many divalent metal ions are readily taken up by plants because they are essential nutrients for plant growth and development. Since plants actively take up many divalent metals,

Cd can enter the plant efficiently through the roots and can then be translocated to the leaves and fruits, thus entering into the food chain (Clemens, 2006). The only biological function of Cd has been described in marine diatoms where it acts as a Cd-carbonic anhydrase; other than that Cd has no known biological function (Benavides et al., 2005).

High doses of Cd result in growth inhibition, leaf chlorosis, inhibition of stomatal opening (Clemens, 2006; Benavides et al., 2005), reduced transpiration and photosynthesis (Benavides et al., 2005). Reduced photosynthesis is likely caused because Cd inhibits Fe(III) reductase, which leads to an Fe(II) deficiency (Benavides et al., 2005). Although Cd is not a redox-active metal, symptoms of oxidative stress are observed; this is most likely due to decreased availability of glutathione (GSH) from the formation of phytochelates (PCs) and Cd binding directly to GSH (Clemens, 2006; Benavides et al., 2005). Another source of oxidative stress is thought to be from the disruption of the photosynthetic electron transport chain resulting in the production of singlet oxygen and superoxide (Benavides et al., 2005). Cd also could interfere with Zn-dependent and Zn-binding molecules because of the chemical similarity of Cd and Zn. Ca binding proteins may also be affected by Cd for the same reasons that Zn binding proteins would, this may interfere with molecules such as calmodulin, which could interrupt cellular signaling cascades (Clemens, 2006).

Exposure to Cd has been shown to up-regulate sulfate assimilation, biosynthesis of cysteine and GSH. This would account for the building blocks for PC synthesis. Another response to Cd exposure is the up-regulation of ROS scavenging proteins and heat shock proteins (Clemens, 2006). Within hours of Cd exposure, many genes involved in photosynthesis and glucosinolate biosynthesis were downregulated, but genes involved in sulfur metabolism, cell

wall metabolism, and phenylpropanoid metabolism are rapidly induced (Mendoza-Cózatl et al., 2011).

Cd enters the roots as a hydrated ion from soil solutions via the ubiquitous ZIP family (ZRT, IRT-like protein) metal transporters (mainly those for Fe^{2+} and Zn^{2+}) (Clemens, 2006; Benavides et al., 2005; Verbruggen et al., 2009; Mendoza-Cózatl et al., 2011) and Ca^{2+} channels (Figure 2.10; Clemens, 2006; Benavides et al., 2005). Studies have shown that IRT1 (a ZIP family iron transporter) has a broad range of substrates. Besides iron, it also transports Zn, which alludes to its ability to transport Cd as well (Benavides et al., 2005; Verbruggen et al., 2009).

In order to maintain the negative membrane potential that is required for the uptake of cations, metals have to become trapped inside the cells through metal binding or sequestration sites (Clemens, 2006; Benavides et al., 2005). Most divalent metals have a high affinity for binding to N and S donors. Generally Cd becomes bound to low molecular weight (LMW) ligands, which are either constitutively present or synthesized in response to the presence of Cd (Clemens, 2006). Cd preferentially binds to glutathione (GSH) and phytochelatins (PCs). GSH is constitutively present in cells but PCs are synthesized in response to Cd exposure (Clemens, 2006) and are highly distributed in the plant kingdom (Benavides et al., 2005). PCs are polypeptides with the general structure $(\gamma\text{-Glu-Cys})_n\text{-Gly}$ ($n = 2\text{--}11$). PCs are synthesized in the cytosol from GSH by phytochelatin synthase (PCS) (EC 2.3.2.15) in a transpeptidase reaction (Clemens, 2006; Mendoza-Cózatl et al., 2011; Benavides et al., 2005). PCS expression is constitutive and the enzyme is activated by the excessive presence of metal ions and/or GS-metal complexes in cells, not just by Cd (Clemens, 2006). In fact, PC biosynthesis happens within minutes of Cd exposure (Benavides et al., 2005). PC deficiency in plants leads to Cd

hypersensitivity. Interestingly, overexpression of PCS1 in *Arabidopsis* caused a higher sensitivity to Cd as well. The overexpression leads to the accumulation of gamma glutamine cysteine but a large depletion of GSH, which may have caused sensitivity. PCS doesn't exert enough control over rate of GSH synthesis (Verbruggen et al., 2009). The chelation of excess and/or toxic metals prevents the metals from binding to important proteins and facilitates transport to vacuoles (Verbruggen et al., 2009).

PC-Cd complexes are transported to the vacuoles; the complexes pass through the tonoplast via an unknown ABC-type transporter (Figure 2.10). Once inside the vacuoles, the LMW complexes are formed into high molecular weight (HMW) complexes (Clemens, 2006). A half-sized ABC transporter has been identified in yeast (*S. pombe*) as the transporter required to move PC-metal complexes into the vacuole (Figure 2.10; Mendoza-Cózatl et al., 2011; Verbruggen et al., 2009). Over-expression of HMT1 in *S. pombe* and *S. cerevisiae* increased tolerance to Cd. This was independent of PC synthesis but dependent on GSH synthesis, showing that GS-Cd complexes are also substrates for HMT1 (Verbruggen et al., 2009). While past studies have shown that PC-Cd complexes are found in the vacuoles of plants the ABC-type transporter required to facilitate the movement across the tonoplast has remained unknown until recently (Benavides et al., 2005; Verbruggen et al., 2009). AtABCC1 and AtABCC2 were recently identified as vacuolar PC transporters. These transporters are constitutively expressed. This may allow for rapid storage and detoxification of toxic compounds in the vacuole (Mendoza-Cózatl et al., 2011).

While most Cd is chelated shortly after entering the cytoplasm, free cadmium ions may still exist in the cell. In which case, a $\text{Cd}^{2+}/\text{H}^{+}$ antiport proteins have been suggested as a possible means for hydrated Cd ions to enter into the vacuole. Evidence has been found that

divalent cation/H⁺ transporters (CAX) are involved in transport of Cd across the tonoplast (Figure 2.10). Specifically the overexpression of CAX2 transporter in Arabidopsis has been shown to increase the Cd, Ca, and Mn content in roots (Clemens, 2006). Studies also suggest that CAX4 and possibly MHX may be involved in the movement of hydrated cations into the vacuoles (Verbruggen et al., 2009). Another transporter known as a heavy metal transporting P-type ATPase (HMA), more precisely HMA3, has been shown to facilitate the transport of Cd²⁺ across the tonoplast (Figure 2.10). HMA3 in Arabidopsis is a pseudogene, containing a premature stop codon. Deletion of HMA3 promotes Cd sensitivity, while overexpression has been shown to enhance tolerance and accumulation of Zn and Cd. The expression of TcHMA3 in Arabidopsis enhanced the accumulation of Cd and to a lesser extent Zn (Mendoza-Cózatl et al., 2011).

Once Cd is in the vacuole, it is unknown whether it is formed into HMW complexes, precipitated, or in hydrated ion state. It is thought that at least some of the Cd is in its ion state through work done on AtNramp3. The function of AtNramp3 is proposed to be involved in the mobilization of Fe, Mn, and Zn from the vacuole to the cytosol; because AtNramp3 transports divalent cations, it most likely could transport Cd as well as the micronutrients listed above (Figure 2.10; Clemens, 2006). Further studies have suggested NRAMP3 and NRAMP4 are responsible for the efflux of Cd from the vacuole. This was demonstrated by the overexpression of NRAMP3/4 proteins leading to increased Cd sensitivity. Knock outs suffered from Fe deficiency because the proteins are responsible for Fe homeostasis (Verbruggen et al., 2009).

In order for Cd to move from the roots to the vascular tissue, the metal ions and/or ligand complexes must be transported across a cell membrane. It is suggested that heavy metal transporting P-type ATPases (HMA) are responsible for this transport. AtHMA2 and AtHMA4

are involved in the loading of Zn into the vascular tissue. It is thought that these two proteins may also be involved in the loading of Cd into the xylem as well (Figure 2.10; Clemens, 2006; Mendoza-Cózatl et al., 2011). In fact, the overexpression of AtHMA4 showed an increased accumulation of Zn and Cd in the leaves of *A. thaliana* demonstrating that it is responsible for the translocation of Cd from the root to the shoot (Clemens, 2006; Verbruggen et al., 2009). AtHMA2 may also play a role in this transport but not as significant as AtHMA4, as AtHMA2 only showed Cd transport activity in AtHMA4 knockouts (Verbruggen et al., 2009).

The accumulation of Cd in the shoots yields a high risk of damage to photosynthetic machinery. In order to reduce this risk, plants can move the Cd via the phloem in a source to sink manner. It has recently been shown that PCS is highly expressed in companion cells (Figure 2.10; Mendoza-Cózatl et al., 2011). Furthermore the main metal-ligand molecules found in phloem sap are nicotianamine (NA), GSH, and PCs. NA forms complexes with essential metals while GSH and PCs have higher affinities for non-essential metals (Mendoza-Cózatl et al., 2011). This suggests that GSH and PCs synthesized in, or transported to companion cells are likely to be loaded into the phloem for transport to sink such as seeds or roots (Mendoza-Cózatl et al., 2011). Interestingly, analysis of Arabidopsis seeds showed high levels of GSH but not PCs; suggesting that thiol complexes found in seeds are GS-Cd complexes and that PC-Cd complexes are most likely sequestered in the root vacuoles. To support this more, ABCC1/2 transcript levels are about 3-fold higher in the roots compared to shoots (Mendoza-Cózatl et al., 2011).

It should be noted that PC participates in long distance transport between root and shoot via the phloem. However, Cd transported in the xylem is considered to be in the hydrated cation state because PC concentrations are negligible in the xylem (Verbruggen et al., 2009).

A low-affinity nitrate transporter (NRT1.8) is highly up-regulated in the roots in response to Cd exposure. NRT1.8 is a nitrate transporter that mediates the nitrate removal from xylem sap. Removal of this gene resulted in Cd sensitivity and accumulation of nitrate in the xylem sap. NRT1.8 transcript levels were shown to increase in a concentration and time dependent manner to Cd exposure. This is the first gene directly linking N metabolism to Cd-stress response. Also, it supports the previous hypothesis that N-containing compounds are partially responsible for translocation of Cd from roots to shoots through xylem (Mendoza-Cózatl et al., 2011).

2.2.2 Arsenic uptake and translocation by plants

Arsenic is considered the number one most hazardous substance on the priority list of the Agency for Toxic Substances and Disease Registry. The list is based on three criteria: frequency of occurrence, toxicity, and potential for human exposure (Francesconi et al., 2002). As(III) is found under reducing conditions and As(V) is found in oxygenated conditions (Srivastava et al., 2012). As(V) is the predominant form of As in terrestrial systems (Verbruggen et al., 2009; Francesconi et al., 2002). The only known functions of As in organisms is the use of As(III) as the sole electron donor for anoxygenic photosynthesis in bacteria found in hot spring biofilms and it may also have beneficial roles in methionine metabolism and gene silencing in animals. No functions have been observed in higher plants (Verbruggen et al., 2009). Arsenic toxicity can occur as hypo- and hyper-pigmentation, keratosis, and cancer of lungs, skin, and urinary bladder (Srivastava et al., 2012).

As(V) is a phosphate analog and enters the roots via high affinity phosphate transporters. As(III) enters the roots through aquaglyceroporin channels of the NIP (nodulin 26-like intrinsic protein) subfamily of aquaporins which transports neutral molecules such as silicic acid and

boric acid (Figure 2.10; Srivastava et al., 2012; Verbruggen et al., 2009; Mendoza-Cózatl et al., 2011; Caille et al., 2004; Kertulis et al., 2005). More specifically, OsLsi1 (a silicic acid transporter found in rice) has been shown to be the primary transporter responsible for As(III) uptake, and it is also responsible for the efflux of As(III) from the roots (Srivastava et al., 2012).

As(V) is a chemical analog of phosphate and can potentially be substituted for processes that involve phosphate, including ATP synthesis (Verbruggen et al., 2009). However, phosphorous is always present as phosphate, but As(V) can be and readily is reduced to As(III) within cells (Figure 2.10). This process can take place either enzymatically by AtARC2 arsenate reductase (Srivastava et al., 2012; Verbruggen et al., 2009; Bleeker et al., 2006) or non-enzymatically by glutathione (Verbruggen et al., 2009; Delnomdedieu et al., 1994). The reduction of As(V) to As(III) is a highly efficient process (Srivastava et al., 2012). The reduction of As(V) to As(III) is a crucial step in the detoxification process because it allows the As to become bound to GSH and PC and also activates PCS, much like Cd (Figure 2.10; Verbruggen et al., 2009). However, As(III) can deplete the pool of reduced glutathione by forming complexes with GSH and also through the activation of PC synthesis (Verbruggen et al., 2009).

PCs display a high affinity for As(III) (Mendoza-Cózatl et al., 2011). The chelation of As(III) by GSH and PC not only inhibits the reactivity of As(III), but it also prevents translocation from the roots to the shoots (Srivastava et al., 2012). As(III)-GS₃ complexes can be transported into the vacuoles by an ABC transporter, like Cd (Figure 2.10; Verbruggen et al., 2009). Post-translational activation of PCS seems to be related to the formation of As(III)-GS thiolates (Verbruggen et al., 2009). As(V) reduction to As(III) proves to be a critical step in As tolerance and detoxification. The activation of the PC biosynthetic pathway is dependent on

As(III) levels. Furthermore, the knockout of arsenate reductase gene AtACR2 (arsenic compounds resistance 2) in Arabidopsis showed that translocation of As from the roots to the shoots was increased by 10-16 fold (Srivastava et al., 2012).

Sequestration of As into the vacuoles is crucial for As tolerance. It has recently been found that *P. vittata* possesses an As(III) efflux permease gene ACR3 (arsenic compounds resistance 3) which encodes the ACR3 protein that can transport As across the tonoplast as As(III). Yet in higher plants, this is not thought to exist and the main method for transporting As into the vacuole is through the transport of As(III)-PC complexes by ABCC 1 and ABCC2 transporters (Figure 2.10; Srivastava et al., 2012). ABCC1 and ABCC2 are not activated by As, but are constitutively expressed allowing for rapid storage of excess metal(oids) in the vacuole for a detoxification strategy (Mendoza-Cózatl et al., 2011). It has been demonstrated that ABCC 1/2 double mutant is As hypersensitive and PC-As in the vacuoles is substantially reduced (Mendoza-Cózatl et al., 2011).

As(V) and As(III) are both found in the xylem suggesting that both forms have the capacity to be loaded into the xylem. While As(III) is predominantly found in the xylem, As(V) can also be found in substantial quantities in the xylem (Verbruggen et al., 2009). Arsenic found in the xylem is not complexed with GSH or PC suggesting that it is predominantly loaded in its inorganic form (Verbruggen et al., 2009). As(V) is most likely loaded by Pi transporters while As(III) is thought to be loaded by aquaporins (Figure 2.10; Verbruggen et al., 2009; Mendoza-Cózatl et al., 2011).

Efflux of As from the roots has also been shown as a detoxification strategy in which As(V) is taken up and reduced to As(III) in the roots and then effluxed from the roots, yet the efflux transporter has not yet been identified in plants (Verbruggen et al., 2009). OsLsi1 has

been shown to be the primary transporter responsible for As(III) uptake, and it is also responsible for the efflux of As(III) from the roots (Srivastava et al., 2012).

As can also be methylated as another potential detoxification strategy. As(V) has been shown to upregulate methyltransferases. Methylated As is less toxic than inorganic As, but this process for detox is not a primary strategy in plants, yet it could play a role in specific organs (Verbruggen et al., 2009). It has yet to be shown whether methylated As leads to volatilization (Srivastava et al., 2012).

2.3 Rationale

While it has been shown that TiO₂ ENPs yield the ability to increase photosynthesis, it should be noted that most of these experiments were carried out with a high concentration of TiO₂ ENPs and were conducted on a short time frame. The concentration for the majority of the enhanced photosynthesis experiments was at 2,500 mg L⁻¹ because that is the application rate which warranted the highest increases in photosynthetic rates in early studies. However, there seems to be little to no literature as to whether plants can sustain this rate of photosynthesis for an extended period of time (i.e. the length of a growing season).

That being said, there is still much research to be done before the use of TiO₂ ENPs should be considered for mass usage in a plant-based agricultural setting. There is a dire need for food safety research, as there is currently no apparent data on nanoparticle retention in vegetative tissues, or the translocation/retention in fruits. The use of TiO₂ ENPs in an agricultural system would also increase environmental exposure significantly via the direct release of ENPs on crop lands.

This increased exposure has the potential to be detrimental to numerous microfauna, both terrestrial and aquatic, because it has been observed to be toxic to many organisms. While the toxic concentrations vary widely, TiO₂ ENPs would likely have an extremely long residence time in these systems due to the fact that they are highly stable (Tourinho et al. 2012). This long residence time would allow for environmental concentrations to compound throughout time, and while there has been research involving the use of nanoparticles in remediation; there seems to be no research being done for the remediation of nanoparticles.

In summary, nanotechnology could provide to be a useful tool in many aspects of agriculture, but there is still much research to be done in this area. There are currently many gaps to be filled in as far as effects on chemical and physical soil properties, as well as, a more detailed understanding of how it may affect plants and other forms of biota.

2.4 Objectives

2.4.1 Influence of TiO₂ ENPS on photosynthetic efficacy

Objective 1: Assess the enhancement of CO₂ assimilation following foliar application of TiO₂ ENPs.

Objective 2: Determine whether the increase in CO₂ assimilation influences seed quality and quantity.

2.4.2 Influence of TiO₂ on the Toxicity of Cadmium and Arsenic

Objective 3: Assess the growth parameters of broccoli treated with TiO₂ ENPs and/or As(V) and Cd to determine if the TiO₂ ENPs with or without the metal contaminants have an adverse effect on overall plant health and growth.

Objective 4: Determine if TiO₂ enhances the accumulation of arsenic and cadmium in broccoli.

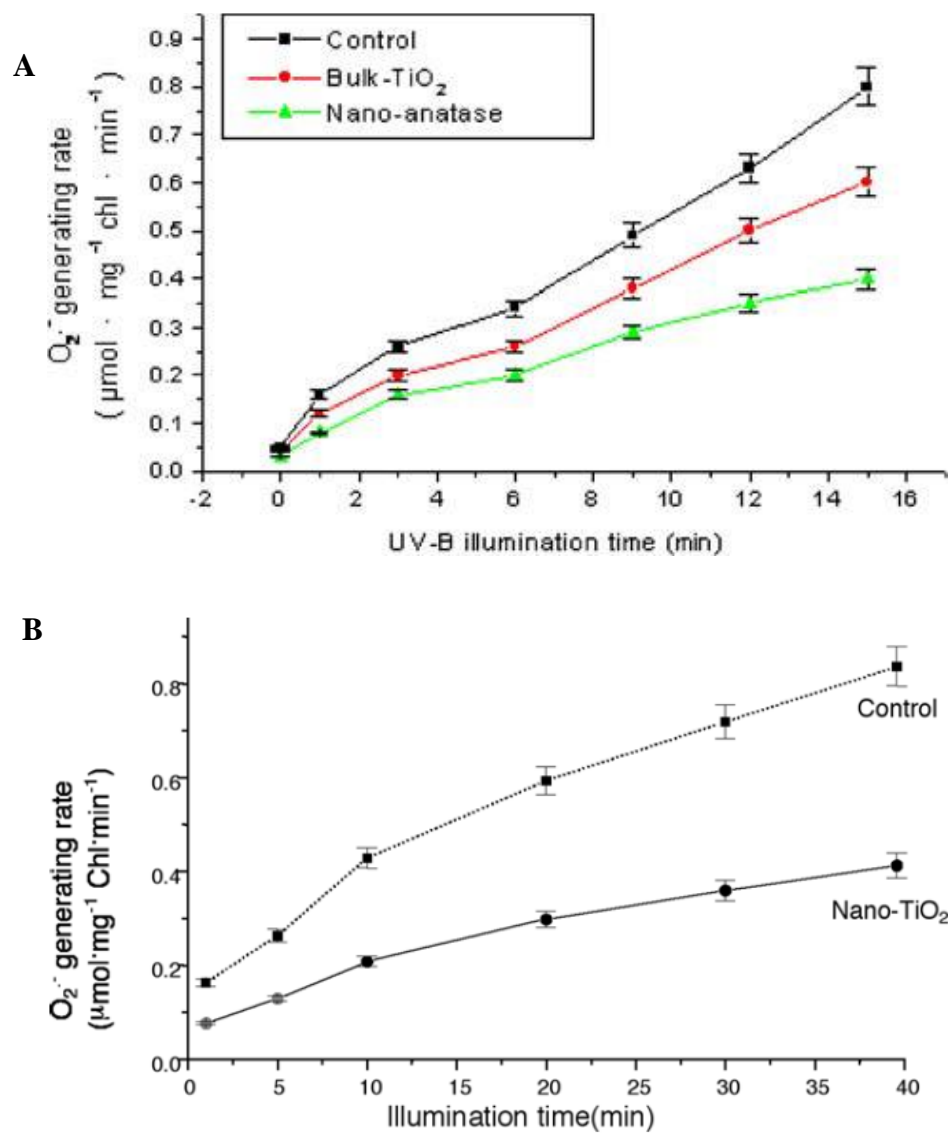


Figure 2.1: Superoxide ion generation rate from isolated chloroplasts from spinach plants treated with 2,500 mg L⁻¹ TiO₂ ENPs when exposed to (A) UV-B radiation (Zheng et al., 2008) and (B) 500 μmol m⁻² s⁻¹ light intensity (Hong et al., 2005a).

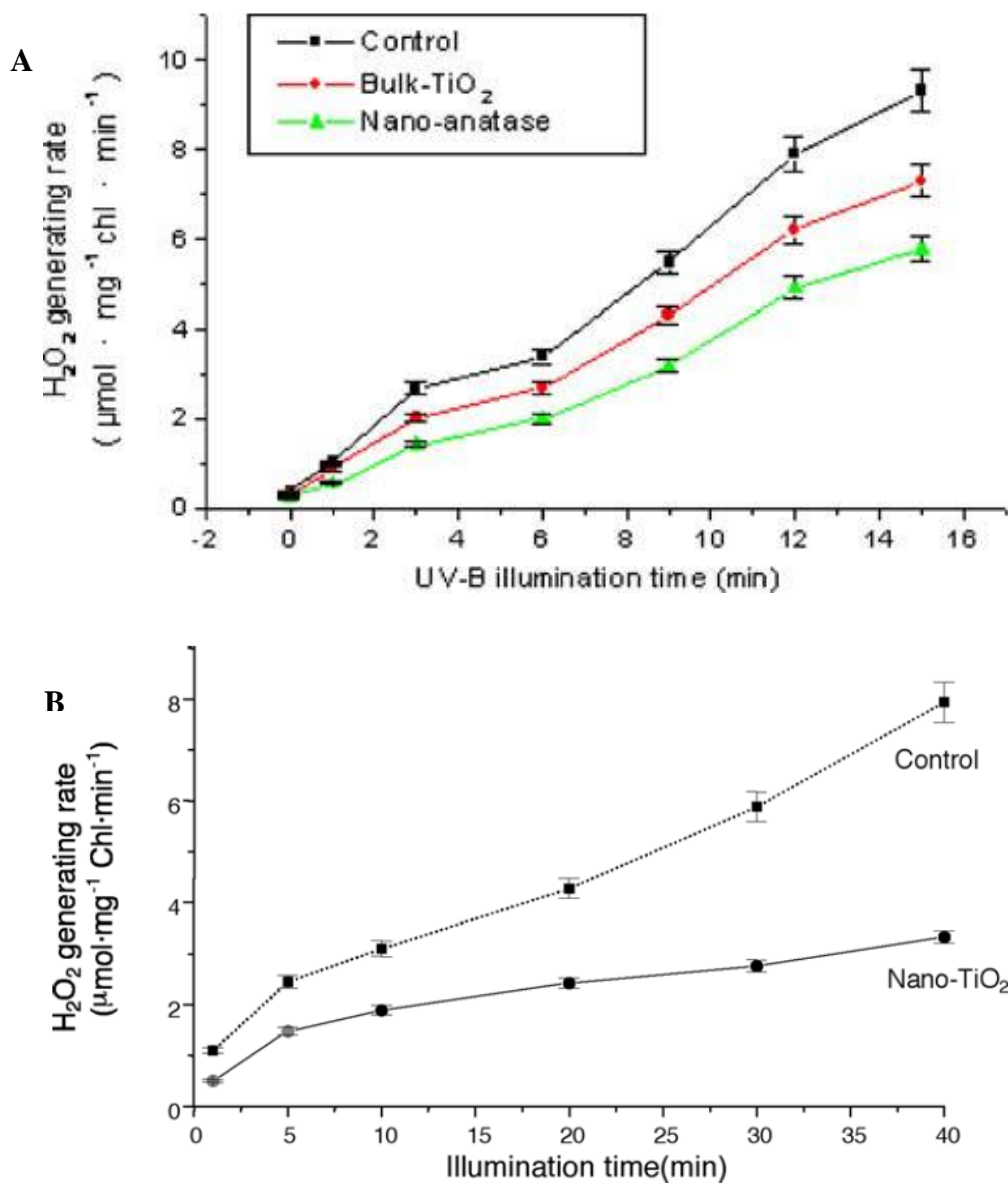


Figure 2.2: Hydrogen peroxide generation rate from isolated chloroplasts from spinach plants treated with $2,500 \text{ mg L}^{-1}$ TiO₂ ENPs when exposed to (A) UV-B radiation (Zheng et al., 2008) and (B) $500 \text{ μmol m}^{-2} \text{ s}^{-1}$ light intensity (Hong et al., 2005a).

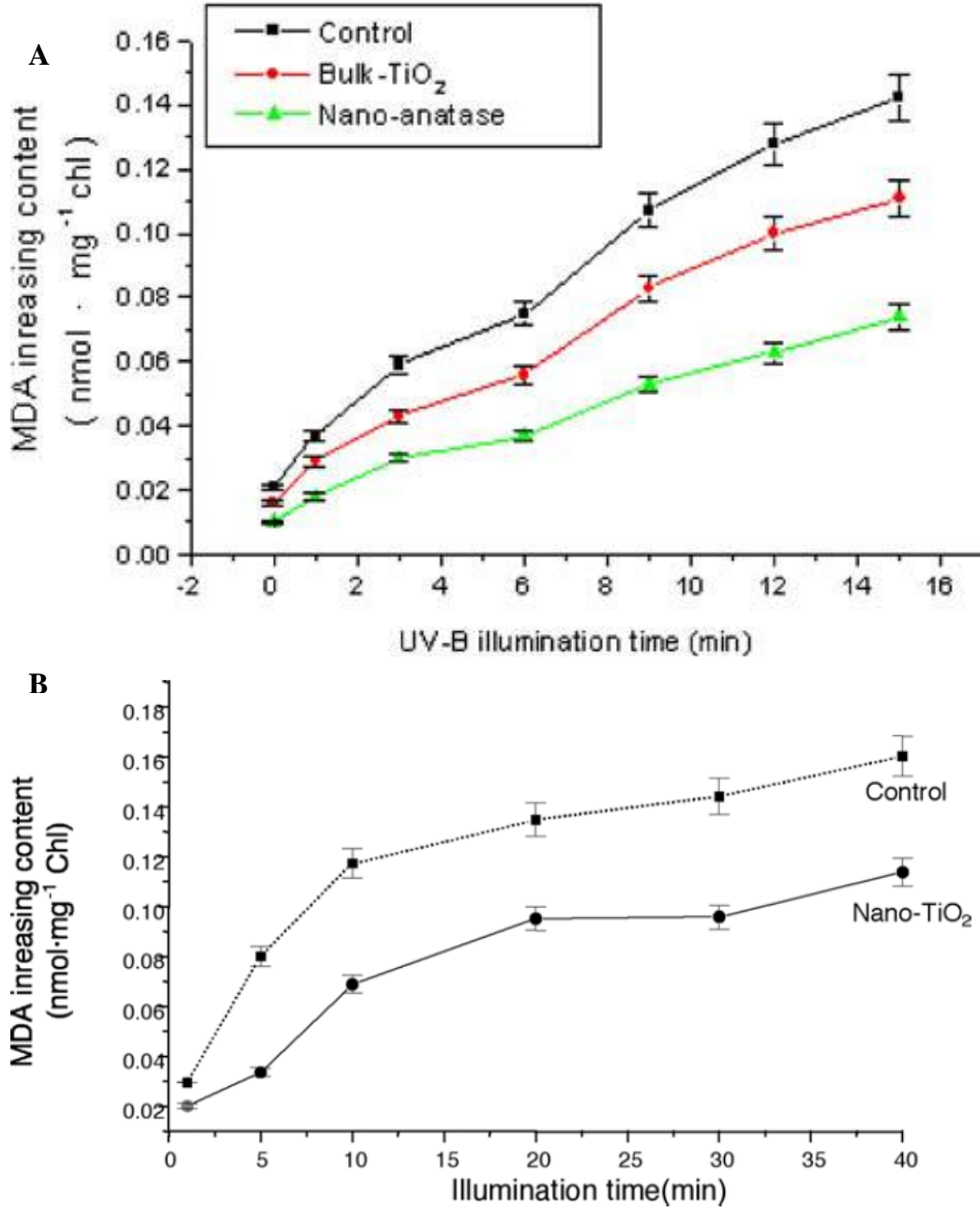


Figure 2.3: Malondialdehyde (MDA) content from isolated chloroplasts from spinach plants treated with 2,500 mg L⁻¹ TiO₂ ENPs when exposed to (A) UV-B radiation (Zheng et al., 2008) and (B) 500 μmol m⁻² s⁻¹ light intensity (Hong et al., 2005a).

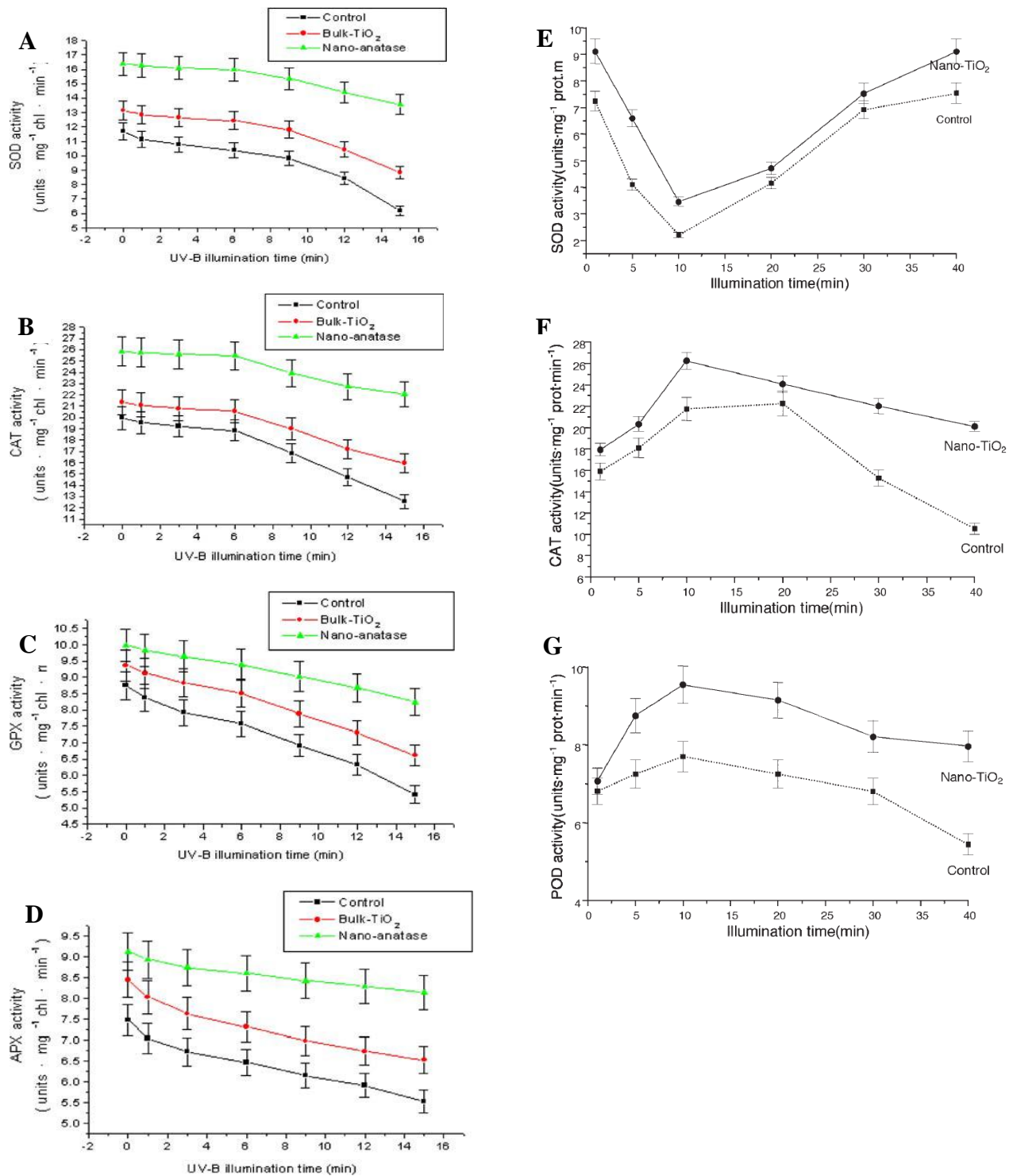


Figure 2.4: Antioxidant enzyme activity for chloroplasts from spinach plants treated with 2,500 mg L⁻¹ TiO₂ ENPs and bulk TiO₂ under (A-D) UV-B radiation (Zheng et al. 2008) and (E-G) 500 μmol m⁻² s⁻¹ light intensity (Hong et al., 2005a).

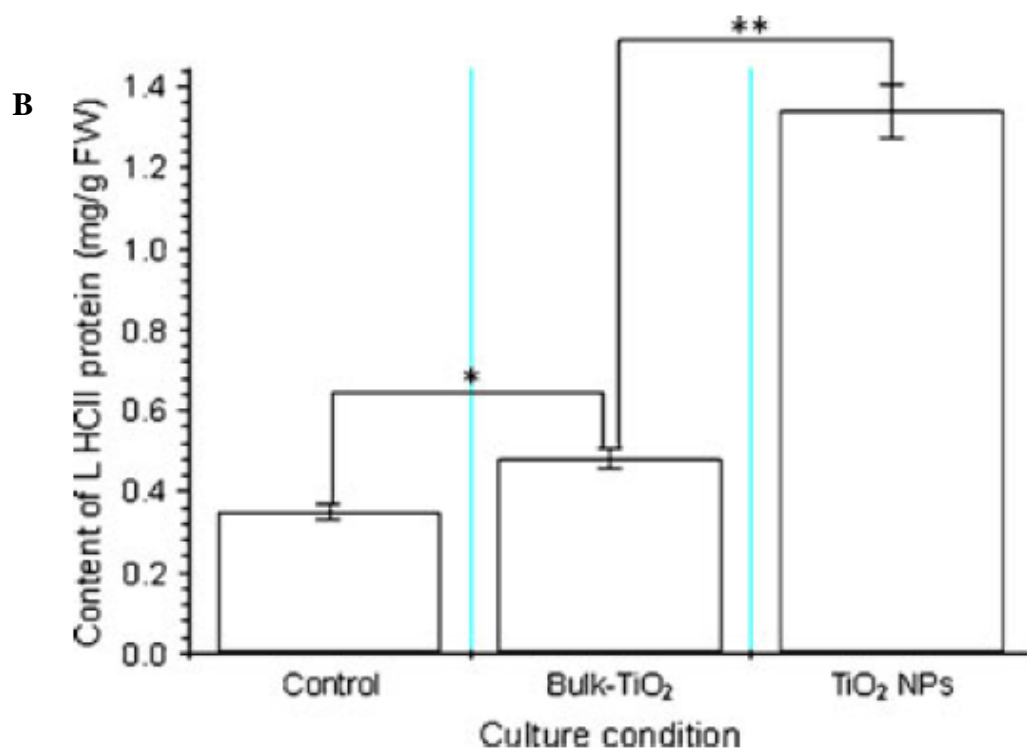
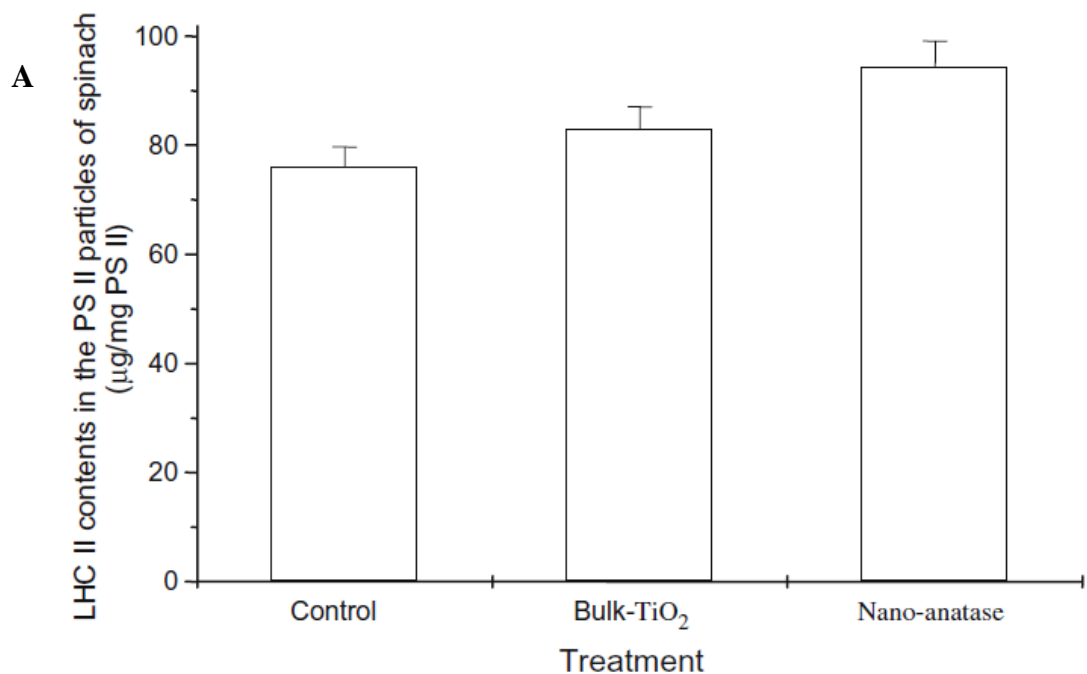


Figure 2.5: Content of LHCII from (A) spinach (Zheng et al. 2007) and (B) *A. thaliana* (Ze et al. 2011) treated with 2,500 mg L⁻¹ TiO₂ ENPs and Bulk TiO₂.

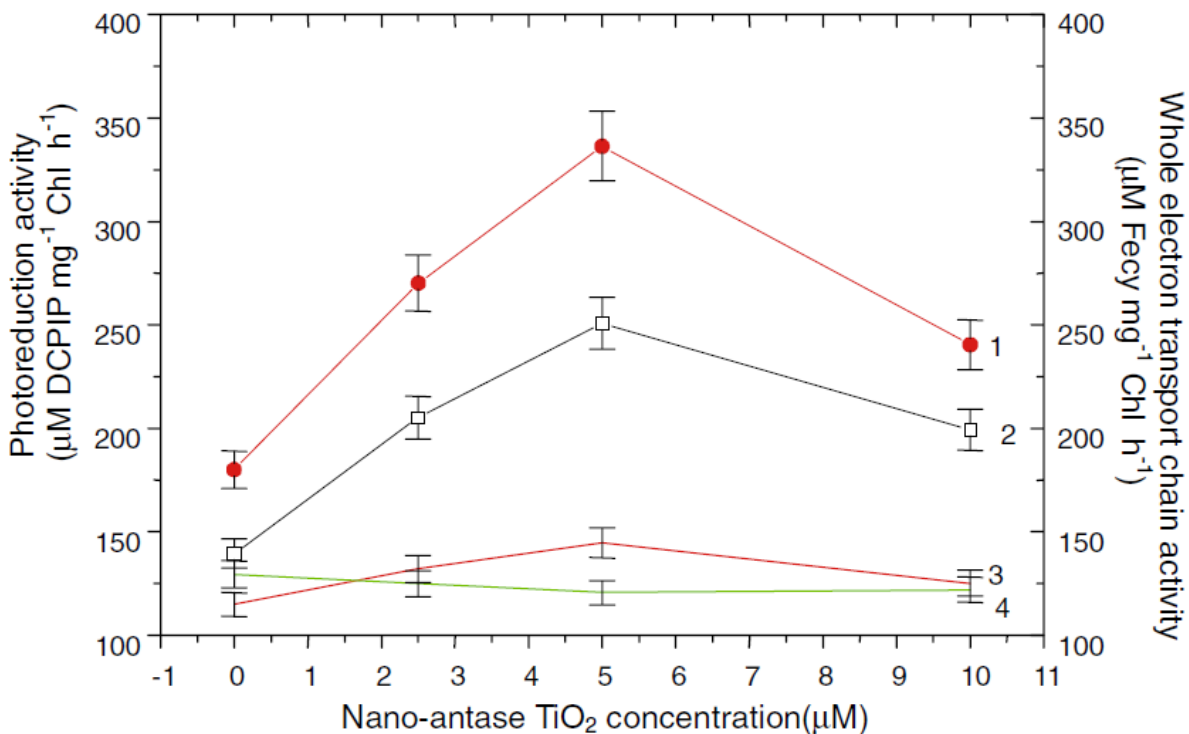


Figure 2.6: Effects of TiO₂ ENPs on the electron transport rate of spinach chloroplasts. (1) whole chain electron transport (H₂O to MV) rate; (2) photochemical activity of DCPIP photoreduction of PSII reducing side (H₂O to DCPIP); (3) photochemical activity of DCPIP photoreduction of PSII oxidative side (DPC to DCPIP); (4) photochemical activity of DCPIP photoreduction of PSI (DCPIP to MV) from Su et al. 2007.

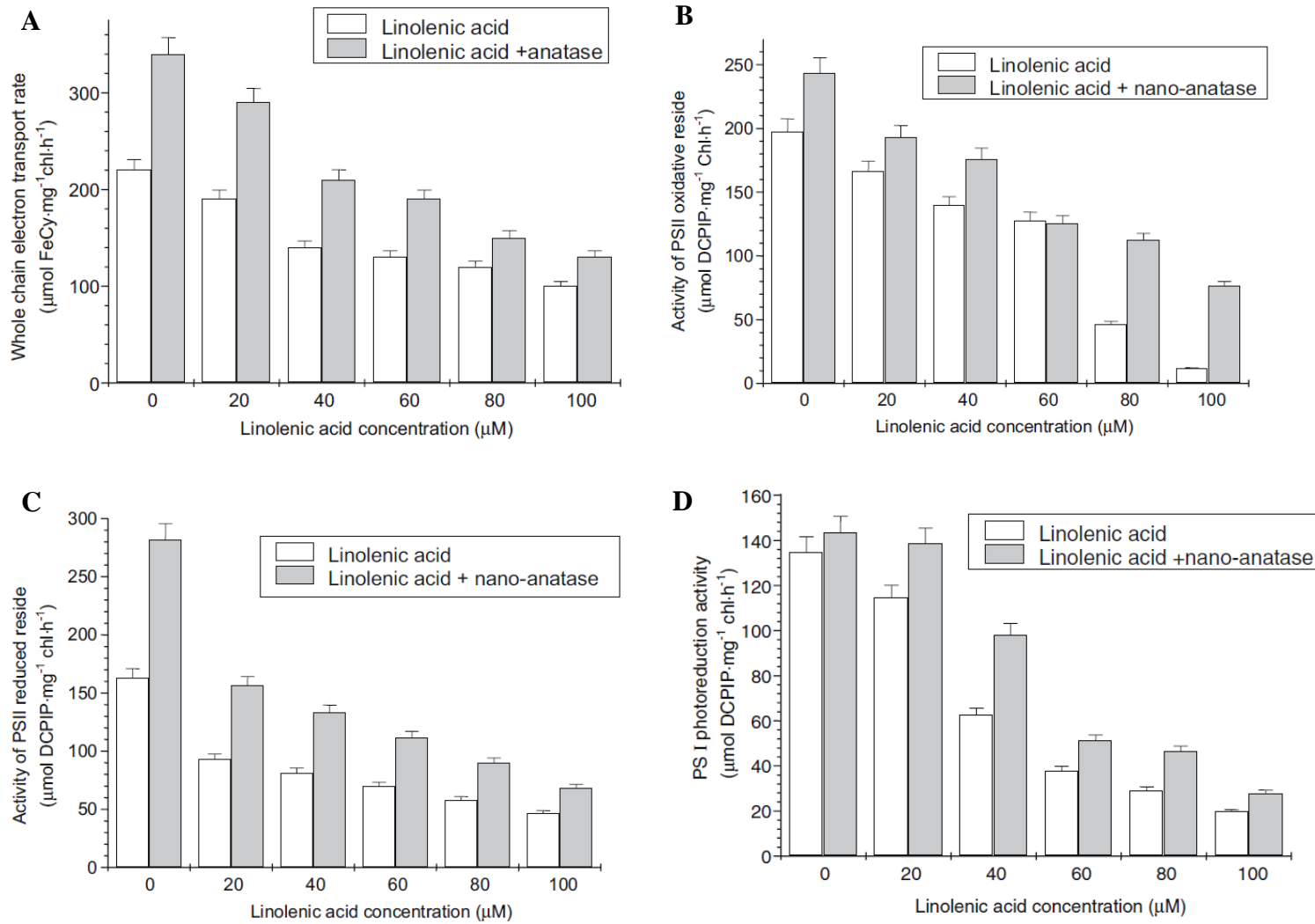


Figure 2.7: Effects of $5\mu\text{M}$ of TiO_2 ENPs on electron transport chain from isolated chloroplasts treated with linolenic acid from Su et al. 2008.

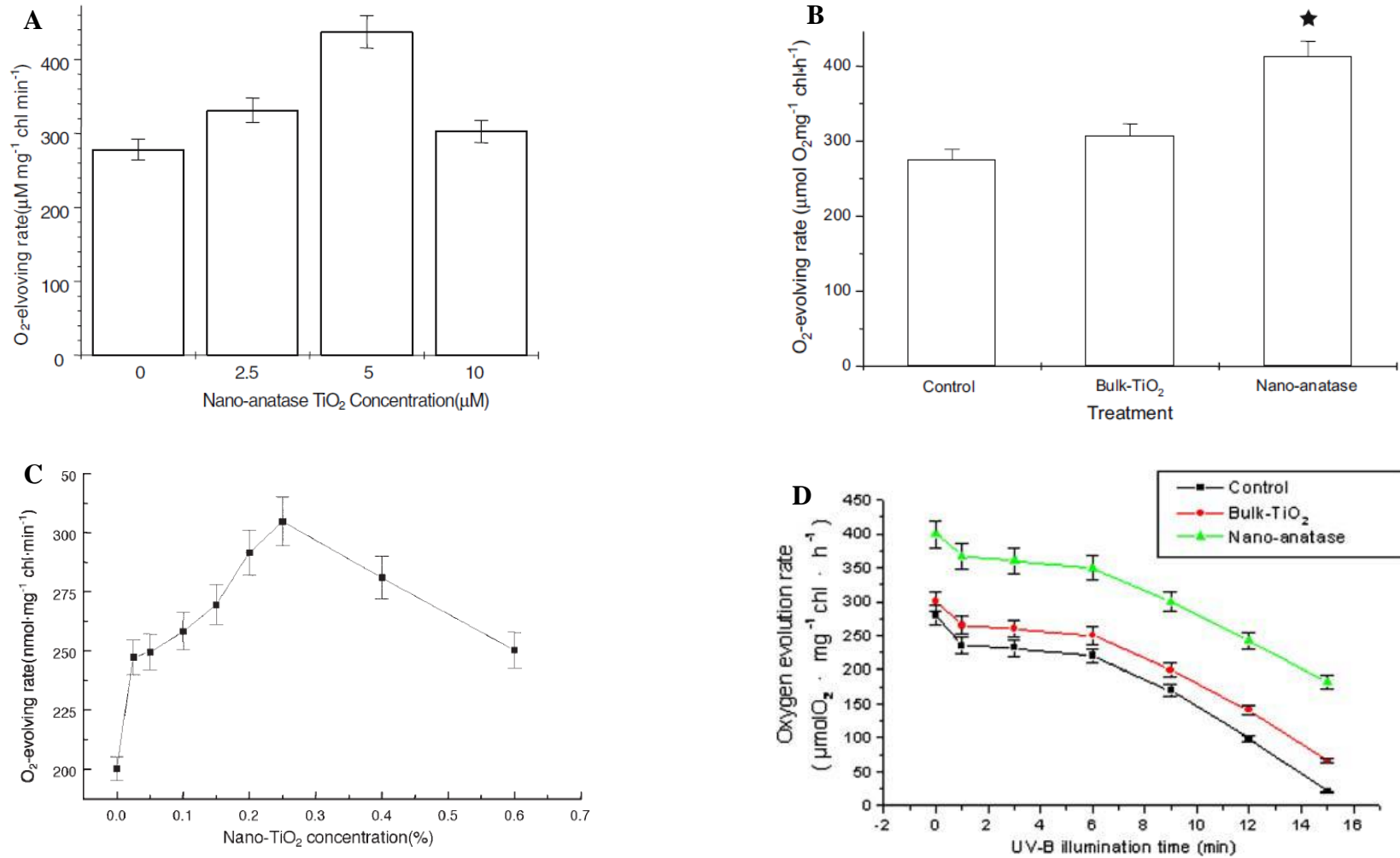


Figure 2.8: Oxygen evolution rates for spinach plants that were soaked in various TiO₂ ENP concentrations as seeds (A Su et al.

2007; C Hong et al. 2005b) and seeds that were soaked in 2,500 mg L⁻¹ TiO₂ ENPs and bulk TiO₂ which were sprayed with the same concentration when the plants had four mature leaves (B Zheng et al. 2007; D Zheng et al. 2008).

Table 2.1: Activity of enzymes involved in the nitrogen assimilation pathway for spinach plants that were soaked in 2,500 mg L⁻¹ TiO₂ ENPs as seeds and received a single foliar application at the same concentration when the plants had two leaves. a,b the differences of values followed by different letters in the same column are significant at the *p*=0.05 level (t-test). Data from Yang et al. (2006).

Culture Time (Day)		20	25	30	35	40	45
Glutamate dehydrogenase activity ($\mu\text{mol NADH mg}^{-3}\text{ prot. min}$)	Control	4.45 \pm 0.03a	3.33 \pm 0.02a	1.00 \pm 0.01a	1.37 \pm 0.01a	1.79 \pm 0.02a	2.65 \pm 0.02a
	Nano-anatase TiO ₂	8.00 \pm 0.04b	4.67 \pm 0.03b	1.74 \pm 0.01b	2.16 \pm 0.01b	3.36 \pm 0.02b	3.88 \pm 0.03b
Glutamate synthase activity ($\mu\text{ mg}^{-1}\text{ prot. min}$)	Control	2.83 \pm 0.03a	1.91 \pm 0.02a	1.01 \pm 0.01a	1.48 \pm 0.01a	1.92 \pm 0.02a	2.57 \pm 0.03a
	Nano-anatase TiO ₂	6.19 \pm 0.04b	2.21 \pm 0.02b	1.88 \pm 0.01b	2.11 \pm 0.01b	2.13 \pm 0.02b	3.50 \pm 0.03b
Glutamate-pyruvic transaminase activity ($\mu\text{mol NADH mg}^{-1}\text{ prot. min}$)	Control	7.81 \pm 0.03a	6.82 \pm 0.03a	4.06 \pm 0.01a	4.46 \pm 0.02a	6.26 \pm 0.03a	7.66 \pm 0.04a
	Nano-anatase TiO ₂	14.19 \pm 0.05b	8.06 \pm 0.04b	4.13 \pm 0.01b	6.76 \pm 0.03b	7.43 \pm 0.03b	8.63 \pm 0.04b

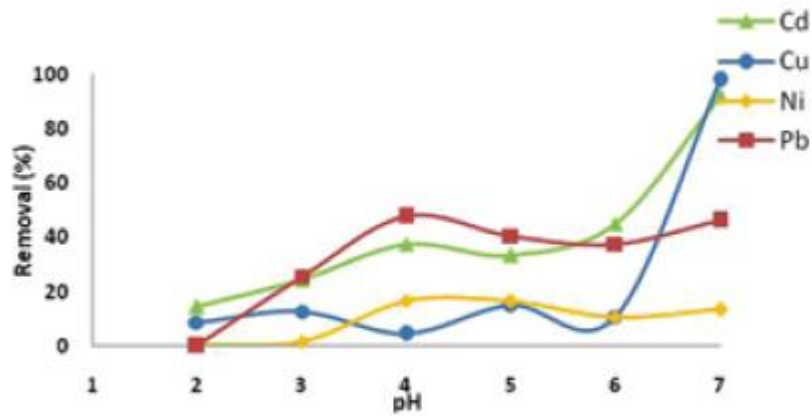


Figure 2.9: Multi-metal batch experiment with four metals (Cd^{2+} , Cu^{2+} , Ni^{2+} , and Pb^{2+}) at 100 mg L^{-1} in combination with $2,000 \text{ mg L}^{-1}$ TiO_2 ENPs (17 nm) at a pH range from 2-7 (Mahdavi et al. 2013).

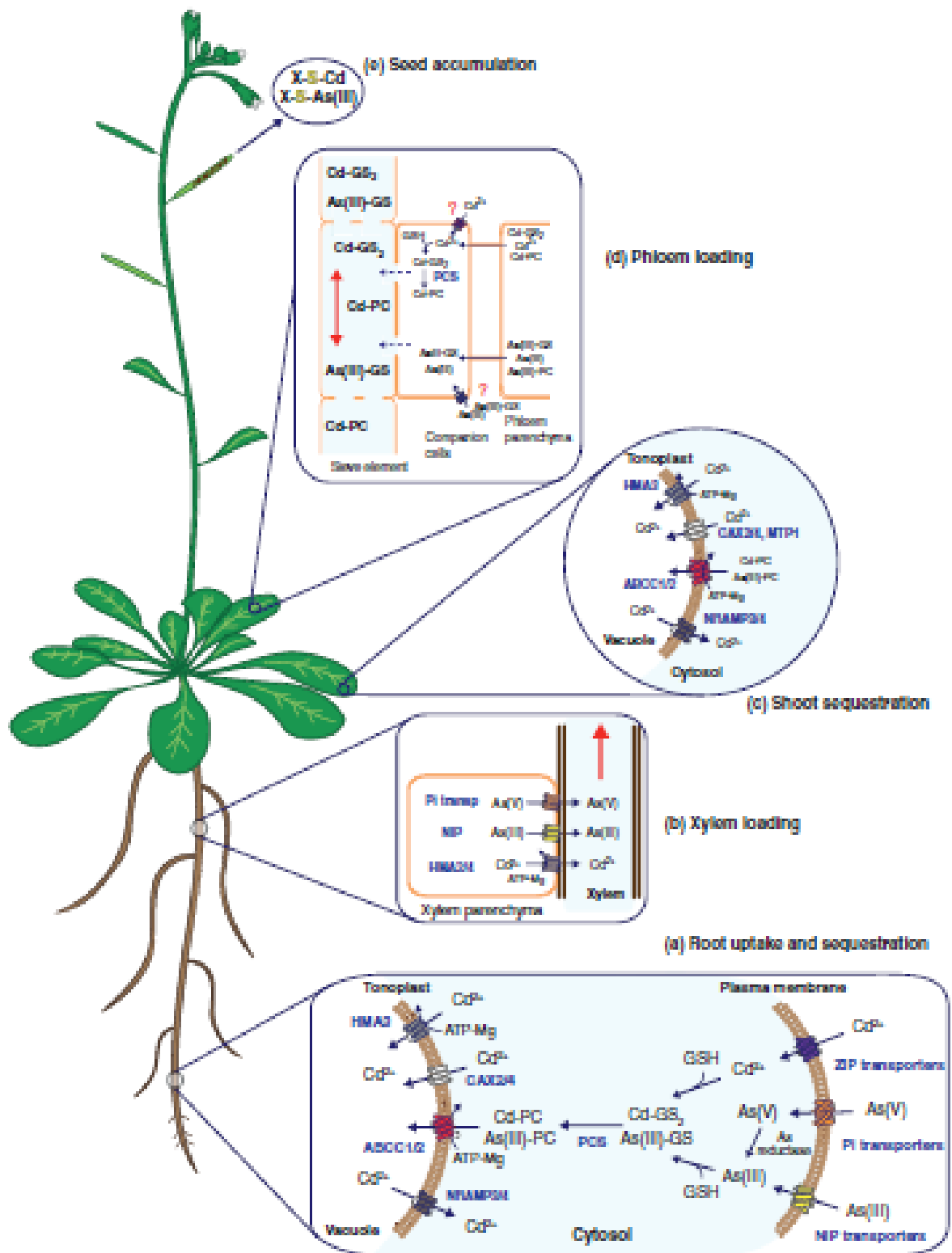


Figure 2.10: Schematic of uptake, translocation, and sequestration of cadmium, arsenate, and arsenite (image from Mendoza-Cozatal et al. 2011).

CHAPTER 3

INFLUENCE OF TiO₂ ENPS ON PHOTOSYNTHETIC EFFICACY

3.1 Introduction

Nanotechnology is developing rapidly into a trillion-dollar industry (Nel et al., 2006). Substantial amounts of engineered nanoparticles are expected to be released into the environment, both intentionally and unintentionally. A nanoparticle is described as a material with at least two dimensions between 1 and 100nm (American Society for Testing and Materials, 2006; Scientific Committee on Emerging and Newly Identified Health Risk, 2007). Of the metal oxide nanoparticles, TiO₂ ENPs is one of the most widely used and produced.

The reason TiO₂ is one of the most widely used nanoparticles is due to its UV absorption and photoactive properties. This photoactivity has been shown to make TiO₂ a photocatalyst, mediating oxidation-reduction reactions on the surface of the ENP (Dodd and Jha, 2011). The properties of TiO₂ ENPs have also prompted investigation of potential uses in agricultural settings, including use of it as a UV protectant, a defense against harmful bacteria and fungi, or a catalyst for the degradation of pesticides and herbicides (Ghormade et al., 2011; Gogos et al., 2012). However, TiO₂ ENPs have also been proposed for the use of a foliar spray to promote plant growth and yield (Choi et al., 2012).

In fact, the foliar application of TiO₂ ENPs have been shown to increase several aspects of the photosynthetic process in spinach (*Spinacia oleracea* L.), including Rubisco and Rubisco activase activity, chlorophyll synthesis, and oxygen evolution (Hong et al., 2005a; Hong et al., 2005b; Gao et al., 2006; Linglan et al., 2008). Moreover, Foliar application of TiO₂ ENPs on spinach resulted in a significant increase in plant fresh weight, dry weight, chlorophyll content,

net photosynthetic rate, and carboxylase activity of Rubisco (Linglan et al., 2008; Hong et al., 2005b; Gao et al., 2006; Gao et al., 2008; Su et al., 2007; Zheng et al., 2007; Zheng et al., 2008). However, the majority of these studies was conducted for short periods of time in a controlled environment, and in some cases used isolated chloroplasts instead of intact plants.

This study aims to focus on how effective TiO₂ ENPs may be at promoting photosynthesis when applied to *Z. mays* for the duration of five weeks under natural environment settings, as well as to determine if the increased photosynthesis results in an increase in seed quantity and/or quality.

3.2 Materials and Methods

3.2.1 Reagents and Plants

A dispersion of 5-15 nm anatase TiO₂ engineered nanoparticles (ENPs) with a purity of 99.9% were obtained from US Research Nanomaterials, Inc. (Houston, TX). Bulk TiO₂ was obtained from Fisher Scientific (Fair Lawn, NJ). Corn (*Zea mays* L. cv. Dekalb A1028584) seeds were obtained from Southern Illinois University College of Agriculture at SIUC. Scotts Osmocote 14-14-14 Slow Release Fertilizer was obtained from Hummert International (Earth City, MO).

3.2.2 Influence of TiO₂ ENPS on photosynthetic efficacy

Corn plants were grown over the summer of 2013 outside the Plant Biology Greenhouse at Southern Illinois University Carbondale. Corn seed was planted on June 18, 2013. Corn was grown in 18.9 L closed bottom pots with a drain hole on the side 5.5 cm from bottom of the pot.

Corn plants were grown in 4.95 kg of 3B Farfard potting mix (consisting of Canadian Sphagnum peat moss, processed pine bark, perlite, and vermiculite) and amended with a 14-14-14 Osmocote fertilizer at a rate of 5.25 g fertilizer kg⁻¹ substrate, yielding final concentrations of 0.4305 g NH₄⁺ kg⁻¹ DW soil, 0.3045 g NO₃ kg⁻¹ DW soil, 0.735 g P₂O₅ kg⁻¹ DW soil, 0.735 g K₂O kg⁻¹ DW soil. Three seeds were sown directly into the pots at a depth of 5 cm and were thinned to plant per pot one week after emergence. Plants received water from rainfall, and were supplemented as needed with tap water to ensure that the pots remained hydrated. The plants were grown for 45 days after sowing seeds until plants reached the R1 stage, at which time the desired treatments were imposed.

There were two different foliar treatment regimens for this experiment, a repeated treatment where a lower treatment concentration of TiO₂ was applied weekly for five weeks, and a single treatment, where a higher concentration of TiO₂ was applied in a single dose. These two treatment strategies were designed so that the final amount of the TiO₂ received by each plant was the same between pairs of repeated and single treatments. The repeated treatments consisted of two different concentrations of TiO₂ 500 and 1,000 mg L⁻¹, applied weekly over five weeks (i.e., total intended application was equivalent to 2,500 and 5,000 mg L⁻¹). The single treatments consisted of two treatments equaling the final concentration of the repeated treatments (2,500 and 5,000 mg L⁻¹). Treatments were applied using a fine mist sprayer; a single layer of the treatment was applied to the adaxial surface of each leaf. Since the treatment applications began after the onset of reproduction, there was no generation of new leaves during the treatment period. Corn plants received 50 ml of treatment for each application; with retention of approximately a 70% for each application. For each of the treatment regimen there were two forms of TiO₂: one being 5-15 nm TiO₂ ENPs and the other being bulk TiO₂ (greater than 100

nm). There were a total of 4 treatments per form (500 repeated, 1,000 repeated, 2,500 single, and 5,000 single) and two forms (ENP and bulk), as well as a control. Each treatment had five replicates, so there was a total of 45 corn plants total. The position of the pots was completely randomized weekly to ensure there were no positional effects.

Measurements of plant physiological performance were made with a CI-340 portable photosynthesis system (CID Bio-Science; Camas, WA) after the initiation of treatment. The physiological parameters measured with the CI-340 were photosynthetically active radiation ($\mu\text{mol photon m}^{-2} \text{s}^{-1}$), net photosynthesis ($\mu\text{mol CO}_2 \text{ m}^{-2} \text{s}^{-1}$), transpiration ($\text{mmol H}_2\text{O m}^{-2} \text{s}^{-1}$), stomatal conductance ($\text{mmol H}_2\text{O m}^{-2} \text{s}^{-1}$), and leaf temperature ($^{\circ}\text{C}$). The CI-340 measurements were taken on the V6 leaf twice per week, generally on Mondays and Fridays, between 8:00 A.M. and 12:00 P.M. using a chamber head with an area of 6.25 cm^2 and a gas flow rate of $0.3 \text{ liter min}^{-1}$. The instrument was allowed to warm up for 1 hour prior to taking the measurements. A Minolta Spad 502 (Konica Minolta, Inc.; Ramsey, NJ) chlorophyll meter was used to measure relative chlorophyll levels. The relative chlorophyll levels were collected on the V4, V6, and V8 leaves the values from the three leaves were averaged to obtain the relative chlorophyll for the whole plant. Relative chlorophyll was measured three times throughout the treatment period; 1, 16, and 25 days after treatment.

Once the plants reached reproductive maturity, the fruits were removed and allowed to air dry in a phytotron under ambient conditions. The shoot tissues were harvested above the second highest set of prop roots for corn. The vegetative tissues were cut into manageable pieces and placed into large paper bags. The tissues were placed in a dry, storage area in the greenhouse to dry under ambient conditions to constant mass. Once the fruits had dried, the husks and silks of the corn were removed and the fruits were removed from the cob. Yield parameters consisting of

total seed count, total seed weight, and weight per seed were collected. Seed quality for corn was measured with a Zeltex ZX-50 Grain Analyzer (Zeltex, Inc.; Hagerstown, Maryland) to determine the percent oil, protein, and moisture content. The Zeltex ZX-50 Grain Analyzer was calibrated and the grains were analyzed according to the manufacturer's protocol.

3.2.3 Data Analysis

Radiation use efficiency (RUE) was derived from data collected with the CI-340 portable photosynthesis system. Using the formula according to Ma et al. (2004):

$$RUE = \frac{Pn}{PAR} \times 1,000$$

In which Pn represents the Net Photosynthesis and PAR represents the Photosynthetically Active Radiation. The units for RUE are expressed as mmol CO₂ mol⁻¹ photon. Water Use Efficiency (WUE) was also derived from data collected with the CI-340 portable photosynthesis system using the formula according to Ma et al. (2004):

$$WUE = \frac{Pn}{E}$$

In which Pn represents the net photosynthesis and E represents evapotranspiration. The units for WUE are expressed as mmol CO₂ mol⁻¹ H₂O.

Data for each treatment were also expressed relative to the corresponding control to provide another means of expressing the treatment effects. The percent differences were calculated using the following formula:

$$\% \text{ Change} = \left(\frac{\text{measured value from treatment effect}}{\text{mean control value for treatment effect}} \times 100 \right) - 100$$

As there were no paired treatments in this experiment, data had to be expressed relative to the mean value of that parameter from control plants.

All data were subjected to a two-way analysis of variance (ANOVA) with repeated measures with the main effects of concentration and form compared using Tukey's honestly significant difference (HSD) using SPSS ver. 22. The repeated measure was time. For the parameters that showed a significant interaction term, the data were subjected to a one-way ANOVA and the interaction means were compared using the HSD of Tukey test at $p < 0.05$ using SAS 9.3 computer software.

3.3 Results

3.3.1 Meteorological Data

The average daily high temperature for the month of August in 2013 was 29.32 °C and the average low temperature was 17.81 °C. A sharp drop in temperature occurred on August 5, in which the highest temperature was 21.67 °C (7.65 °C less than the average). There was another drop in temperature on August 14 in which the temperature was 23.33 °C. After August 14, the temperature continuously increased until it plateaued at 34.44 °C. There was a total of 7.47 cm of precipitation throughout the month with the majority occurring on August 5, 8, and 9th (Figure 3.1).

3.3.2 Influence of TiO₂ on Photosynthetic Efficacy on *Z. mays*

The analysis of the net photosynthesis data showed that there was a significant interaction between the concentration and form of TiO₂ ($p=0.028$). While the foliar application of TiO₂ ENPs and bulk TiO₂ resulted in a substantial increase in net photosynthesis (Table 3.1), the subsequent one-way ANOVA of the interaction means revealed only the 5,000 mg L⁻¹ TiO₂ ENP

and bulk TiO₂ showed a significant increase on 1 DAT. The 5,000 mg L⁻¹ TiO₂ ENP was found to be significantly greater than all of the other treatments except for the 500 mg L⁻¹ TiO₂ ENP treatment and the 500, 2,500, and 5,000 mg L⁻¹ bulk TiO₂ treatments on 1 DAT. The 5,000 mg L⁻¹ bulk TiO₂ treatment was found to be significantly greater than the control, but was not significantly greater than any of the other treatments. There was no significant difference between any of the treatments on any of the days from 4 DAT to 29 DAT, showing that the increased net photosynthesis is a rather short lived transient response to the foliar application of TiO₂ (Figure 3.2).

To clarify the trends, the data were expressed as the percent difference relative to the control for each treatment and on each day measurements were made (Figure 3.2). On days when there were evident differences in the percent differences, the data were subjected to a one-way ANOVA for that individual day (Table 3.2). As mentioned before, there was a sharp increase in net photosynthesis on 1 DAT. On this day, the 5,000 mg L⁻¹ TiO₂ ENP showed an increase in net photosynthesis of 1,275.8% (Figure 3.2). This increase was found to be significantly greater than the 1,000 mg L⁻¹ bulk TiO₂ as well as the 1,000 and 2,500 mg L⁻¹ TiO₂ ENP treatments ($p=0.0038$; Table 3.2). However, it was not significantly greater than the remaining treatments, nor was there a significant difference found between any of the other treatments (Table 3.2). There were no significant differences found on any of the other days for net photosynthesis (Table 3.2).

In terms of internal leaf temperature, there was no significant difference found from the two-way ANOVA (Table 3.3). Even though there wasn't a significant difference, there was an increase in the leaf temperature compared to the control on 1 DAT. Yet, on all days after that the leaf temperature appears to be similar to or less than that of the control (Figure 3.3). The internal

leaf temperature followed the same trend as the net photosynthesis in terms of percent relative to the control on 1 DAT. On this day, the 5000 mg L⁻¹ TiO₂ ENP treatment showed the greatest increase in leaf temperature (22.1%) (Figure 3.3). This increase was significantly greater than the 1,000 mg L⁻¹ bulk TiO₂ treatment as well as the 1,000 and 2,500 mg L⁻¹ TiO₂ ENP treatments ($p=0.0020$), but was not significantly greater than any of the other treatments (Table 3.4). There were also no significant differences between any of the other treatments on 1 DAT (Table 3.4). On 4 DAT, the 500 mg L⁻¹ TiO₂ ENP, 1,000 mg L⁻¹ bulk TiO₂, and 2,500 mg L⁻¹ bulk TiO₂ were significantly greater than the 2,500 mg L⁻¹ TiO₂ ENP treatment ($p=0.0008$), but there was no significant differences found between any of the other treatments (Table 3.4). There were no other significant differences found for internal leaf temperature on any other days.

Stomatal conductance showed a significant difference for concentration ($p=0.002$), form ($p<0.0001$), and the interaction of concentration and form ($p=0.009$) for the two-way ANOVA with repeated measures. The one-way ANOVA performed on the interaction means showed that there was no significant difference between any of the treatments on 1, 18, and 25 DAT. There was a significant difference on all of the other days measurements were taken (Table 3.5). On 4 DAT, the 2,500 and 5,000 TiO₂ ENP treatments were significantly greater than all of the other treatments except the 5,000 bulk TiO₂ treatment ($p<0.0001$; Figure 3.4). The 5,000 mg L⁻¹ bulk TiO₂ treatment was less than the 2,500 and 5000 mg L⁻¹ TiO₂ treatments and greater than the 1,000 mg L⁻¹ TiO₂ ENP treatment but not to a significant extent; however, it was significantly greater than all of the other treatments (Table 3.5). On 8 DAT, the 2,500 mg L⁻¹ TiO₂ ENP was significantly greater than the 500 mg L⁻¹ TiO₂ ENP, 500 and 1,000 bulk TiO₂ treatments, and the control ($p=0.0032$); there was no other significant differences found between the rest of the treatments on this day (Table 3.5). On 12 DAT, the 1,000 and 5,000 mg L⁻¹ TiO₂ ENP

treatments were significantly greater than the control and all of the bulk TiO₂ treatments ($p < 0.0001$). The 2,500 mg L⁻¹ TiO₂ ENP treatment was significantly greater than the control and all of the bulk treatments except the 5,000 mg L⁻¹ bulk TiO₂ ($p < 0.0001$). The 500 mg L⁻¹ TiO₂ ENP treatment was significantly greater than the 500 mg L⁻¹ bulk TiO₂ and the control ($p < 0.0001$). None of the bulk TiO₂ treatments were found to be greater than the control on 12 DAT (Table 3.5). On 22 DAT, all treatments were significantly greater than the control except for the 500 and 2,500 mg L⁻¹ bulk TiO₂ treatment ($p = 0.0003$). On this day, the 2,500 mg L⁻¹ bulk TiO₂ treatment was found to be significantly less than the 5,000 mg L⁻¹ bulk TiO₂ treatment, but not any of the other treatments (Table 3.5). On 29 DAT, the 2,500 mg L⁻¹ TiO₂ ENP treatment was significantly greater than the 5,000 mg L⁻¹ TiO₂ ENP treatment, as well as the 1,000 and 2,500 mg L⁻¹ bulk TiO₂ treatments ($p = 0.0170$); there were no other significant differences found on this day (Table 3.5). When expressed as percent relative to the control, all of the data showed the exact same results in terms of significant differences for each day (Table 3.5; Table 3.7).

The two-way ANOVA with repeated measures showed that the TiO₂ ENP treatments had significantly higher transpiration rates than the control and the bulk TiO₂ ($p < 0.0001$), but there was no significant difference in response to concentration ($p = 0.608$). There was no significant interaction between concentration and form ($p = 0.356$). In terms of expressing the data as percent change relative to the control, there was an apparent spike in the transpiration rates for the 500 and 5,000 mg L⁻¹ TiO₂ ENP treatments on 1 DAT, but they were not found to be significantly greater than the other treatments due to a high variability about the mean (Figure 3.5; Table 3.8). However, on 4 DAT the 5,000 mg L⁻¹ TiO₂ ENP treatment was significantly greater than all of the treatments except the 2,500 mg L⁻¹ TiO₂ ENP and 5,000 mg L⁻¹ bulk TiO₂ treatments

($p < 0.0001$). The 2,500 mg L⁻¹ bulk TiO₂ was significantly less than the 5,000 mg L⁻¹ bulk TiO₂ but not the 2,500 mg L⁻¹ TiO₂ ENP treatment ($p < 0.0001$). The 500 and 1,000 mg L⁻¹ bulk TiO₂ treatments were found to be significantly less than all of the treatments except the 500 mg L⁻¹ TiO₂ ENP, 1,000 mg L⁻¹ TiO₂ ENP, and 2,500 mg L⁻¹ bulk TiO₂ treatments ($p < 0.0001$; Table 3.8). On 8 DAT, the 2,500 mg L⁻¹ TiO₂ ENP treatment was significantly greater than the 500 mg L⁻¹ TiO₂ ENP treatment ($p = 0.0309$), but there was no significant differences between any of the other treatments on this day (Table 3.8). There were no significant differences found between any of the treatments for any of the remaining days (Table 3.8).

In terms of water use efficiency (WUE) the two-way ANOVA with repeated measures, there was no significant difference found for concentration ($p = 0.632$), but there was a marginally significant difference for the form ($p = 0.051$). The interaction of concentration and form showed a significant difference ($p = 0.048$). However, the one-way ANOVA showed that there were no significant differences on any of the days except for 12 DAT, in which the control displayed a significantly greater WUE than the 1,000 and 2,500 mg L⁻¹ TiO₂ ENP treatments ($p = 0.0027$); there were no other significant differences between any of the other treatments for this day (Table 3.9).

When the WUE was expressed as a percent change relative to the control, there were no significant differences between any of the treatments for any of the days when measurements were recorded (Table 3.10). Even though there were no significant differences found, there was a clear increase in WUE on 1 DAT, in which the 5,000 mg L⁻¹ TiO₂ ENP and bulk TiO₂ treatments had a 404.2 and 394.5% increase (Figure 3.6). All of the other treatments showed an increase of about 200% except the 2,500 mg L⁻¹ TiO₂ ENP treatment which only had a 128.2% increase. One notable point is that there was a high variability about the mean on this day

(Figure 3.6). By 4 DAT, the WUE dropped to levels that were similar to, but often less than, the control and remained that way for the remainder of the experiment (Figure 3.6).

There were no significant differences found for the concentration ($p=0.397$), form ($p=0.646$), or the interaction ($p=0.946$) for radiation use efficiency (RUE) from the two-way ANOVA with repeated measures. However, a large increase in RUE was observed on 1 DAT, but by 4 DAT it dropped back down to levels that were similar to or less than that of the control (Figure 3.7). In terms of expressing the RUE as percent change relative to the control, there were no significant differences found on any of the days except for 12 DAT (Table 3.12). On 12 DAT, the 2,500 mg L⁻¹ bulk TiO₂ treatment was significantly greater than the 2,500 mg L⁻¹ TiO₂ treatment ($p=0.0675$). Even though there was no significant difference between the treatments on 1 DAT, there was still a noticeable increase in RUE for the treated plants (Figure 3.7). The 500 and 2,500 mg L⁻¹ TiO₂ ENP treatments as well as the 500 and 5,000 mg L⁻¹ bulk TiO₂ treatments all had an increased RUE that was 100% or greater compared to the control (Figure 3.7); and the other four treatments all showed increased RUE between the range of 25-90% (Figure 3.7), but there was a high amount a variability about the mean for most of the treatments.

There were no significant differences found for any of the parameters that were used to measure seed quantity and quality. A marginally significant difference was observed for the seed count and the total yield ($p=0.0565$; $p=0.0503$), however this difference was only between the 1,000 and 2,500 mg L⁻¹ bulk TiO₂ treatments.

3.4 Discussion

Previous studies have shown that TiO₂ ENPs have the capability to increase net photosynthetic rates and oxygen evolving rates in intact spinach plants as well as isolated

chloroplasts from spinach plants (Linglan et al., 2008; Gao et al., 2008; Zheng et al., 2005; Hong et al., 2005; Hong et al., 2005; Zheng et al., 2007; Su et al., 2007; Zheng et al., 2008). However, these experiments were mostly conducted for short periods of time in a controlled environment. The aim of this research was to determine how bulk TiO₂ and TiO₂ ENPs would affect various aspects of photosynthesis over a longer period of time in a natural environment.

An unexpected result in the data was that the response to the TiO₂ was transient for the majority of the parameters that were measured rather than a sustained increase in photosynthesis as observed in the studies mentioned above. The foliar application of TiO₂ ENPs resulted in a large increase in net photosynthesis at 1 DAT. This increase caused an increase in radiation use efficiency (RUE), water use efficiency (WUE), and internal leaf temperature. The increase in leaf temperature most likely led to the increased transpiration rates observed on that day. Interestingly, there was not an increase in stomatal conductance on 1 DAT, which might have been expected if the stomates had opened wider to allow for increased transpiration. However by 4 DAT, the net photosynthesis, RUE, WUE, and leaf temperature all dropped to levels that were equal to or less than that of the control, yet the stomatal conductance increased substantially at that time and remained at a higher rate throughout the remainder of the experiment. This resulted in an increased transpiration rate, which would have most likely have been higher if the humidity wasn't so high during this time frame.

Under a light intensity of 1,000-2,000 $\mu\text{mol m}^{-2} \text{s}^{-1}$, the average net photosynthetic rate of corn is generally in the range of 18-30 $\mu\text{mol CO}_2 \text{m}^{-2} \text{s}^{-1}$ (Leakey et al., 2006; Sun et al., 2012). Under lower light intensities of 500-1,000 $\mu\text{mol m}^{-2} \text{s}^{-1}$ the average net photosynthetic rate of corn is generally 10-20 $\mu\text{mol CO}_2 \text{m}^{-2} \text{s}^{-1}$ (Leakey et al., 2006; Sun et al., 2012). Under light intensities less than 500 $\mu\text{mol m}^{-2} \text{s}^{-1}$, the net photosynthetic rate is usually less than 10 μmol

$\text{CO}_2 \text{ m}^{-2} \text{ s}^{-1}$ (Leakey et al., 2006; Sun et al., 2012). It appears that under low light conditions, the TiO_2 ENPs boost the net photosynthesis and RUE in corn, but under high light conditions it causes a reduction in net photosynthesis and RUE.

The findings of this study coincide with that of a study performed with *Ulmus elongata*, in which the tree saplings were sprayed with 0.1%, 0.2%, and 0.4% (1,000 mg L^{-1} , 2,000 mg L^{-1} , and 4,000 mg L^{-1} TiO_2 ENPs) at the beginning of the month for two months. After the second month photosynthetic measurements were taken with a Li-6400XT portable photosynthesis system using two light intensities ($\text{PAR} = 800 \mu\text{mol m}^{-2} \text{ s}^{-1}$ and $\text{PAR} = 1,600 \mu\text{mol m}^{-2} \text{ s}^{-1}$). Under the lower light intensity, the net photosynthetic rate was slightly increased for the 0.2% TiO_2 ENP treatment, but under the high light intensity the net photosynthetic rate was decreased for all three treatments and the 0.2% and 0.4% TiO_2 ENP treatments dropped to about 1/3 that of the control. Furthermore, under both light conditions, the stomatal conductance rate was increased for all three treatments with the 0.2% and 0.4% TiO_2 ENPs showing an increase that was about three times that of the control. Similarly, the transpiration rates for both light conditions were increased for both light conditions with the 0.2% and 0.4% TiO_2 ENP treatments showing an increase that was about two times that of the control (Gao et al., 2013). Since this experiment was conducted in natural field conditions where the PAR is generally greater than $1,000 \mu\text{mol m}^{-2} \text{ s}^{-1}$ and the concentrations of TiO_2 ENPs were similar, it would make sense for the results to coincide with the results reported by Goa et al. (2013) for the treated plants under high light intensities.

A possibility for the decreased photosynthetic rates could be attributed to the capabilities of TiO_2 ENPs to physisorb N_2 on its surface. While pure TiO_2 ENPs have been shown to absorb UV light, TiO_2 ENPs that have been doped with N_2 have been observed to shift their

absorption spectra to allow them to absorb light in the 450-550 nm range. Since the atmosphere is comprised of about 78% N₂ gas, it is easy to speculate that this could easily be adsorbed to the surface of the TiO₂ ENPs that cover the abaxial side of the leaf in this experiment; and this sorption may have resulted in a shift in the absorption spectrum of the TiO₂ ENPs; which may have led to the decreased photosynthetic rate by screening out the higher light intensities used for photosynthesis. In fact, past research has shown that chlorophyll fluorescence and electron transport rates were decreased for *Ulmus elongata* saplings that were treated with TiO₂ ENPs suggesting that the TiO₂ ENPs may be absorbing PAR, thus reducing the amount of PAR that would be available for photosynthesis (Gao et al., 2013).

Since the TiO₂ treatments were only applied to the adaxial side of the leaves and the stomata are located on the abaxial side of the leaf it is unlikely that the TiO₂ is having a direct effect on stomatal opening. However, the TiO₂ could potentially have an effect on the leaf's ability to diffuse heat via sensible heat loss. If this is the case, the increased stomatal conductance could be explained as a measure to cope with the lack of sensible heat loss. By increasing the stomatal conductance (increasing the stomatal aperture) the plant would diffuse excess heat through evaporative cooling (transpiration). In fact this phenomenon was observed in this experiment. As the stomatal conductance was increased at 4 DAT, the transpiration rates increased as well, which appears to have reduced the leaf temperature to levels that were similar to, but often times less, than that of the control plants.

Another possible explanation of the data could be that the TiO₂ is absorbing short wavelength light and fluoresce a shorter wave length light. This would allow for a greater amount of photosynthetically active radiation (PAR) at the leaf surface. The increased PAR could explain why there was a sharp increase in net photosynthesis and RUE as well as why it

decreased shortly after the exposure to the TiO₂. The decrease that was observed by 4 DAT could be a result of photoinhibition caused by an increased bombardment of PAR on PSII. However, this would not explain the increased stomatal conductance and transpiration that was observed from 4 DAT to the end of the experiment.

The increased conductance and transpiration may have resulted from another phenomenon that has been observed with TiO₂, in which it can catalyze the breakdown of organic compounds. If the TiO₂ caused the deterioration of the leaf cuticle, it may have allowed for an increase in non-stomatal gas exchange on the adaxial surface of the leaf. This could have made it appear that there was an increased stomatal conductance and transpiration rates, when there could have just been a greater gas exchange on the adaxial surface of the leaves.

The increase in net photosynthesis did not appear to be substantial enough (nor sustained long enough) for it to result in an increase in seed quantity or quality. However, recent studies have shown that the application of a solution containing 25 ppm TiO₂ ENPs (15-25 nm) resulted in an increased yield in rice and corn plants grown in an agricultural field (Choi et al., 2012). Similar results were observed for cowpea (Owolade et al., 2008) and wheat (Jaberzadeh et al., 2013). Jaberzadeh et al., (2013) reported that if the TiO₂ ENPs exceeded 0.02% (back calculated to 200 mg L⁻¹) it resulted in decreased growth and production of wheat plants. This indicates that there is likely a species specific concentration for the benefits of TiO₂ ENPs in relation to photosynthesis and the current experiment may have exceeded the maximum concentration of TiO₂ ENPs for corn. While the use of TiO₂ ENPs has been proposed for agriculture, the data from this research suggests that it is not a feasible means for increasing crop yield in corn, which contradicts that of previous research.

However, it may be a useful tool for enhancing the degradation of herbicides and pesticides because of its photocatalytic properties. On the other hand, exposure of TiO₂ ENPs to plant roots has shown some negative effects on growth and development, but this is mostly attributed to a reduction in hydraulic conductance caused by the TiO₂ ENPs physically blocking the root pores (Asli et al. 2009). Furthermore, TiO₂ ENPs have been shown to be harmful to both terrestrial and aquatic microorganisms (Ge et al., 2011; Fan et al., 2011; Clement et al., 2013), thus potentially negating the potential benefits of it. Since TiO₂ ENPs are toxic to microorganisms in a non-discriminant manner, the potential for loss of beneficial microorganisms is great. Furthermore, TiO₂ ENPs would likely have an extremely long residence time in these systems due to the fact that they are very stable. This could lead to a compounding concentration increase of TiO₂ ENPs from both the foliar spray and the crop residues as annual inputs for TiO₂ ENPs.

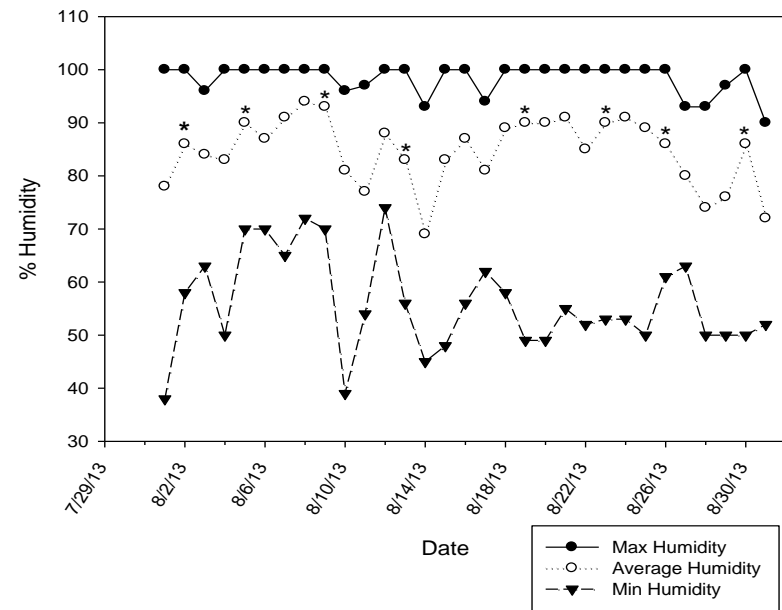
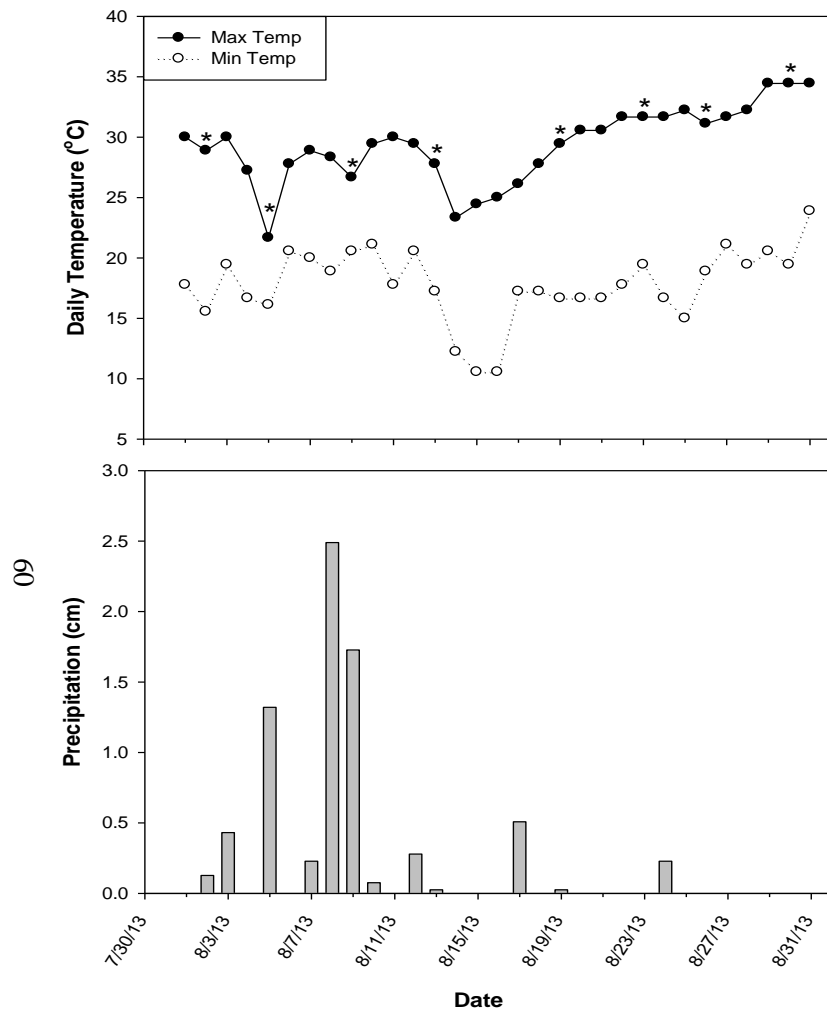


Figure 3.1: Daily temperature, precipitation, and percent humidity for the time span of the treatment and physiological parameter measurements. The data was extracted from Weather Underground (www.wunderground.com). The asterisks represent days when measurements were taken with the CI-340 portable photosynthesis system.

Table 3.1: Net photosynthesis rates ($\mu\text{mol CO}_2 \text{ m}^{-2} \text{ s}^{-1}$) \pm standard error for *Z. mays* treated weekly for five weeks with 500 and 1,000 mg L^{-1} TiO_2 ENPs and bulk TiO_2 , and single bolus 2,500 and 5,000 mg L^{-1} TiO_2 ENPs and bulk TiO_2 . Lettering indicates honestly significant difference (HSD) of Tukey test ($p < 0.05$) ($n=5$).

Net Photosynthesis								
Days After Treatment	1	4	8	12	18	22	25	29
Control	1.9 \pm 0.6 ^c	9.2 \pm 2.9	15.6 \pm 2.9	20.9 \pm 2.6	21.3 \pm 7.0	13.7 \pm 4.6	24.4 \pm 2.9	24.9 \pm 2.5
500 mg L^{-1} ENP	14.1 \pm 4.2 ^{abc}	9.3 \pm 4.7	13.8 \pm 2.1	16.3 \pm 3.4	19.5 \pm 3.0	7.7 \pm 1.5	21.6 \pm 1.8	17.0 \pm 3.2
1,000 mg L^{-1} ENP	6.7 \pm 2.0 ^{bc}	5.3 \pm 0.6	11.5 \pm 1.6	11.7 \pm 3.2	18.8 \pm 4.5	9.2 \pm 1.3	13.5 \pm 0.7	18.2 \pm 3.8
2,500 mg L^{-1} ENP	6.2 \pm 1.4 ^{bc}	4.5 \pm 0.7	16.8 \pm 2.0	14.0 \pm 1.0	9.9 \pm 1.7	12.3 \pm 2.8	13.6 \pm 1.6	17.1 \pm 2.1
5,000 mg L^{-1} ENP	26.1 \pm 3.6 ^a	10.3 \pm 1.4	14.5 \pm 2.4	13.5 \pm 1.5	14.6 \pm 3.5	11.7 \pm 2.2	18.0 \pm 2.7	15.3 \pm 2.7
500 mg L^{-1} Bulk	11.5 \pm 4.0 ^{abc}	4.5 \pm 0.7	14.7 \pm 1.0	15.7 \pm 2.9	14.9 \pm 4.0	7.7 \pm 0.5	14.8 \pm 2.4	16.0 \pm 3.9
1,000 mg L^{-1} Bulk	3.3 \pm 1.3 ^{bc}	5.7 \pm 1.0	13.3 \pm 2.3	16.3 \pm 2.0	23.0 \pm 2.5	8.3 \pm 0.8	26.6 \pm 8.0	15.6 \pm 2.9
2,500 mg L^{-1} Bulk	13.8 \pm 5.7 ^{abc}	7.7 \pm 0.4	15.3 \pm 2.2	14.7 \pm 2.6	17.8 \pm 3.8	7.3 \pm 2.7	16.6 \pm 2.6	18.5 \pm 1.4
5,000 mg L^{-1} Bulk	19.3 \pm 5.5 ^{ab}	5.9 \pm 1.8	16.4 \pm 1.0	13.7 \pm 1.4	21.1 \pm 4.3	5.3 \pm 1.6	15.3 \pm 3.0	14.0 \pm 4.2

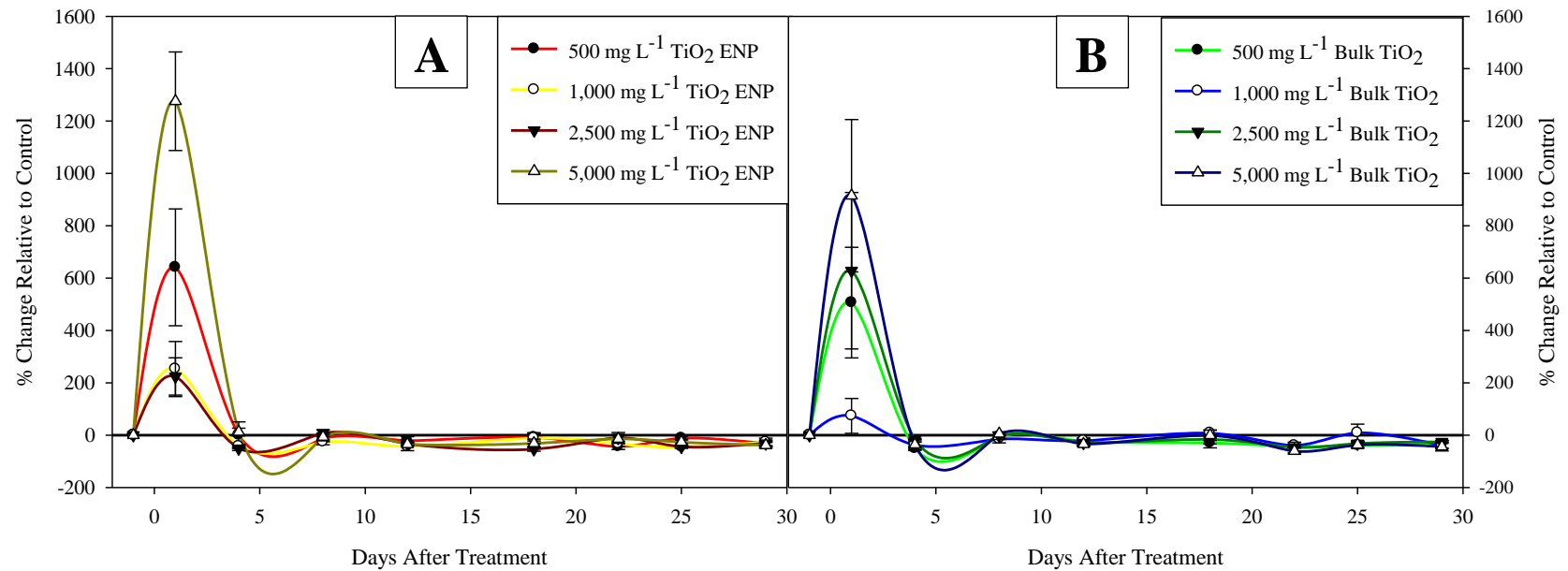


Figure 3.2: Percent change in net photosynthesis relative to the control across the time frame of the experiment for *Z. mays* which received foliar application treatment of (A) TiO₂ ENPs and (B) bulk TiO₂ at concentrations of 500, 1000, 2,500 and 5,000 mg L⁻¹. Bars represent standard error (n=5).

Table 3.2: Post hoc multiple comparison results for the percent difference data for net photosynthesis by *Z. mays*. Letters indicates honestly significant difference (HSD) of Tukey test (n=5).

Days After Treatment	1	4	8	12	18	22	25	29
500 mg L ⁻¹ ENP	AB	A	A	A	A	A	A	A
1,000 mg L ⁻¹ ENP	B	A	A	A	A	A	A	A
2,500 mg L ⁻¹ ENP	B	A	A	A	A	A	A	A
5,000 mg L ⁻¹ ENP	A	A	A	A	A	A	A	A
500 mg L ⁻¹ Bulk	AB	A	A	A	A	A	A	A
1,000 mg L ⁻¹ Bulk	B	A	A	A	A	A	A	A
2,500 mg L ⁻¹ Bulk	AB	A	A	A	A	A	A	A
5,000 mg L ⁻¹ Bulk	AB	A	A	A	A	A	A	A
P Value	<i>p</i> =0.0038	<i>p</i> =0.2820	<i>p</i> =0.5852	<i>p</i> =0.8762	<i>p</i> =0.2393	<i>p</i> =0.1793	<i>p</i> =0.1565	<i>p</i> =0.9741

Table 3.3: Internal leaf temperature ($^{\circ}\text{C}$) \pm standard error for *Z. mays* treated weekly for five weeks with 500 and 1,000 mg L^{-1} TiO_2 ENPs and bulk TiO_2 , and single bolus 2,500 and 5,000 mg L^{-1} TiO_2 ENPs and bulk TiO_2 . Lettering indicates honestly significant difference (HSD) of Tukey test ($p < 0.05$) ($n=5$).

Internal Leaf Temperature								
Days after Treatment	1	4	8	12	18	22	25	29
Control	28.60 \pm 0.05	24.68 \pm 0.05	70.18 \pm 0.85	31.10 \pm 1.02	33.36 \pm 2.00	31.82 \pm 0.57	35.16 \pm 1.08	39.16 \pm 0.83
500 mg L^{-1} ENP	31.72 \pm 0.70	24.94 \pm 0.27	69.18 \pm 0.77	30.36 \pm 1.74	32.86 \pm 1.86	30.48 \pm 0.32	35.60 \pm 0.90	38.64 \pm 1.02
1,000 mg L^{-1} ENP	30.22 \pm 0.54	24.24 \pm 0.12	70.38 \pm 0.88	29.06 \pm 1.79	33.42 \pm 1.65	31.08 \pm 0.33	34.20 \pm 0.90	38.36 \pm 1.27
2,500 mg L^{-1} ENP	29.68 \pm 0.38	23.84 \pm 0.07	70.66 \pm 0.35	30.84 \pm 1.08	30.54 \pm 1.57	30.90 \pm 0.60	33.62 \pm 0.53	38.78 \pm 0.41
5,000 mg L^{-1} ENP	34.92 \pm 0.77	24.66 \pm 0.09	69.94 \pm 0.42	27.00 \pm 1.32	33.74 \pm 1.58	31.36 \pm 0.26	35.22 \pm 0.74	36.64 \pm 1.39
500 mg L^{-1} Bulk	31.92 \pm 0.92	24.92 \pm 0.26	70.16 \pm 0.80	30.28 \pm 1.49	33.22 \pm 1.45	31.00 \pm 0.28	34.52 \pm 1.30	39.00 \pm 1.01
1,000 mg L^{-1} Bulk	30.64 \pm 0.40	24.74 \pm 0.24	70.98 \pm 0.41	29.10 \pm 2.03	31.86 \pm 1.57	30.78 \pm 0.31	36.18 \pm 0.88	37.28 \pm 1.34
2,500 mg L^{-1} Bulk	32.64 \pm 1.25	25.10 \pm 0.22	70.40 \pm 0.69	28.58 \pm 1.49	31.34 \pm 1.60	30.82 \pm 0.32	35.24 \pm 0.35	38.70 \pm 1.27
5,000 mg L^{-1} Bulk	32.08 \pm 0.98	24.20 \pm 0.20	69.40 \pm 1.03	29.54 \pm 2.31	34.70 \pm 0.98	30.60 \pm 0.47	34.76 \pm 1.31	38.44 \pm 0.99

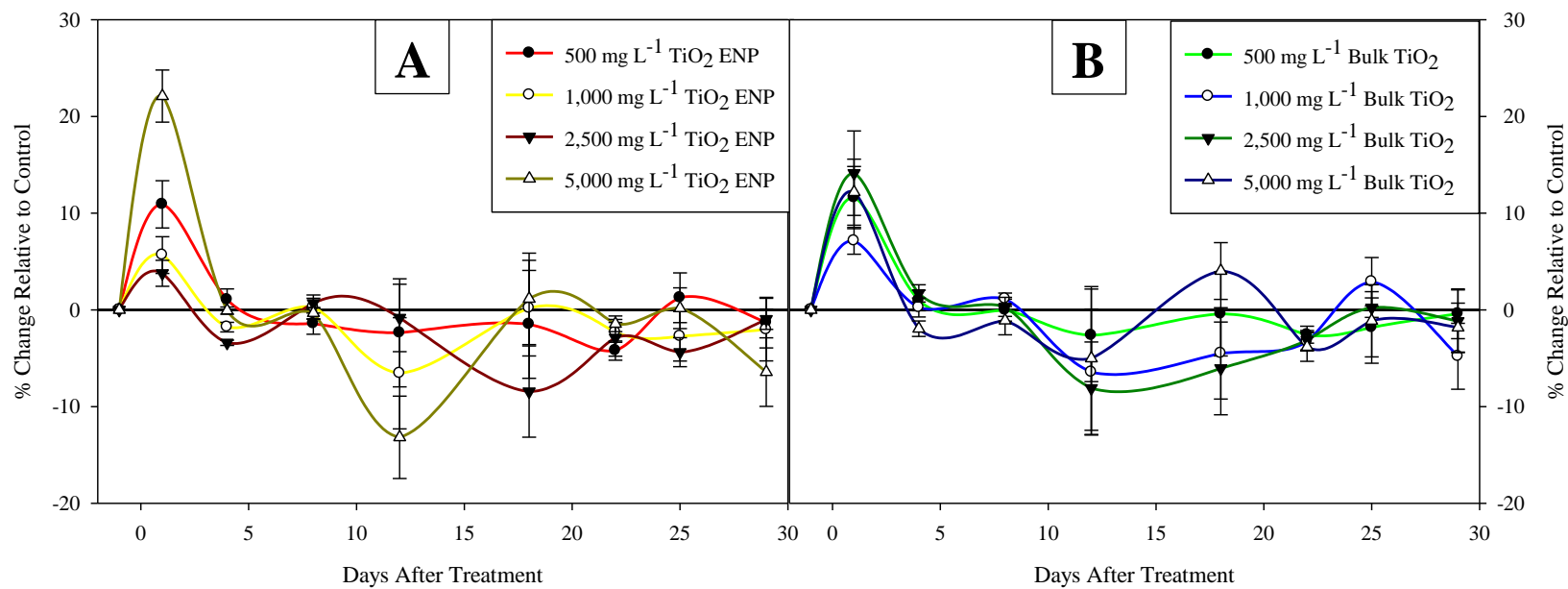


Figure 3.3: Percent change in internal leaf temperature relative to the control across the time frame of the experiment for *Z. mays* which received foliar application treatment of (A) TiO₂ ENPs and (B) bulk TiO₂ at concentrations of 500, 1000, 2,500 and 5,000 mg L⁻¹. Bars represent standard error (n=5).

Table 3.4: Post hoc multiple comparison results for the percent difference data for internal leaf temperature by *Z. mays*. Letters indicates honestly significant difference (HSD) of Tukey test (n=5).

Days After Treatment	1	4	8	12	18	22	25	29
500 mg L ⁻¹ ENP	AB	A	A	A	A	A	A	A
1,000 mg L ⁻¹ ENP	B	AB	A	A	A	A	A	A
2,500 mg L ⁻¹ ENP	B	B	A	A	A	A	A	A
5,000 mg L ⁻¹ ENP	A	AB	A	A	A	A	A	A
500 mg L ⁻¹ Bulk	AB	A	A	A	A	A	A	A
1,000 mg L ⁻¹ Bulk	B	AB	A	A	A	A	A	A
2,500 mg L ⁻¹ Bulk	AB	A	A	A	A	A	A	A
5,000 mg L ⁻¹ Bulk	AB	AB	A	A	A	A	A	A
P Value	<i>p</i> =0.0020	<i>p</i> =0.0008	<i>p</i> =0.6367	<i>p</i> =0.8151	<i>p</i> =0.6092	<i>p</i> =0.7981	<i>p</i> =0.6069	<i>p</i> =0.7985

Table 3.5: Stomatal conductance rates ($\text{mmol CO}_2 \text{ m}^{-2} \text{ s}^{-1}$) \pm standard error for *Z. mays* treated weekly for five weeks with 500 and 1,000 mg L^{-1} TiO_2 ENPs and bulk TiO_2 , and single bolus 2,500 and 5,000 mg L^{-1} TiO_2 ENPs and bulk TiO_2 . Lettering indicates honestly significant difference (HSD) of Tukey test ($p < 0.05$) ($n = 5$).

Stomatal Conductance								
Days after Treatment	1	4	8	12	18	22	25	29
Control	78.8 \pm 7.3	138.2 \pm 16.6 ^c	7.4 \pm 0.4 ^b	135.2 \pm 9.6 ^d	177.4 \pm 36.7	159.4 \pm 43.1 ^c	180.2 \pm 28.4	157.6 \pm 50.2 ^{ab}
500 mg L^{-1} ENP	107.2 \pm 23.1	172.4 \pm 18.9 ^c	6.9 \pm 0.5 ^b	372.4 \pm 24.5 ^{abc}	384.0 \pm 46.3	403.8 \pm 57.7 ^{ab}	305.0 \pm 41.7	302.4 \pm 92.4 ^{ab}
1,000 mg L^{-1} ENP	108.2 \pm 32.8	279.4 \pm 64.5 ^{bc}	9.1 \pm 0.7 ^{ab}	460.0 \pm 17.0 ^a	329.4 \pm 39.9	420.4 \pm 42.4 ^{ab}	316.0 \pm 35.0	242.7 \pm 80.2 ^{ab}
2,500 mg L^{-1} ENP	106.4 \pm 18.8	556.8 \pm 57.7 ^a	11.2 \pm 0.5 ^a	447.8 \pm 28.6 ^{ab}	389.4 \pm 62.3	381.8 \pm 61.9 ^{ab}	331.0 \pm 30.4	443.4 \pm 8.8 ^a
5,000 mg L^{-1} ENP	112.2 \pm 18.9	507.4 \pm 46.3 ^a	9.9 \pm 0.5 ^{ab}	520.2 \pm 34.1 ^a	382.7 \pm 99.3	421.6 \pm 20.6 ^{ab}	324.0 \pm 60.8	137.0 \pm 33.8 ^b
500 mg L^{-1} Bulk	59.8 \pm 23.1	152.4 \pm 21.2 ^c	7.4 \pm 0.7 ^b	150.4 \pm 12.8 ^d	174.4 \pm 47.3	291.8 \pm 21.5 ^{abc}	161.2 \pm 45.4	201.6 \pm 52.4 ^{ab}
1,000 mg L^{-1} Bulk	44.4 \pm 7.6	164.2 \pm 6.4 ^c	6.8 \pm 0.8 ^b	265.0 \pm 47.4 ^{cd}	245.8 \pm 26.5	385.4 \pm 36.3 ^{ab}	237.8 \pm 32.4	127.4 \pm 52.6 ^b
2,500 mg L^{-1} Bulk	72.2 \pm 9.6	173.6 \pm 10.9 ^c	9.2 \pm 1.0 ^{ab}	216.4 \pm 32.0 ^{cd}	230.4 \pm 75.2	225.8 \pm 46.5 ^{bc}	212.8 \pm 42.1	147.0 \pm 72.2 ^b
5,000 mg L^{-1} Bulk	75.4 \pm 28.6	423.2 \pm 95.8 ^{ab}	9.0 \pm 1.4 ^{ab}	291.2 \pm 66.4 ^{bcd}	311.6 \pm 72.8	434.2 \pm 48.1 ^a	283.8 \pm 48.8	153.0 \pm 74.7 ^{ab}

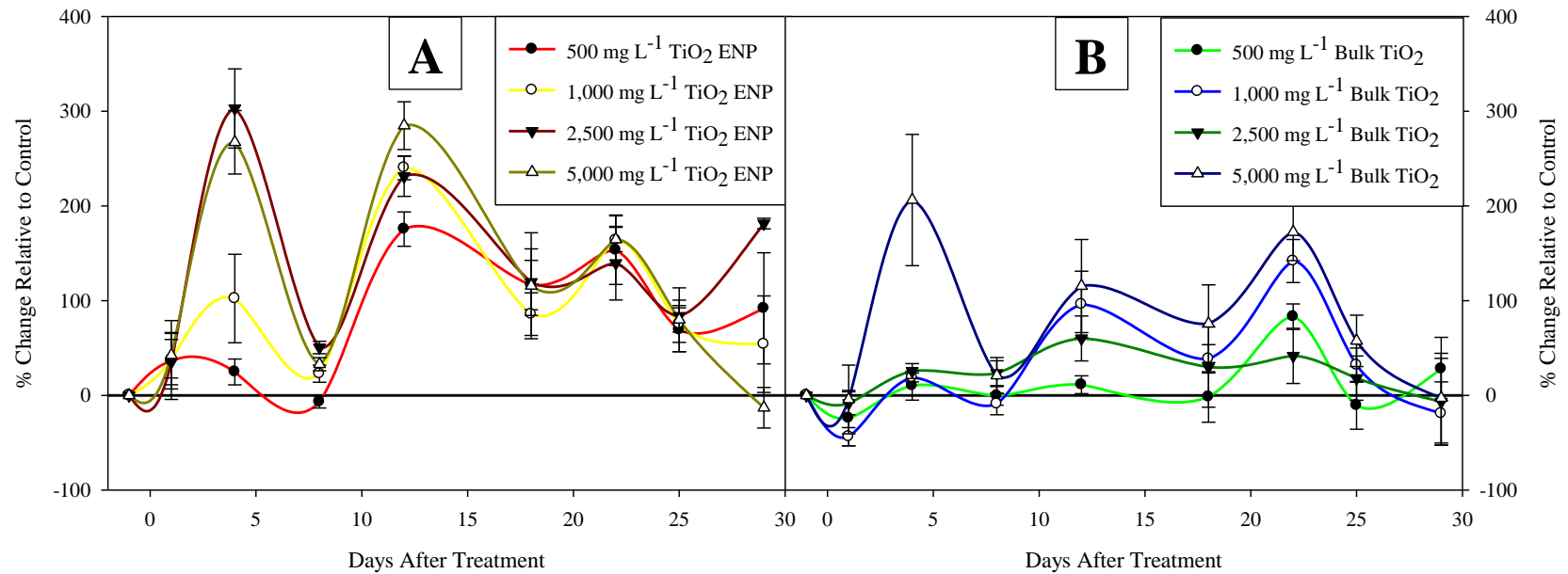


Figure 3.4: Percent change in stomatal conductance relative to the control across the time frame of the experiment for *Z. mays* which received foliar application treatment of (A) TiO₂ ENPs and (B) bulk TiO₂ at concentrations of 500, 1000, 2,500 and 5,000 mg L⁻¹. Bars represent standard error (n=5).

Table 3.6: Post hoc multiple comparison results for the percent difference data for stomatal conductance by *Z. mays*. Letters indicates honestly significant difference (HSD) of Tukey test (n=5).

Days After Treatment	1	4	8	12	18	22	25	29
500 mg L ⁻¹ ENP	A	C	B	ABC	A	AB	A	AB
1,000 mg L ⁻¹ ENP	A	BC	AB	A	A	AB	A	AB
2,500 mg L ⁻¹ ENP	A	A	A	AB	A	AB	A	A
5,000 mg L ⁻¹ ENP	A	A	AB	A	A	AB	A	B
500 mg L ⁻¹ Bulk	A	C	B	D	A	AB	A	AB
1,000 mg L ⁻¹ Bulk	A	C	B	CD	A	AB	A	B
2,500 mg L ⁻¹ Bulk	A	C	AB	CD	A	B	A	B
5,000 mg L ⁻¹ Bulk	A	AB	AB	BCD	A	A	A	AB
P Value	$p=0.2298$	$p<0.0001$	$p=0.0060$	$p<0.0001$	$p=0.1488$	$p=0.0231$	$p=0.0825$	$p=0.0178$

Table 3.7: Transpiration rates ($\text{mmol H}_2\text{O m}^{-2} \text{s}^{-1}$) \pm standard error for *Z. mays* treated weekly for five weeks with 500 and 1,000 mg L^{-1} TiO_2 ENPs and bulk TiO_2 , and single bolus 2,500 and 5,000 mg L^{-1} TiO_2 ENPs and bulk TiO_2 . Lettering indicates honestly significant difference (HSD) of Tukey test ($p < 0.05$) ($n=5$).

Transpiration								
Days After Treatment	1	4	8	12	18	22	25	29
Control	0.88 \pm 0.08	0.96 \pm 0.14	2.08 \pm 0.18	2.36 \pm 0.34	2.92 \pm 0.85	1.88 \pm 0.56	3.10 \pm 0.61	4.06 \pm 1.27
500 mg L^{-1} ENP	1.90 \pm 0.46	1.22 \pm 0.17	1.82 \pm 0.15	3.84 \pm 0.61	3.98 \pm 0.70	2.50 \pm 0.27	4.28 \pm 0.58	5.62 \pm 1.62
1,000 mg L^{-1} ENP	1.16 \pm 0.20	1.30 \pm 0.11	2.62 \pm 0.27	3.70 \pm 0.73	3.94 \pm 0.75	2.70 \pm 0.24	3.88 \pm 0.50	4.90 \pm 1.47
2,500 mg L^{-1} ENP	1.26 \pm 0.16	1.72 \pm 0.06	3.26 \pm 0.16	4.22 \pm 0.40	3.16 \pm 0.81	2.60 \pm 0.45	3.46 \pm 0.27	7.52 \pm 0.42
5,000 mg L^{-1} ENP	2.46 \pm 0.46	2.04 \pm 0.17	2.70 \pm 0.13	3.34 \pm 0.43	3.24 \pm 0.87	2.94 \pm 0.15	4.14 \pm 0.65	3.10 \pm 0.78
500 mg L^{-1} Bulk	1.12 \pm 0.50	1.02 \pm 0.11	2.08 \pm 0.26	2.34 \pm 0.38	2.68 \pm 0.73	2.38 \pm 0.20	2.66 \pm 0.83	4.70 \pm 1.18
1,000 mg L^{-1} Bulk	0.72 \pm 0.12	1.10 \pm 0.07	1.94 \pm 0.28	2.98 \pm 0.39	2.92 \pm 0.61	2.70 \pm 0.13	4.06 \pm 0.54	2.96 \pm 1.18
2,500 mg L^{-1} Bulk	1.44 \pm 0.31	1.20 \pm 0.09	2.66 \pm 0.41	2.58 \pm 0.55	2.60 \pm 0.89	2.10 \pm 0.25	3.21 \pm 0.56	3.66 \pm 1.70
5,000 mg L^{-1} Bulk	1.28 \pm 0.56	1.86 \pm 0.21	2.52 \pm 0.49	3.20 \pm 0.82	3.70 \pm 0.56	2.56 \pm 0.15	3.72 \pm 0.26	3.56 \pm 1.66

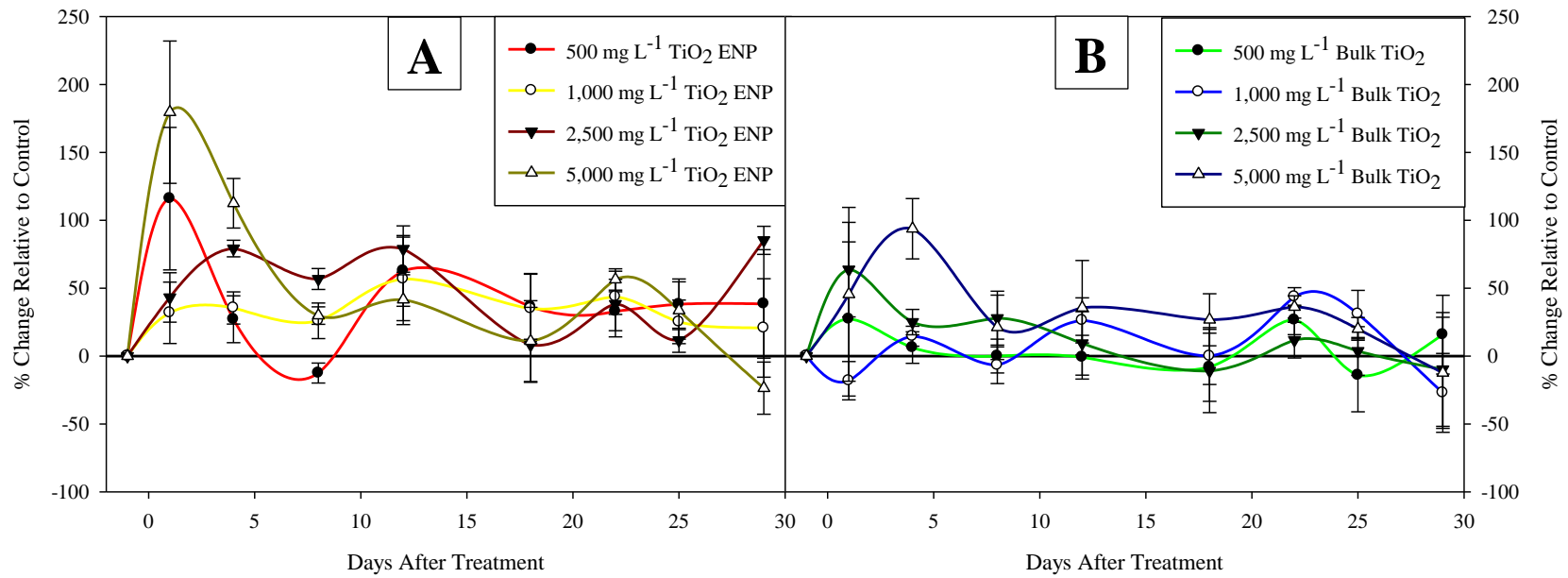


Figure 3.5: Percent change in transpiration relative to the control across the time frame of the experiment for *Z. mays* which received foliar application treatment of (A) TiO₂ ENPs and (B) bulk TiO₂ at concentrations of 500, 1000, 2,500 and 5,000 mg L⁻¹. Bars represent standard error (n=5).

Table 3.8: Post hoc multiple comparison results for the percent difference data for transpiration by *Z. mays*. Letters indicates honestly significant difference (HSD) of Tukey test (n=5).

Days After Treatment	1	4	8	12	18	22	25	29
500 mg L ⁻¹ ENP	A	CD	B	A	A	A	A	A
1,000 mg L ⁻¹ ENP	A	BCD	AB	A	A	A	A	A
2,500 mg L ⁻¹ ENP	A	ABC	A	A	A	A	A	A
5,000 mg L ⁻¹ ENP	A	A	AB	A	A	A	A	A
500 mg L ⁻¹ Bulk	A	D	AB	A	A	A	A	A
1,000 mg L ⁻¹ Bulk	A	D	AB	A	A	A	A	A
2,500 mg L ⁻¹ Bulk	A	CD	AB	A	A	A	A	A
5,000 mg L ⁻¹ Bulk	A	AB	AB	A	A	A	A	A
P Value	<i>p</i> =0.0915	<i>p</i> <0.0001	<i>p</i> =0.0309	<i>p</i> =0.2878	<i>p</i> =0.8074	<i>p</i> =0.4586	<i>p</i> =0.4722	<i>p</i> =0.2617

Table 3.9: Water Use Efficiency ($\text{mmol CO}_2 \text{ mol}^{-1} \text{ H}_2\text{O}$) \pm standard error for *Z. mays* treated weekly for five weeks with 500 and 1,000 mg L^{-1} TiO_2 ENPs and bulk TiO_2 , and single bolus 2,500 and 5,000 mg L^{-1} TiO_2 ENPs and bulk TiO_2 . Lettering indicates honestly significant difference (HSD) of Tukey test ($p < 0.05$) ($n=5$).

Water Use Efficiency								
Days after Treatment	1	4	8	12	18	22	25	29
Control	2.4 \pm 0.8	13.0 \pm 6.0	7.3 \pm 0.9	9.1 \pm 0.8 ^a	6.8 \pm 1.3	5.8 \pm 1.0	8.4 \pm 0.7	5.8 \pm 0.9
500 mg L^{-1} ENP	7.1 \pm 0.9	10.9 \pm 7.2	7.4 \pm 0.8	4.3 \pm 0.7 ^{ab}	5.0 \pm 0.5	3.1 \pm 0.6	5.3 \pm 0.6	9.3 \pm 6.8
1,000 mg L^{-1} ENP	6.9 \pm 2.5	4.2 \pm 0.7	4.3 \pm 0.3	3.3 \pm 0.8 ^b	5.4 \pm 1.6	3.7 \pm 0.8	3.8 \pm 0.6	3.8 \pm 0.7
2,500 mg L^{-1} ENP	5.4 \pm 1.5	2.7 \pm 0.5	5.1 \pm 0.4	3.4 \pm 0.2 ^b	3.4 \pm 0.6	5.2 \pm 1.4	4.0 \pm 0.5	2.4 \pm 0.4
5,000 mg L^{-1} ENP	11.9 \pm 2.1	5.0 \pm 0.4	5.5 \pm 1.0	4.1 \pm 0.2 ^b	17.2 \pm 13.7	3.9 \pm 0.6	4.5 \pm 0.7	6.7 \pm 2.7
500 mg L^{-1} Bulk	9.3 \pm 2.0	4.7 \pm 0.8	7.3 \pm 0.5	6.7 \pm 0.9 ^{ab}	4.5 \pm 1.4	3.4 \pm 0.4	9.6 \pm 4.5	4.1 \pm 1.1
1,000 mg L^{-1} Bulk	6.9 \pm 3.9	5.2 \pm 0.9	7.7 \pm 2.2	5.5 \pm 0.3 ^{ab}	8.9 \pm 1.3	3.1 \pm 0.2	7.6 \pm 3.2	5.1 \pm 1.3
2,500 mg L^{-1} Bulk	8.3 \pm 2.0	6.4 \pm 0.2	5.9 \pm 0.6	6.7 \pm 1.7 ^{ab}	16.4 \pm 10.6	3.7 \pm 1.5	5.4 \pm 0.6	19.3 \pm 10.2
5,000 mg L^{-1} Bulk	14.5 \pm 5.2	3.6 \pm 1.3	7.8 \pm 1.7	5.2 \pm 0.9 ^{ab}	7.1 \pm 2.5	2.1 \pm 0.6	4.0 \pm 0.6	8.7 \pm 3.1

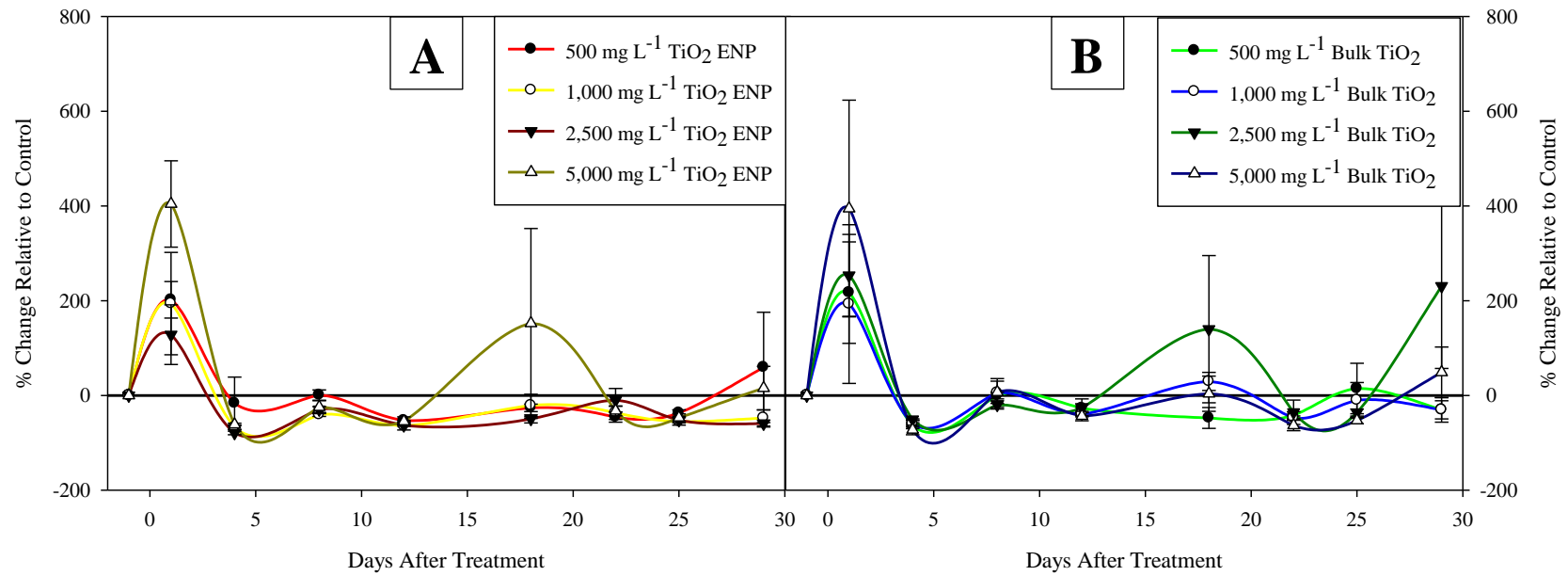


Figure 3.6: Percent change in water use efficiency relative to the control across the time frame of the experiment for *Z. mays* which received foliar application treatment of (A) TiO₂ ENPs and (B) bulk TiO₂ at concentrations of 500, 1000, 2,500 and 5,000 mg L⁻¹. Bars represent standard error (n=5).

Table 3.10: Post hoc multiple comparison results for the percent difference data for water use efficiency by *Z. mays*. Letters indicates honestly significant difference (HSD) of Tukey test (n=5).

Days After Treatment	1	4	8	12	18	22	25	29
500 mg L ⁻¹ ENP	A	A	A	A	A	A	A	A
1,000 mg L ⁻¹ ENP	A	A	A	A	A	A	A	A
2,500 mg L ⁻¹ ENP	A	A	A	A	A	A	A	A
5,000 mg L ⁻¹ ENP	A	A	A	A	A	A	A	A
500 mg L ⁻¹ Bulk	A	A	A	A	A	A	A	A
1,000 mg L ⁻¹ Bulk	A	A	A	A	A	A	A	A
2,500 mg L ⁻¹ Bulk	A	A	A	A	A	A	A	A
5,000 mg L ⁻¹ Bulk	A	A	A	A	A	A	A	A
P Value	<i>p</i> =0.7231	<i>p</i> =0.5163	<i>p</i> =0.2608	<i>p</i> =0.0359	<i>p</i> =0.6158	<i>p</i> =0.4659	<i>p</i> =0.4100	<i>p</i> =0.2270

Table 3.11: Radiation Use Efficiency ($\text{mmol CO}_2 \text{ mol}^{-1} \text{ photon}$) \pm standard error for *Z. mays* treated weekly for five weeks with 500 and 1,000 mg L^{-1} TiO_2 ENPs and bulk TiO_2 , and single bolus 2,500 and 5,000 mg L^{-1} TiO_2 ENPs and bulk TiO_2 . Lettering indicates honestly significant difference (HSD) of Tukey test ($p < 0.05$) ($n=5$).

Radiation Use Efficiency								
Days after Treatment	1	4	8	12	18	22	25	29
Control	22.3 \pm 5.3	85.8 \pm 35.5	61.9 \pm 3.4	40.6 \pm 5.1	30.6 \pm 4.8	33.5 \pm 8.0	39.4 \pm 3.2	37.7 \pm 3.0
500 mg L^{-1} ENP	48.3 \pm 4.8	65.8 \pm 22.8	58.7 \pm 4.9	26.8 \pm 3.5	28.0 \pm 6.0	31.8 \pm 8.3	30.6 \pm 4.7	35.9 \pm 4.5
1,000 mg L^{-1} ENP	42.6 \pm 6.3	62.5 \pm 9.8	50.2 \pm 3.2	35.0 \pm 4.4	27.4 \pm 8.0	27.3 \pm 4.4	31.7 \pm 4.7	21.8 \pm 3.1
2,500 mg L^{-1} ENP	52.4 \pm 14.0	50.2 \pm 4.7	54.5 \pm 3.3	25.3 \pm 3.6	22.3 \pm 1.5	25.6 \pm 5.6	25.4 \pm 4.4	26.4 \pm 3.4
5,000 mg L^{-1} ENP	38.4 \pm 7.3	55.4 \pm 3.5	50.3 \pm 2.5	31.2 \pm 5.3	29.3 \pm 2.0	29.4 \pm 7.1	27.1 \pm 3.0	21.7 \pm 2.7
500 mg L^{-1} Bulk	44.6 \pm 5.9	44.2 \pm 5.1	74.3 \pm 15.9	29.5 \pm 3.0	30.4 \pm 6.2	36.0 \pm 5.6	34.3 \pm 1.4	26.3 \pm 1.9
1,000 mg L^{-1} Bulk	27.7 \pm 10.1	58.9 \pm 8.3	48.9 \pm 7.6	31.4 \pm 5.3	31.3 \pm 2.3	40.5 \pm 5.7	29.8 \pm 1.7	38.3 \pm 12.5
2,500 mg L^{-1} Bulk	34.2 \pm 4.5	56.5 \pm 5.1	52.1 \pm 2.6	30.1 \pm 4.8	44.6 \pm 2.1	29.1 \pm 2.4	22.4 \pm 2.3	29.5 \pm 4.3
5,000 mg L^{-1} Bulk	56.5 \pm 20.1	41.5 \pm 7.3	65.2 \pm 4.6	29.5 \pm 2.6	23.5 \pm 4.4	24.2 \pm 3.1	24.8 \pm 4.5	23.8 \pm 2.9

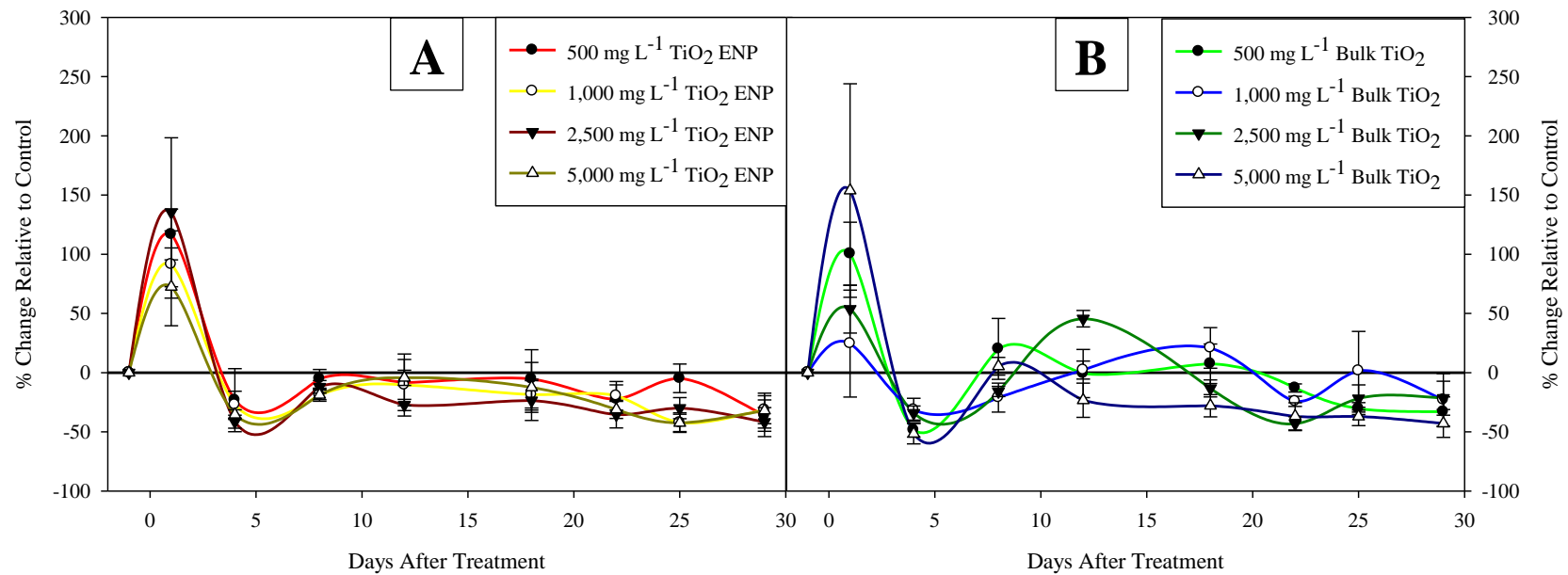


Figure 3.7: Percent change in radiation use efficiency relative to the control across the time frame of the experiment for *Z. mays* which received foliar application treatment of (A) TiO₂ ENPs and (B) bulk TiO₂ at concentrations of 500, 1000, 2,500 and 5,000 mg L⁻¹. Bars represent standard error (n=5).

Table 3.12: Post hoc multiple comparison results for the percent difference data for radiation use efficiency by *Z. mays*. Letters indicates honestly significant difference (HSD) of Tukey test (n=5).

Days After Treatment	1	4	8	12	18	22	25	29
500 mg L ⁻¹ ENP	A	A	A	AB	A	A	A	A
1,000 mg L ⁻¹ ENP	A	A	A	AB	A	A	A	A
2,500 mg L ⁻¹ ENP	A	A	A	B	A	A	A	A
5,000 mg L ⁻¹ ENP	A	A	A	AB	A	A	A	A
500 mg L ⁻¹ Bulk	A	A	A	AB	A	A	A	A
1,000 mg L ⁻¹ Bulk	A	A	A	AB	A	A	A	A
2,500 mg L ⁻¹ Bulk	A	A	A	A	A	A	A	A
5,000 mg L ⁻¹ Bulk	A	A	A	AB	A	A	A	A
P Value	<i>p</i> =0.5705	<i>p</i> =0.6678	<i>p</i> =0.1605	<i>p</i> =0.0675	<i>p</i> =0.4725	<i>p</i> =0.3183	<i>p</i> =0.2753	<i>p</i> =0.9548

Table 3.13: Seed yield data for *Z. mays* treated weekly for five weeks with 500 and 1,000 mg L⁻¹ TiO₂ ENPs and bulk TiO₂, and single bolus 2,500 and 5,000 mg L⁻¹ TiO₂ ENPs and bulk TiO₂.

	Seed Count	Total Yield (g)	% Protein	% Water	% Oil
Control	706.50±27.88	253.50±7.69	12.20±0.54	9.40±0.33	5.68±0.06
500 mg L ⁻¹ ENP	657.25±23.57	232.65±10.60	12.05±0.64	8.90±0.27	5.53±0.22
1,000 mg L ⁻¹ ENP	661.50±13.73	235.85±4.35	13.40±0.48	8.85±0.13	5.90±0.08
2,500 mg L ⁻¹ ENP	661.00±10.00	236.25±3.25	10.70±1.70	9.65±0.15	6.15±1.15
5,000 mg L ⁻¹ ENP	711.75±36.52	234.70±8.02	12.93±0.31	8.88±0.21	6.03±0.30
500 mg L ⁻¹ Bulk	662.20±33.71	243.42±7.67	11.72±0.62	8.88±0.18	5.66±0.13
1,000 mg L ⁻¹ Bulk	738.00±18.91	254.42±3.56	12.32±0.87	8.86±0.26	5.76±0.20
2,500 mg L ⁻¹ Bulk	594.25±17.90	218.28±6.58	12.53±0.42	9.40±0.37	5.80±0.25
5,000 mg L ⁻¹ Bulk	663.80±35.31	234.44±8.53	10.80±1.06	9.42±0.18	5.34±0.18
P value	<i>p</i> =0.0565	<i>p</i> =0.0503	<i>p</i> =0.3020	<i>p</i> =0.2261	<i>p</i> =0.5304

CHAPTER 4

INFLUENCE OF TiO_2 ON THE TOXICITY OF CADMIUM AND ARSENIC

4.1 Introduction

Cadmium and arsenic are two of the top ten most hazardous substances on the priority list of the Agency for Toxic Substances and Disease Registry. The list is based on three criteria: frequency of occurrence, toxicity, and potential for human exposure (Francesconi et al., 2002). Sources for Cd and As contamination include atmospheric deposition resulting from mining, smelting, and fuel combustion, phosphate fertilizers, and sewage sludge (Clemens, 2006). Both of these contaminants can readily be taken up by plants because they are chemical analogues of essential nutrients for plant growth and development (Clemens, 2006). Once inside the plants they can be translocated to the leaves and fruits, thus entering the food chain (Clemens, 2006). Arsenic toxicity can occur as hypo- and hyper-pigmentation, keratosis, and cancer of lungs, skin, and urinary bladder (Srivastava et al., 2012).

The production of nanomaterials is quickly growing into a trillion dollar industry, in which there are already over 140 companies currently manufacturing engineered nanoparticles (ENPs) (Sun et al., 2009). At this rate of production, there is a great potential for engineered nanomaterials to be released into the environment, both intentionally and unintentionally. TiO_2 engineered nanoparticles (ENPs) are one of the most widely produced nanoparticles with a broad range of applications in paints, inks, sunscreens, cosmetics, astronautics, and air/water purification.

It is because of their vast range of applications that concerns have been raised about the introduction of TiO_2 ENPs into the environment. The release of TiO_2 ENPs into domestic and

industrial wastewaters is expected to represent the largest release of these nanoparticles. There has been data showing that up to 99% of TiO₂ ENPs that enter wastewater treatment plants are retained in the sludge (Tourinho et al., 2012). In addition, TiO₂ ENPs are being used at some water treatment plants because of their strong adsorption strength for hazardous materials, such as cadmium, arsenic, and copper (Zhang et al., 2007; Sun et al., 2007; Fan et al., 2011) and also the photocatalytic breakdown of harmful organic compounds. Since sewage sludge from wastewater treatment plants is applied to agricultural lands as a soil conditioner and fertilizer, this has resulted in the introduction of an estimated 120 µg kg⁻³ per year of TiO₂ ENPs (Tourinho et al., 2012).

The simultaneous introduction of heavy metals and TiO₂ ENPs to agricultural fields via sewage sludge begs the question of how the interaction of the two contaminants may alter the bioavailability and uptake of the heavy metal contaminants. TiO₂ has been shown to enhance the exposure of cadmium and arsenate in carp (*Cyprinus carpio*) (Zhang et al. 2007; Sun et al. 2007). The accumulation of cadmium was increased more in the gills and viscera of the carp than it was the skin and muscle tissue (Zhang et al. 2007). This same trend was observed for carp upon exposure to TiO₂ exposure to arsenate (Sun et al. 2007).

Furthermore, it has been observed that when *Daphnia magna* were exposed to TiO₂ ENPs prior to treatment with Cd there was a significantly greater accumulation of Cd in the organism (Tan and Wang, 2014). This data suggests that the TiO₂ ENPs provide an increased binding surface for the Cd in the gut of *D. magna*. Yet when the daphnids were fed algae after the combination of exposures, the accumulated Cd concentration returned to a level similar to that of *D. magna* that were exposed to Cd alone. This indicated that the consumption of algae allowed the daphnids to purge their guts of TiO₂ ENPs as well as bolstered the hypothesis that the TiO₂

ENPs acted as a binding site for Cd ions which resulted in the increased accumulation (Tan and Wang, 2014). Similarly, TiO₂ ENPs were shown to increase copper accumulation in *Daphnia*, but resulted in a decreased mortality rate (Fan et al. 2011). This was most likely due to the fact that the copper entering into the *Daphnia* weren't entering as free ions, but rather adsorbed to the TiO₂ ENPs. However, in the absence of copper, there has been evidence that TiO₂ ENPs do yield toxic effects to *D. Magna*. In fact, it is a rather acute toxicity, showing an LC50 (Lethal Concentration to 50% of the population) at 1 mg L⁻¹ for 15 nm TiO₂ ENPs (Clement et al., 2013). As with most organisms, the toxicity of the ENPs decreases with increasing size.

Previous studies performed with carbonaceous nanomaterials and persistent pesticides have shown mixed results (Torre-Roche et al., 2012; Torre-Roche et al., 2013; Kelsey and White, 2013). It was demonstrated that multi-walled carbon nanotubes (MWCN) reduced the uptake of weathered chlorodane and DDX in a dose dependent manner for zucchini, corn, tomato, and soybean. On the other hand, C₆₀ fullerenes only reduced the bioaccumulation of the pesticides for corn and zucchini, but had little to no effect on the accumulation for tomato and soybean (Torre-Roche et al., 2013). However, it was shown that the combination of C₆₀ fullerenes and DDE (a persistent metabolite of DDT) resulted in a significantly greater bioaccumulation than exposure to DDE alone for tomato, soybean, and zucchini plants (Torre-Roche et al., 2012). Yet a parallel experiment showed that the C₆₀ fullerenes had no significant effect on the accumulation of DDE in zucchini (Kelsey and White, 2013). These experiments used similar concentrations of both substances, but the study done by Torre-Rouche et al. (2012) used vermiculite as a growth media and Kelsey and White (2013) used a Cheshire fine sandy loam soil.

These results have led to speculation by researchers that TiO₂ ENPs retained the majority metal ions adsorbed on the surface of the nanoparticle. This information gives rise to two alternative hypotheses on how TiO₂ ENPs may affect the fate of heavy metal contaminants in a single substrate growth media. The first is that the TiO₂ ENPs may sequester the heavy metals in the soil thus decreasing the amount of the heavy metals that can be taken up by the plant. The alternative is that the TiO₂ ENPs could act as a carrier of the metals i.e. if the plant is able to take up the intact TiO₂ ENP doped with heavy metals, it could potentially increase the amount of the metals that enter the plants.

To date, there has been very little research done for ENP and contaminant interactions in a terrestrial environment, and even less done with respect to plants, especially agricultural plants. The majority of ENP and contaminant interactions are focused on aquatic and/or microorganisms. The main objective of this study was to determine which of these scenarios is true for broccoli plants that were grown in cadmium and arsenate contaminated growth media.

4.2 Materials and Methods

4.2.1 Reagents and Plants

A dispersion of 5-15 nm anatase TiO₂ engineered nanoparticles (ENPs) with a purity of 99.9% were obtained from US Research Nanomaterials, Inc. (Houston, TX). Cadmium nitrate (CdNO₃) and arsenic acid (NaH₃AsO₄) were obtained from Fisher Scientific (Fair Lawn, NJ). *Brassica oleracea* var. *botrytis* L. cv. Waltham 29 was obtained from NK Lawn and Garden.

4.2.2 Experimental Design

Field capacity was determined by adding known volumes of DI H₂O to a known volume of vermiculite until it reached saturation. The volume of water for field capacity was then back calculated to determine that 40 mL of H₂O was approximately 85-90% field capacity. Thus, the experimental pots were prepared by adding 40 mL of TiO₂ ENPs suspensions and then stirring in 12 g of autoclaved vermiculite. The pots were then placed in a Percival E-36L growth chamber (Perry, IA) under 16 hr light regime with a light intensity of 300 $\mu\text{mol photon m}^{-2} \text{s}^{-1}$ at 60-70% relative humidity and hydration levels were maintained for four days to allow the TiO₂ ENPs and vermiculite to come to equilibrium. Broccoli seeds were imbibed on filter paper for 48 hr and then transferred to the experimental pots, which remained in a growth chamber for 47 days. After 47 days, the pots were transferred to the SIUC Plant Biology phytotron in order to obtain a more natural light setting; the pots remained in the phytotron throughout the remainder of the experiment. The initial mass of the pots after planting was determined to be 55.8 g (40 g of H₂O, 12 g of vermiculite, and 3.8 g for the pot). The pot mass was recorded daily to determine water loss (as an estimate of evapotranspiration), and deionized water was added to return the pot mass to the initial value. The mass data was used to determine cumulative transpiration over the course of the experiment. The plants received 5 mL of nutrient solution once per week. The nutrient solution consisted of 1.2 mM KNO₃, 0.8 mM Ca(NO₃)₂, 0.1 mM NH₄H₂PO₄, 0.2 mM MgSO₄, 50 μM KCl, 12.5 μM H₃BO₃, 1.0 μM MnSO₄, 1.0 μM ZnSO₄, 0.5 μM CuSO₄, 0.1 μM H₂MoO₄, 0.1 μM NiSO₄, 12.5 μM Fe(III)-EDDHA. The nutrient solution was buffered with 1 mM *n*-morpholinoethanesulfonic acid (MES) and pH was adjusted to 6.0 with KOH. Once the plants developed their first fully expanded true leaf (35 days after sowing seeds), Cd or As(V) treatments were applied. The treatments were applied in two 5 mL aliquots (7 days apart) each

adding half the amount needed to achieve final treatment concentrations of cadmium (0, 2, and 20 mg kg⁻¹) or arsenate (0, 20, and 200 mg kg⁻¹). The array of treatments (Table 4.1) had five replicates each (total 45 plants). The position of the pots was completely randomized in the growth chamber daily.

Weekly measurements of plant height and leaf number were taken to determine relative growth rate throughout the entire experiment. Broccoli plants were harvested 70 days after sowing seeds (35 days after the initiation of the As or Cd treatment). Relative chlorophyll was measured with a Minolta Spad 502 (Konica Minolta, Inc.; Ramsey, NJ) at harvest.

Measurements were made on three randomly selected leaves and then averaged to create a single value for each replicate. The harvested plants were separated into roots and shoots. The tissue samples were then dried at 56°C to constant mass and the total dry biomass of each tissue was determined.

Both tissue types were then ground and subjected to acid digestion by the US EPA 3050b (USEPA, 1996) method in which 67-70% trace metal grade nitric acid was added to the sample and heated on a heat block cycling between 94 and 45 °C. Once this phase of the digest was completed, 30% hydrogen peroxide was added and the samples were heated in the same manner again. The samples were then sent to the Connecticut Agricultural Experiment Station (New Haven, CT) for analysis of arsenic and cadmium concentrations inductively coupled plasma mass spectroscopy (ICP-MS, Agilent 7500ce, Santa Clara, CA).

4.2.3 Data Analysis

The chlorophyll data was expressed as the percent of control and obtained by dividing the value for treated plants by the value obtained for control plants. Relative growth rate was

determined by counting the number of fully expanded leaves once a week. The data was then entered into the following equation from Evans (1972):

$$\text{Relative growth rate} = \frac{\ln(W_2) - \ln(W_1)}{t_2 - t_1}$$

All data except cumulative transpiration and RGR were subjected to a two-way analysis of variance (ANOVA) with the main effects of TiO₂ concentration and concentration of the metal [As(V) or Cd]. Means were compared using the honestly significant difference (HSD) of Tukey test at $p < 0.05$ using SAS 9.3 computer software. For the parameters that showed a significant interaction term, the data were subjected to a one-way ANOVA and interaction means were compared using the HSD of Tukey test at $p < 0.05$ using SAS 9.3 computer software. Cumulative transpiration and RGR data were subjected to a two-way ANOVA with repeated measures (time). Means were compared using the honestly significant difference (HSD) of Tukey test at $p < 0.05$ using SPSS ver. 22.

4.3 Results

4.3.1 Influence of the TiO₂ ENPs and Cd treatments

The results from the two-way ANOVA indicated that there was no significant difference in shoot dry weight, root dry weight; root to shoot ratio, final plant height, or relative chlorophyll (Table 4.2). Furthermore, the two-way ANOVA with repeated measures showed that there were no significant differences found for cumulative transpiration (Figure 4.1), height RGR (Figure 4.2), and leaf RGR (Figure 4.3), showing that the Cd and TiO₂ ENP treatments did not have any effect on these growth and development parameters of the plants.

There was a significant difference between the Cd concentrations in the shoots, with the 200 mg kg⁻¹ treatment being significantly greater than the 20 and 0 mg kg⁻¹ treatments, and the 20 mg kg⁻¹ treatment was significantly greater than the 0 mg kg⁻¹ treatment (Figure 4.4). Broccoli plants treated with 2 and 20 mg kg⁻¹ cadmium accumulated 29.96 and 79.13 mg kg⁻¹ dry weight cadmium in the shoots respectively. The two-way ANOVA for Cd concentration in the shoots revealed that there was no significant differences in response to TiO₂ concentration nor was there a significant interaction term. While there were no significant differences found for the interaction, the application of 333 and 3,333 mg kg⁻¹ TiO₂ ENPs resulted in a 58.59 and 40.29% decrease of cadmium accumulation in the shoots for plants treated with 2 mg kg⁻¹, respectively. However, plants treated with 20 mg kg⁻¹ resulted in a 0.07% increase when treated with 333 mg kg⁻¹ TiO₂ ENPs and a 6.50% decrease in the shoots when treated with 3,333 mg kg⁻¹ TiO₂ ENPs.

The two-way ANOVA for Cd concentration in broccoli roots showed that there was significant variation with respect to the interaction of TiO₂ ENPs and Cd ($p=0.0024$). The roots of broccoli plants treated with 2 and 20 mg kg⁻¹ cadmium accumulated 154.52 and 571.41 mg kg⁻¹ DW (Figure 4.5). Plants that received TiO₂ ENP treatments of 333 and 3,333 mg kg⁻¹ resulted in a decrease of 24.69% and a significant decrease of 60.05% ($p < 0.001$) cadmium accumulation, respectively, for plants treated with 2 mg kg⁻¹ cadmium. Whereas plants that received the same TiO₂ ENP treatments with a 20 mg kg⁻¹ cadmium treatment only showed a 3.29 and 29.23% decrease. It should be noted Cd concentrations reported for the roots includes all contaminants associated with the roots, without distinction between Cd adsorption and absorption.

4.3.2 Influence of the TiO₂ ENPs and As(V)

The two-way ANOVA showed that there was a significant difference for the TiO₂ ENP concentrations with respect to root and shoot dry biomass ($p=0.0040$; $p=0.0042$) (Table 4.3). For both tissue types, the 3,333 mg kg⁻¹ TiO₂ ENP treatment had a significantly greater biomass than the 0 mg kg⁻¹ TiO₂ ENP treatment, but the 333 mg kg⁻¹ TiO₂ ENP treatment was not significantly different from the 3,333 mg kg⁻¹ TiO₂ ENP treatment or the 0 mg kg⁻¹ TiO₂ ENP treatment. The As(V) concentration also had a significant effect on root and shoot dry biomass ($p<0.0001$; $p<0.0001$). For both tissue types, the 0 and 20 mg kg⁻¹ As(V) treatments were significantly greater than the 200 mg kg⁻¹ As(V) treatment, but there was no significant difference between the 0 and 20 mg kg⁻¹ As(V) treatment. There was not a significant interaction between TiO₂ and As(V) concentration. There were also no significant differences found for any of the main effects or an interaction in relation to the root:shoot ratio or relative chlorophyll (Table 4.3). However, there was a significant difference found for both the TiO₂ ENP and As(V) concentrations in relation to final plant height ($p=0.0009$; $p=0.0010$) (Table 4.3). The plant height followed the same pattern as the dry biomass, in which the 3,333 mg kg⁻¹ TiO₂ treatment was significantly greater than the 0 mg kg⁻¹ TiO₂ ENP treatment, but the 333 mg kg⁻¹ TiO₂ ENP treatment was not significantly different than the 0 or 3,333 mg kg⁻¹ TiO₂ ENP treatments. Also, the 0 and 20 mg kg⁻¹ As(V) treatments were significantly greater than the 200 mg kg⁻¹ As(V) treatment, but there was no significant difference between the 0 and 200 mg kg⁻¹ As(V) treatments.

The two-way ANOVA with repeated measures revealed that there was a significant difference for TiO₂ concentrations ($p=0.005$) and As(V) concentrations ($p=0.016$), but the interaction term was not significant in relation to cumulative transpiration (Figure 4.6). Plants

which receive the 333 and 3,333 mg kg⁻¹ TiO₂ ENP treatment had a significantly greater cumulative transpiration than plants that received 0 mg kg⁻¹ TiO₂ ENPs. In relation to As(V) concentrations, the 0 mg kg⁻¹ treatment had a significantly greater cumulative transpiration than the 200 mg kg⁻¹ treatment; the 20 mg kg⁻¹ treatment was not significantly different than either of the other treatments. For the height RGR there was a significant difference for As(V) concentrations, but there was no significant differences found for the TiO₂ concentrations or the interaction term (Figure 4.7). All three As(V) treatments showed a significant difference from one another, with the 0 mg kg⁻¹ treatment having the greatest height RGR, followed by the 20 mg kg⁻¹ treatment, and the 200 mg kg⁻¹ had the lowest height RGR. There were no significant differences found in relation to leaf RGR (Figure 4.8).

The two-way ANOVA revealed that there was significant differences with respect to the interaction of TiO₂ ENPs and As(V) concentrations ($p=0.0105$) in relation to the As concentration found in the shoots. However, the only a significant difference found for the As(V) concentration found in the roots was for the As concentration ($p=0.0075$), in which the 200 mg kg⁻¹ As(V) was significantly greater than the 0 and 20 mg kg⁻¹ As(V) treatments; there was no significant difference between the 0 and 20 mg kg⁻¹ As(V) treatments. Broccoli plants treated with 20 and 200 mg kg⁻¹ As(V) accumulated 44.04 and 50.23 mg kg⁻¹ dry weight of As(V) in their shoots, respectively (Figure 4.9). The addition of 333 and 3,333 mg kg⁻¹ TiO₂ ENPs resulted in a 20.74 and 63.66% decrease in As(V) accumulated in plants treated with 20 mg kg⁻¹ As(V). The one-way ANOVA showed that the 20 mg kg⁻¹ As(V) treated plants which received 3,333 mg kg⁻¹ TiO₂ ENPs had a significant reduction in As accumulation in the shoots ($p<0.0001$) compared to those which received 0 mg kg⁻¹ TiO₂ ENPs, yet the ones that received 333 mg kg⁻¹ TiO₂ ENPs were not significantly different than those which received 0 or 3,333 mg

kg⁻¹ TiO₂ ENPs (Figure 4.9). Interestingly, for plants treated with 200 mg kg⁻¹ As(V) the addition of 333 and 3,333 mg kg⁻¹ TiO₂ ENPs resulted in an increase of 59.19 and 18.54% As(V) accumulation in the shoots, and the addition of 333 mg kg⁻¹ TiO₂ ENPs was found to be significantly greater than the plants that received 0 mg kg⁻¹ TiO₂ ENPs (Figure 4.9).

The two-way ANOVA for As concentration in the roots showed that there was a significant difference for the interaction of TiO₂ ENP and As(V) concentration ($p=0.0069$). For plants treated with 20 mg kg⁻¹ As(V), the one-way ANOVA revealed that the plants which received 0 mg kg⁻¹ TiO₂ ENPs had a significantly greater concentration of As than plants that received 3,333 mg kg⁻¹ TiO₂ ENPs ($p<0.0001$); plants that received 333 mg kg⁻¹ TiO₂ ENPs did not have an As concentration than the other two treatments (Figure 4.10). For broccoli plants which were treated with 200 mg kg⁻¹ As(V), the one-way ANOVA showed that there was no significant differences in As concentration between the 0 and 333 mg kg⁻¹ TiO₂ treatments, but both treatments were found to have a significantly greater As concentration than plants which received 3,333 mg kg⁻¹ TiO₂ ENPs ($p<0.0001$; Figure 4.10). The roots of broccoli plants treated with 20 and 200 mg kg⁻¹ As(V) accumulated 2,881.27 and 7,547.32 mg kg⁻¹ dry weight of As, respectively (Figure 4.10). The addition of 333 and 3,333 mg kg⁻¹ TiO₂ ENPs resulted in a decrease of 33.80 and 82.80% in As accumulation for plants treated with 20 mg kg⁻¹ As(V). For plants treated with 200 mg kg⁻¹ As(V), the addition of 333 mg kg⁻¹ showed an increase in As accumulation of 10.06%, but the addition of 3,333 mg kg⁻¹ brought about a decrease in As accumulation of 32.78% (Figure 4.10). It should be noted As concentrations reported for the roots includes all contaminants associated with the roots, without distinction between the adsorption and absorption of As.

4.4 Discussion

The emphasis on nanomaterial-contaminant interactions is a new focus for nanotoxicology. Recent studies performed with carp have shown that the accumulation of As and Cd was significantly increased with the addition of TiO₂ ENPs compared to expose of As or Cd alone (Sun et al., 2007; Zhang et al., 2007). For both studies, the greatest increase in As or Cd concentration was found in the gills and viscera of the fish. Similarly, TiO₂ ENPs have been shown to increase the concentration of Cd and Cu in *D. magna* (Tan and Wang, 2014; Fan et al. 2011). These studies indicated TiO₂ ENPs have the capacity to directly adsorb the contaminants and act as a carrier, thus increasing the total amount of the contaminants that enter the organism. However, the increase in Cu in the daphnids didn't result in an increased mortality rate (Fan et al. 2011), and once the daphnids purged their guts by consuming algae, the Cd concentration was similar to the daphnids that were exposed to Cd treatment with no TiO₂ ENPs (Tan and Wang 2014). These experiments involving *D. magna* suggest that if the heavy metal contaminants is adsorbed to the surface of the TiO₂ ENPs, preventing it from being biologically available (Tan and Wang, 2014; Fan et al. 2011). Regardless of the bioavailability, all of the experiments conducted with aquatic organisms resulted in an increased contaminant concentration within the organism being exposed to TiO₂ ENPs and the contaminants.

The results from this study were found to unexpectedly contradict those of the previous studies mentioned for TiO₂ ENP and contaminant interactions, in which the addition of TiO₂ ENPs seemed to reduce the uptake of Cd and As by broccoli instead of increasing it. There are several differences between this study and previous contaminant and ENP interaction studies that may have influenced the results. First, plant cells are structurally different than animal cells in that plant cells possess a cell wall which may prevent the movement of TiO₂ ENPs into the

interior of the cells. A recent study examining the combined effects of polyacrylate-coated TiO₂ ENPs and Cd with the green algae *Chlamydomonas reinhardtii* showed that the TiO₂ alleviated the toxicity of Cd due to the binding of free Cd to the surface of the TiO₂ ENPs (Yang et al. 2012). Furthermore, TEM imaging and EDX spectroscopy found no TiO₂ ENPs within the cells suggesting that the presence of the cell wall may have prevented the movement of the TiO₂ ENPs within the cells (Yang et al. 2012).

Secondly, this study was conducted with a solid substrate growth media as opposed to an aquatic system. While there has been recent studies focusing on ENP-contaminant interactions, the majority of them have been conducted in aquatic systems focusing on fish, daphnids, and algae (Zhang et al. 2007; Sun et al. 2007; Tan and Wang, 2014; Fan et al. 2011; Yang et al. 2012). ENPs may behave differently in a solid substrate as opposed to an aquatic system because the ENPs may become adsorbed to the growth media restricting the mobility of the ENPs (Tourinho et al. 2012).

Finally, the properties of TiO₂ ENPs are inherently different than the properties of carbon based nanoparticles. While both ENPs are photoactive, fullerenes are considered photosensitizers and TiO₂ ENPs are semiconductors. Furthermore, the light absorption range is different for the two ENPs; TiO₂ ENPs absorb light in the UV range (<390 nm) and fullerenes are capable of absorbing light in the UV/visible spectrum (Brunet et al. 2009). Both ENPs generate reactive oxygen species, but TiO₂ ENPs have been shown to generate hydroxyl ions, superoxide ions, and singlet oxygen whereas fullerenes were only shown to generate superoxide ions and singlet oxygen (Brunet et al. 2009). Furthermore, TiO₂ ENPs tended to generate a greater amount of the ROS under UV light. Brunet et al. (2009) demonstrated that TiO₂ ENPs were only toxic to *E. coli* under light while fullerenes were toxic to the bacteria in both light and

darkness. It is likely their toxicity is linked to the disruption of cell membranes; indicating that when in a soil environment, fullerenes would be more destructive to plant root membranes than TiO₂ ENPs. The disruption of root membranes could allow for ENPs as well as contaminants to enter the root system whether the contaminants are adsorbed to ENPs or not.

The reason for a greater decrease in As accumulation compared to Cd accumulation could be attributed to the difference in the bonds that are formed between the metals and the TiO₂ ENPs. Much of this difference in bonds is based on the nature of the metals. Cadmium is present as a cationic divalent ion in aqueous solution, whereas arsenate is present as a negatively charged molecule in aqueous solutions. The negatively charged oxygen molecules that surround the As(V) molecule have the potential to form bidentate bonds (mononuclear or binuclear) with the TiO₂ ENPs (Jegadeesan et al., 2010) giving them the ability to adhere more strongly to the TiO₂ ENPs. Alternatively, the Cd ions do not bind directly to the TiO₂ ENPs; rather, they interact with the hydration sphere that surrounds the TiO₂ ENPs and form bonds with the hydroxyl groups (Chen et al., 2012). Given this alone it is clear as to why the As accumulation had a greater reduction compared to the Cd accumulation. However, it is also important to consider the competition for binding sites on the TiO₂ ENPs from the nutrient solution that was present in the pots. When this is taken into consideration, it is clear that there are an abundance of cations, such as: Cu²⁺, Zn²⁺, Ca²⁺, Mg²⁺, Mn²⁺, Ni²⁺, K⁺ etc., which could potentially be competing for binding sites on the TiO₂ ENPs with Cd (Chen et al., 2012; Mahdavi et al. 2013). On the other hand, there are only a small number of molecules, such as: SO₄, H₂PO₄, and H₂MoO₄, that could potentially compete with As(V) for binding sites (Jegadeesan et al., 2010).

There is a very limited body of literature involving the influence of ENPs on the bioaccumulation of environmental contaminants because it is a relatively new area of study. The

data from this study suggests that TiO₂ ENPs may act as a binding site for Cd and As and prevent them from being available for uptake by roots. However, the capability of TiO₂ ENPs to bind such metals and metalloids is highly dependent on the surface charge of the TiO₂ ENP, which is mainly dictated by the pH of its environment (Chen et al., 2012; Jegadeesan et al., 2010; Lui et al., 2013). There needs to be further research to determine how TiO₂ ENPs may influence the bioaccessibility of these substances at a range of different pH levels, in various soil types, and under various soil hydration states. Furthermore, future work should be done to determine adsorption/desorption kinetics, binding strengths, and binding site competition for the aforementioned ions and molecules to TiO₂ ENPs.

Table 4.1: Matrix demonstrating the treatment strategy for TiO₂ interaction with Cd or As(V).

	0 mg TiO₂ kg⁻¹	333 mg TiO₂ kg⁻¹	3,333 mg TiO₂ kg⁻¹
0 mg Cd kg⁻¹	0 TiO ₂ + 0 Cd	333 TiO ₂ + 0 Cd	3,333 TiO ₂ + 0 Cd
2 mg Cd kg⁻¹	0 TiO ₂ + 2 Cd	333 TiO ₂ + 2 Cd	3,333 TiO ₂ + 2 Cd
20 mg Cd kg⁻¹	0 TiO ₂ + 20 Cd	333 TiO ₂ + 20 Cd	3,333 TiO ₂ + 20 Cd
0 mg As(V) kg⁻¹	0 TiO ₂ + 0 As(V)	333 TiO ₂ + 0 As(V)	3,333 TiO ₂ + 0 As(V)
20 mg As(V) kg⁻¹	0 TiO ₂ + 20 As(V)	333 TiO ₂ + 20 As(V)	3,333 TiO ₂ + 20 As(V)
200 mg As(V) kg⁻¹	0 TiO ₂ + 200 As(V)	333 TiO ₂ + 200 As(V)	3,333 TiO ₂ + 200 As(V)

Table 4.2: The means \pm standard error for shoot dry weight, root dry weight, root:shoot ratio, final height, and relative chlorophyll for broccoli plants treated with Cd and TiO₂ ENPs. The bottom three rows indicate the results (*p* value) from the two-way ANOVA. Relative chlorophyll is expressed as percentage relative to control (0 TiO₂ + 0 Cd), thus excluding the control data point.

mg Cd/TiO ₂ kg ⁻¹	Shoot Dry Weight (g)	Root Dry Weight (g)	Root to Shoot Ratio	Height (cm)	Relative Chlorophyll
0 TiO ₂ + 0 Cd	0.069 \pm 0.004	0.024 \pm 0.002	0.35 \pm 0.04	3.80 \pm 0.23 ab	-
0 TiO ₂ + 2 Cd	0.067 \pm 0.006	0.020 \pm 0.001	0.30 \pm 0.01	4.52 \pm 0.18 a	99.09 \pm 5.25
0 TiO ₂ + 20 Cd	0.076 \pm 0.004	0.023 \pm 0.002	0.30 \pm 0.03	4.14 \pm 0.22 ab	104.04 \pm 8.73
333 TiO ₂ + 0 Cd	0.065 \pm 0.008	0.019 \pm 0.002	0.30 \pm 0.02	3.40 \pm 0.07 b	105.79 \pm 3.72
333 TiO ₂ + 2 Cd	0.074 \pm 0.003	0.021 \pm 0.001	0.28 \pm 0.02	3.80 \pm 0.17 ab	111.40 \pm 1.95
333 TiO ₂ + 20 Cd	0.076 \pm 0.007	0.019 \pm 0.003	0.25 \pm 0.03	4.04 \pm 0.19 ab	104.80 \pm 1.95
3,333 TiO ₂ + 0 Cd	0.072 \pm 0.007	0.021 \pm 0.002	0.30 \pm 0.04	4.06 \pm 0.21 ab	109.88 \pm 2.64
3,333 TiO ₂ + 2 Cd	0.069 \pm 0.010	0.020 \pm 0.002	0.30 \pm 0.04	3.64 \pm 0.28 ab	116.34 \pm 8.23
3,333 TiO ₂ + 20 Cd	0.067 \pm 0.006	0.021 \pm 0.002	0.31 \pm 0.01	4.04 \pm 0.17 ab	100.34 \pm 4.30
Cd	0.8888	0.2868	0.2831	0.0545	0.2162
TiO ₂	0.7489	0.7968	0.4858	0.1414	0.4459
Interaction	0.6773	0.7198	0.7807	0.0508	0.4745

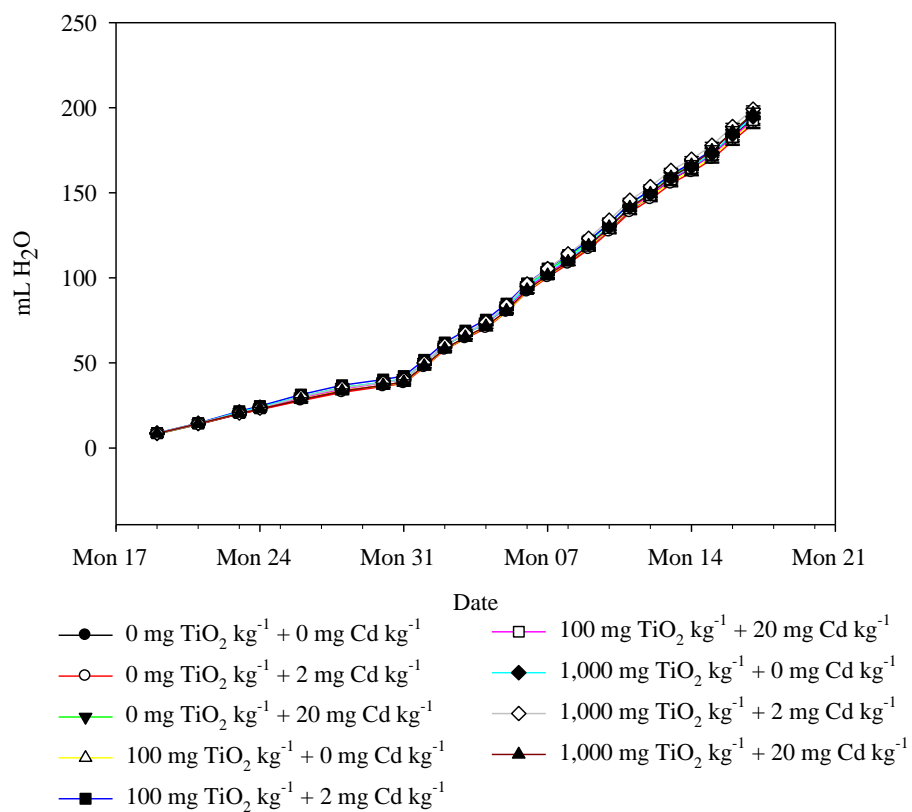


Figure 4.1: Cumulative transpiration for broccoli plants treated with Cd and TiO₂ ENPs as described in Table 4.1. The bars represent standard error (n=5).

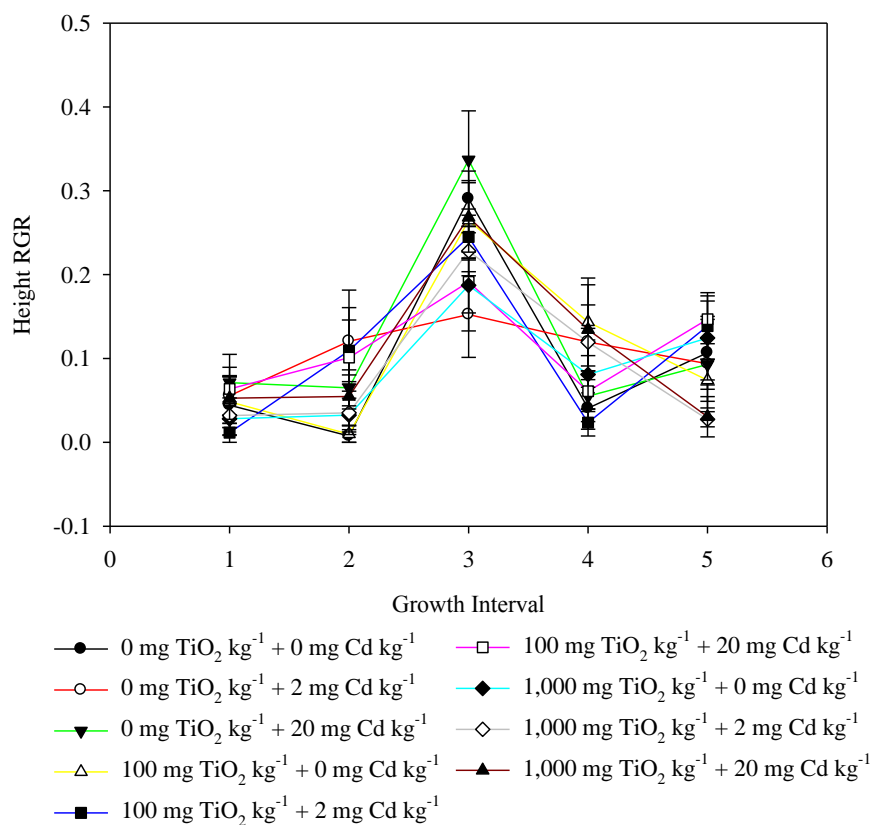


Figure 4.2: Height relative growth rate (RGR) for broccoli plants treated with Cd and TiO₂ ENPs as described in Table 4.1. The bars represent standard error (n=5).

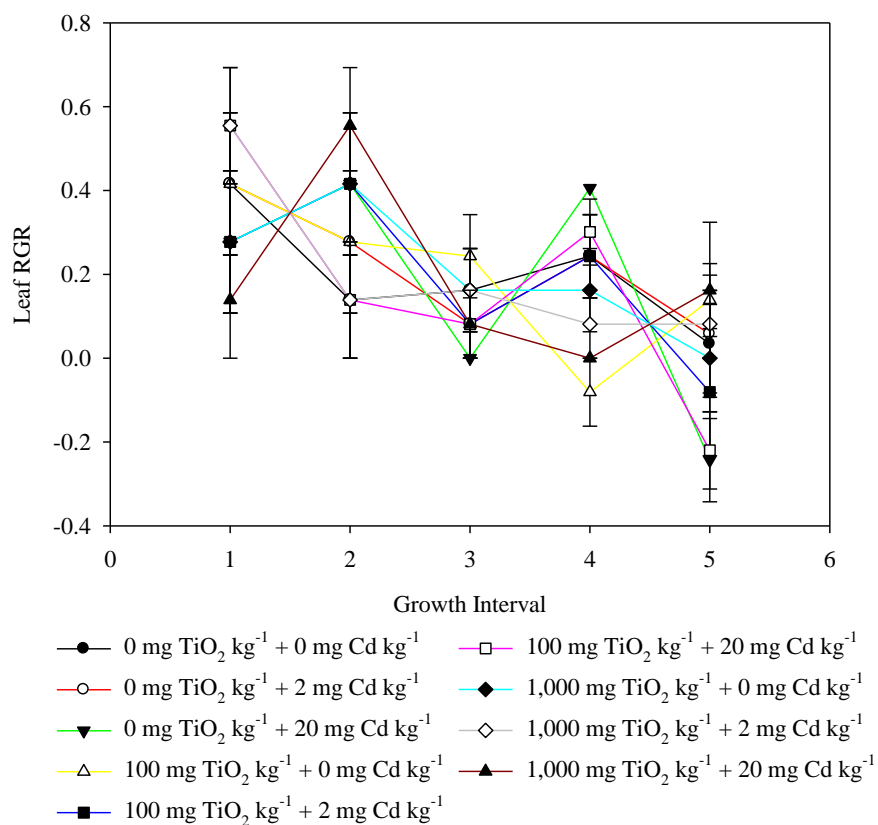


Figure 4.3: Leaf number relative growth rate (RGR) for broccoli plants treated with Cd and TiO₂ ENPs as described in Table 4.1. The bars represent standard error (n=5).

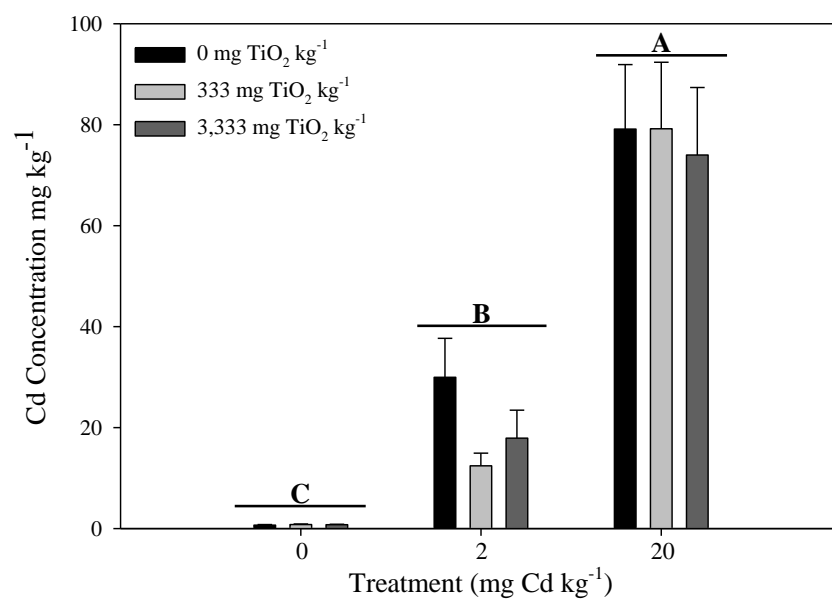


Figure 4.4: Total shoot concentration of Cd for broccoli plants treated with Cd and TiO₂ ENPs as described in Table 4.1. The bars represent standard error and the lettering indicates honestly significant difference (HSD) of Tukey test ($p < 0.05$) for cadmium concentration from the two-way ANOVA.

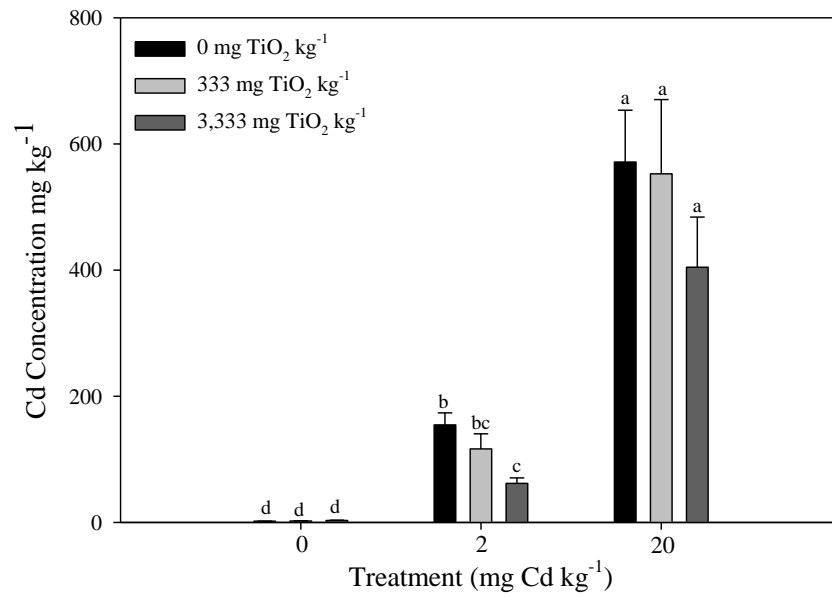


Figure 4.5: Total root concentration of Cd for broccoli plants treated with Cd and TiO₂ ENPs as described in Table 4.1. The bars represent standard error and the lettering indicates honestly significant difference (HSD) of Tukey test ($p < 0.05$) ($n=5$).

Table 4.3: The means \pm standard error for shoot dry weight, root dry weight, root:shoot ratio, final height, and relative chlorophyll for broccoli plants treated with As(V) and TiO₂ ENPs. The bottom three rows indicate the results (*p* value) from the two-way ANOVA. Relative chlorophyll is expressed as percentage relative to control [0 TiO₂ + 0 As(V)], thus excluding the control data point.

mg As(V)/TiO ₂ kg ⁻¹	Shoot Dry Weight (g)	Root Dry Weight (g)	Root to Shoot Ratio	Height (cm)	Relative Chlorophyll
0 TiO ₂ + 0 As(V)	0.050 \pm 0.007	0.018 \pm 0.002	0.40 \pm 0.10	2.60 \pm 0.22	-
0 TiO ₂ + 20 As(V)	0.040 \pm 0.005	0.014 \pm 0.001	0.38 \pm 0.05	2.48 \pm 0.23	117.93 \pm 9.46
0 TiO ₂ + 200 As(V)	0.024 \pm 0.005	0.007 \pm 0.002	0.28 \pm 0.04	2.08 \pm 0.19	113.01 \pm 26.57
333 TiO ₂ + 0 As(V)	0.063 \pm 0.004	0.020 \pm 0.001	0.33 \pm 0.02	2.68 \pm 0.12	103.27 \pm 10.76
333 TiO ₂ + 20 As(V)	0.054 \pm 0.009	0.017 \pm 0.002	0.32 \pm 0.02	3.00 \pm 0.18	99.26 \pm 8.84
333 TiO ₂ + 200 As(V)	0.025 \pm 0.003	0.009 \pm 0.001	0.37 \pm 0.04	2.34 \pm 0.17	105.66 \pm 11.68
3,333 TiO ₂ + 0 As(V)	0.066 \pm 0.003	0.020 \pm 0.001	0.30 \pm 0.02	3.28 \pm 0.35	95.78 \pm 3.83
3,333 TiO ₂ + 20 As(V)	0.061 \pm 0.004	0.018 \pm 0.001	0.31 \pm 0.03	3.42 \pm 0.19	96.07 \pm 3.44
3,333 TiO ₂ + 200 As(V)	0.031 \pm 0.004	0.014 \pm 0.001	0.48 \pm 0.09	2.54 \pm 0.11	122.61 \pm 6.06
As	0.0042	0.0040	0.8649	0.0009	0.7242
TiO ₂	<0.0001	<0.0001	0.5945	0.0010	0.3473
Interaction	0.6229	0.4341	0.0694	0.6838	0.6400

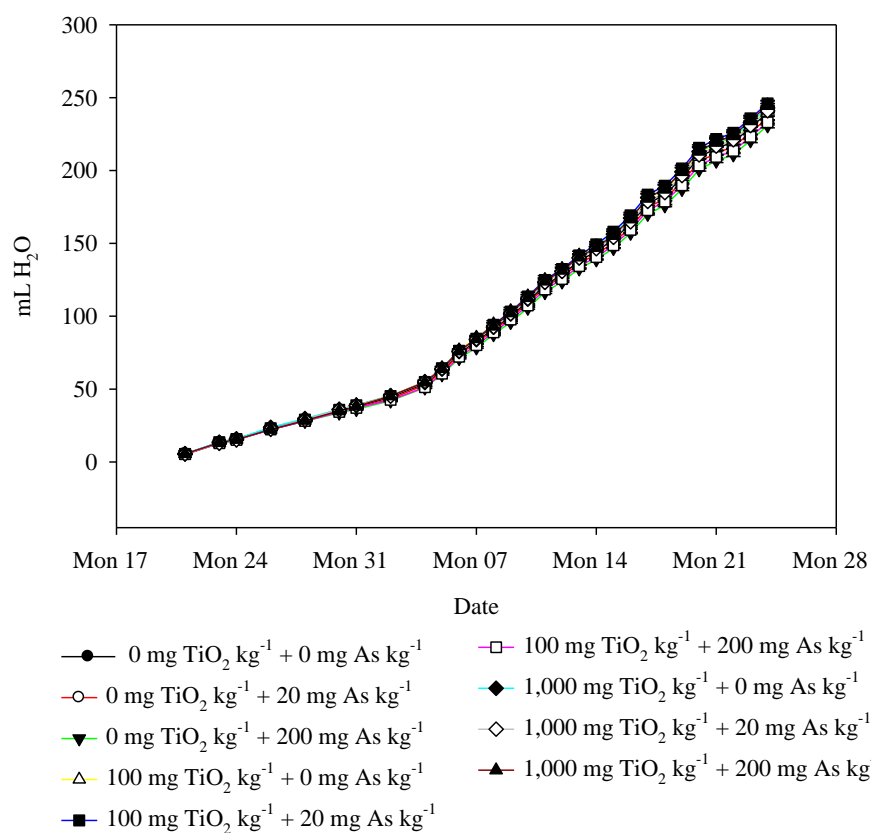


Figure 4.6: Cumulative transpiration data for broccoli plants treated with As(V) and TiO₂ ENPs as described in table 4.1. The bars represent standard error (n=5).

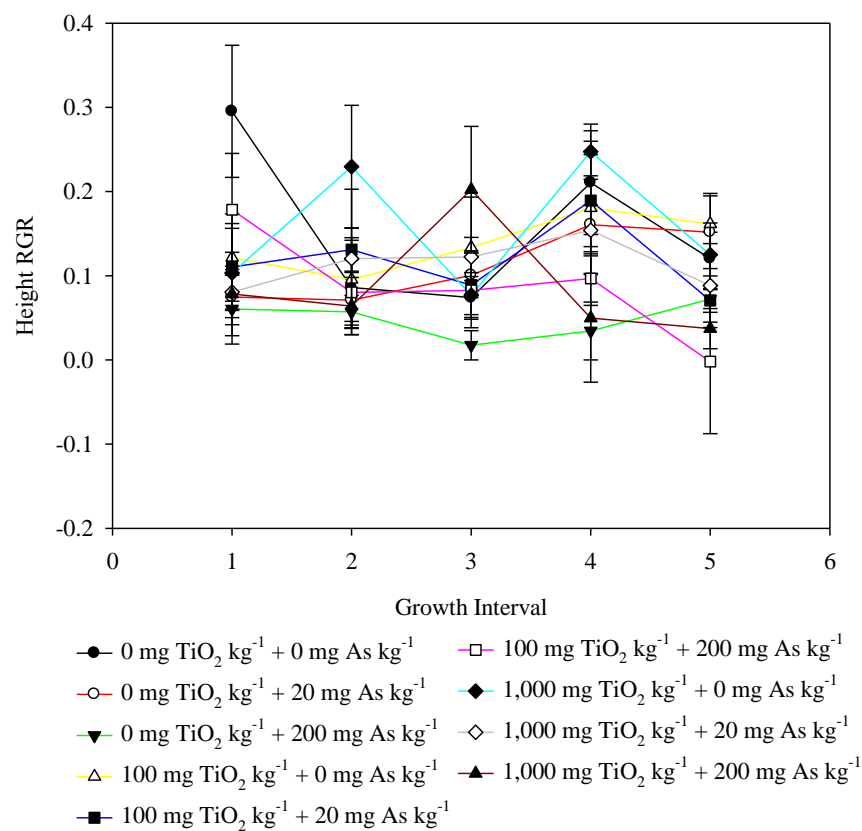


Figure 4.7: Height relative growth rate (RGR) for broccoli plants treated with As(V) and TiO₂ ENPs as described in Table 4.1. The bars represent standard error (n=5).

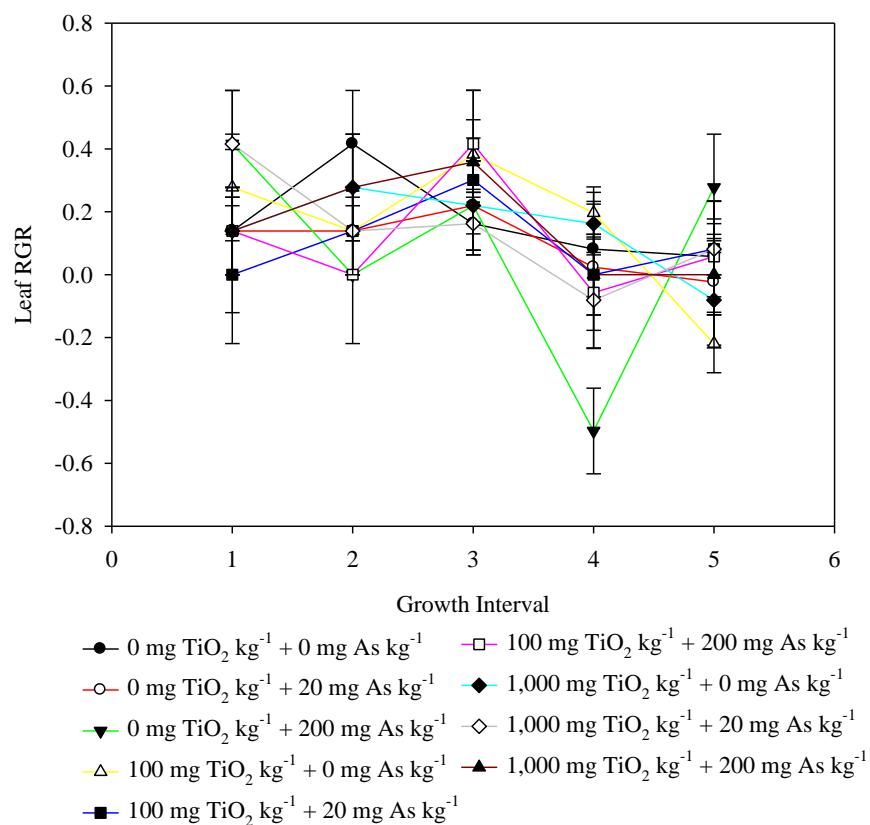


Figure 4.8: Leaf number relative growth rate (RGR) for broccoli plants treated with As(V) and TiO₂ ENPs as described in Table 4.1. The bars represent standard error (n=5).

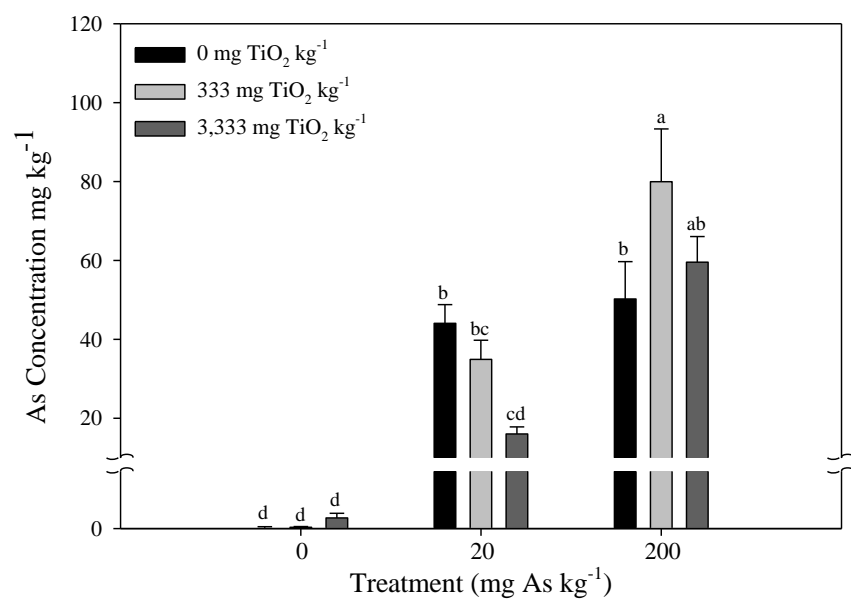


Figure 4.9: Total shoot concentration of As for broccoli plants treated with As(V) and TiO₂ ENPs as described in Table 4.1. The bars represent standard error and the lettering indicates honestly significant difference (HSD) of Tukey test ($p < 0.05$) ($n=5$).

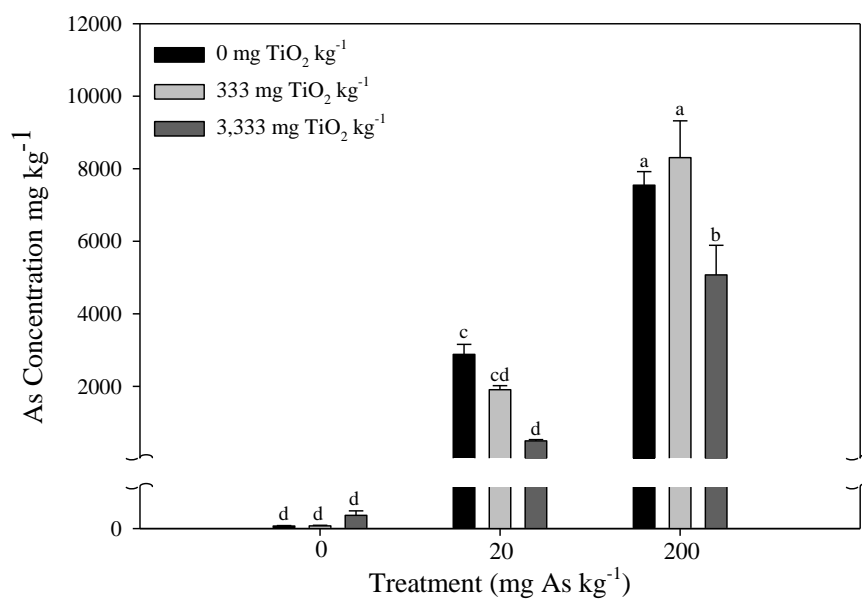


Figure 4.10: Total root concentration of As for broccoli plants treated with As(V) and TiO₂ ENPs as described in Table 4.1. The bars represent standard error and the lettering indicates honestly significant difference (HSD) of Tukey test ($p < 0.05$) ($n=5$).

CHAPTER 5

CONCLUSIONS

The results for the foliar application of bulk TiO₂ and TiO₂ ENPs on corn plants indicated that at there was transient rather than sustained. Furthermore, the transient increase in net photosynthesis did not increase the seed quantity or quality of the corn. A recent study performed with wheat plants indicated that at concentrations below 0.02% (200 mg L⁻¹) resulted in an increase in seed yield, but at concentrations greater than that resulted in a decreased yield (Choi et al., 2012). This indicates that TiO₂ may have a somewhat hormetic effect on plants, which may vary between species, and the concentrations used in this study were far too high to sustain the beneficial properties of dosing a plant with TiO₂ via foliar application. Future research should include a broad range of TiO₂ concentrations in a species specific manner.

However, there was a sustained increase in stomatal conductance. This may be the result of the TiO₂ preventing sensible heat loss which may have forced the plant to increase its stomatal opening to cool the leaf via evapotranspiration. However, this is just speculative and further research needs to be conducted to determine the underlying mechanism that caused the increased stomatal conductance that was observed in this study and the one performed on *Ulmus elongata* by Gao et al. (2013).

The results for the TiO₂ ENP and heavy metal interaction results suggested that the TiO₂ ENPs were capable of reducing the amount of the heavy metals that accumulated in the broccoli plants. These findings were contradictory to previous research that has been done involving fish (Zhang et al., 2007; Sun et al., 2007). The most likely of reasons for the discrepancy is due to the fact that plants possess a cell wall which may prevent the TiO₂ ENPs from entering the root

system. One of the shortcomings of this research was the failure to analyze the growth media for its final concentration of free ionic Cd and As. Future research should focus on the sorption capacities of TiO₂ ENPs with Cd and As(V) under different pH regimes as well as binding site competition with essential plant nutrients. Furthermore, it would have been interesting to investigate how the interaction may affect the levels of oxidative stress in the plants. It would also be prudent for future research to conduct these experiments in a soil substrate as opposed to vermiculite because the complex chemistry of soil may yield much different results compared to the vermiculite.

LITERATURE CITED

- American Society for Testing and Materials. Standard terminology relating to nanotechnology. E2456-06. 2006, West Conshohocken, PA.
- Asli S, Neumann, P. Colloidal suspensions of clay or titanium dioxide nanoparticles can inhibit leaf growth and transpiration via physical effects on root water transport. *Plant, Cell, and Environment* 2009, 32. 577-584.
- Benavides MP, Gallego SM, and Tomaro ML. Cadmium toxicity in plants. *Brazilian Journal of Plant Physiology*. 2005, 17(1). 21-34.
- Bleeker P, Hakvoort H, Blik M, Souer E, and Schat H. Enhanced arsenate reduction by a CDC25-like tyrosine phosphatase explains increased phytochelatin accumulation in arsenate-tolerant *Holcus lanatus*. *The Plant Journal*. 2006, 45. 917-929.
- Brunet L, Lyon DY, Hotze EM, Alvarez PJJ, Wiesner MR. Comparative photoactivity and antibacterial properties of C₆₀ fullerenes and titanium dioxide nanoparticles. *Environmental Research and Technology* 2009, 43. 4355-4360.
- Bystrejska-Piotrowska G, Asztemborska M, Giska I, Mikoszewski A. Influence of earthworms on extractability of metals from soils contaminated with Al₂O₃, TiO₂, Zn, and ZnO nanoparticles and microparticles. *Polish Journal of Environmental Studies* 2012, 21:2. 313-319.
- Caille N, Swanwick S, Zhao F, and McGrath S. Arsenic hyperaccumulation by *Pteris vittata* from arsenic contaminated soils and the effect of liming and phosphate fertilization. *Environmental Pollution*. 2004, 132. 113-120.
- Choi KS, Wansan-Gu, Jeollabuk-do. Liquid composition for promoting plant growth containing titanium dioxide nanoparticles. U.S. Patent US 8,188,005 B2. May 29, 2012.

- Clemens S. Toxic metal accumulation, responses to exposure and mechanisms of tolerance in plants. *Biochimie*. 2006, 88. 1707-1719.
- Clement L, Hurel C, Marmier N. Toxicity of TiO₂ nanoparticles to cladocerans, algae, rotifers, and plants – Effects of size and crystalline structure. *Chemosphere* 2013, 90. 1083-1090.
- Curie C, Cassin G, Couch D, Divol F, Higuchi K, Le Jean M, Misson J, Schikora A, Czernic P, and Mari S. Metal movement within the plant: contribution of nicotianamine and yellow stripe 1-like transporters. *Annals of Botany*. 2009, 103. 1-11.
- Delnomdedieu M, Basti M, Otvos JD, and Thomas DJ. Reduction and binding of arsenate and dimethylarsinate by glutathione: a magnetic resonance study. *Chemico-Biological Interactions*. 1994, 90. 139–155.
- Dodd N and Jha A. Photoexcitation of aqueous suspensions of titanium dioxide nanoparticles: an electron spin resonance spin trapping study of potentially oxidative reactions. *Photochemistry and Photobiology*. 2011, 87. 632-640.
- Dunphy Guzman KA, Finnegan MP, Banfield JF. Influence of surface potential on aggregation and transport of titania nanoparticles. *Environmental Science and Technology* 2006b, 40. 7688-7693.
- Dunphy Guzman KA, Taylor MR, Banfield JF. Environmental risks of nanotechnology: National Nanotechnology Initiative Funding 2000-2004. *Environmental Science and Technology* 2006, 40. 1401-1407.
- Dutta PK, Ray AK, Sharma VK, Millero FJ. Adsorption of arsenate and arsenite on titanium dioxide suspensions. *Journal of Colloid and Interface Science* 2004, 278(2). 270-275.

- Engates KE, Shipley HJ. Adsorption of Pb, Cd, Cu, Zn, and Ni to titanium dioxide nanoparticles: effect of particle size, solid concentration, and exhaustion. *Environmental Science and Pollution Research* 2011, 18. 386-395.
- Evans GC. *The quantitative analysis of plant growth*. Berkeley, CA: University of California Press. 1972, 734.
- Fan W, Cui M, Liu H, Wang C, Shi Z, Tan C, Yang X. Nano-TiO₂ enhances the toxicity of copper in natural water to *Daphnia magna*. *Environmental Pollution* 2011, 159. 729-734.
- Francesconi K, Visoottiviset P, Sridokchan W, and Goessler W. Arsenic species in an arsenic hyperaccumulating fern, *Pityrogramma calomelanos*: a potential phytoremediator of arsenic-contaminated soils. *The Science of the Total Environment*. 2002, 284. 27-35.
- Gao F, Hong F, Liu C, Zheng L, Su M, Wu X, Yang F, Wu C, and Yang P. Mechanism of Nano-anatase TiO₂ on Promoting Photosynthetic Carbon Reaction of Spinach. *Biological Trace Element Research* 2006, 111. 239-253.
- Gao F, Liu C, Qu C, Zheng L, Yang F, Su M, Hong F. Was the improvement of spinach growth by nano-TiO₂ treatment related to the changes of Rubisco activase?. *Biometals* 2008, 21. 211-217.
- Gao J, Xu G, Quin H, Liu P, Zhao P, and Hu Y. Effects of nano-TiO₂ on photosynthetic characteristics of *Ulmus elongata* seedlings. *Environmental Pollution*. 2013, 176. 63-70.
- Ge Y, Schimel JP, Holden PA. Evidence for negative effects of TiO₂ and ZnO nanoparticles on soil bacterial communities. *Environmental Science and Technology* 2011, 45. 1659-1664.
- Ghormade V, Deshpande M, and Paknikar K. Perspectives for nano-biotechnology enabled protection and nutrition of plants. *Biotechnology Advances* 2011, 29. 792-803.

- Ghosh M, Bandyopadhyay M, and Mukherjee A. Genotoxicity of titanium dioxide (TiO₂) nanoparticles at two trophic levels: Plant and human lymphocytes. *Chemosphere*. 2010, 81. 1253-1262.
- Gogos A, Knauer K, and Bucheli T. Nanomaterials in plant protection and fertilization: current state, foreseen applications, and research priorities. *Journal of Agricultural and Food Chemistry* 2012, 60. 9781-9792.
- Gottschalk F, Sonderer T, Scholz RW, Nowack B. Modeled environmental concentrations of engineered nanomaterials (TiO₂, ZnO, Ag, CNT, Fullerenes) for different regions. *Environmental Science and Technology* 2009, 43. 9216-9222.
- Hartmann NB, Von der Kammer F, Hofmann T, Baalousha M, Ottofuelling S, Baun A. Algal testing of titanium dioxide nanoparticles-testing considerations, inhibitory effects and modification of cadmium bioavailability. *Toxicology* 2010, 269. 190-197.
- Hong F, Yang F, Liu C, Gao Q, Wan Z, Gu F, Wu C, Ma Z, Zhou J, and Yang P. Influences of Nano-TiO₂ on the Chloroplast Aging of Spinach Under Light. *Biological Trace Element Research* 2005a, 104. 249-260.
- Hong F, Zhou J, Liu C, Yang F, Wu C, Zheng L, and Yang P. Effect of Nano-TiO₂ on Photochemical Reaction of Chloroplasts of Spinach. *Biological Trace Element Research* 2005b, 105. 269-279.
- Jaberzadeh A, Moaveni P, Tohidimoghadam HR, and Zahedi H. Influence of bulk and nanoparticles titanium foliar application on some agronomic traits, seed gluten and starch contents of wheat subjected to water deficit stress. *Notulae Botanicae Horti Agrobotanici Cluj-Napoca*. 2013, 41:1. 201-207.

- Jegadeesan G, Al-Abed S, Sundaram V, Choi H, Scheckel K, and Dionysiou D. Arsenic sorption on TiO₂ nanoparticles: size and crystallinity effects. *Water Research* 2010, 44. 965-973.
- Kelsey JW and White JC. Effect of C₆₀ fullerenes on the accumulation of weathered p,p'-DDE by plant and earthworm species under single and multispecies conditions, *Environmental Toxicology and Chemistry*. 2013, 32:5. 1117-1123.
- Kertulis G, Ma, L, MacDonald G, Chen R, Winefordner J, and Cai Y. Arsenic speciation and transport in *Pteris vittata* L. and the effects on phosphorus in the xylem sap. *Environmental and Experimental Botany*. 2005, 54. 239-247.
- Leakey ADB, Uribe-larrea M, Ainsworth EA, Naidu SL, Rogers A, Ort DR, Long SP. Photosynthesis, productivity, and yield of maize are not affected by open-air elevation of CO₂ concentration in the absence of drought. *Plant Physiology* 2006, 140. 779-790
- Lin D, Ji J, Long Z, Yang K, and Wu F. The influence of dissolved and surface-bound humic acid on the toxicity of TiO₂ nanoparticles to *Chlorella* sp. *Water Research*. 2012, 46. 4477-4487.
- Linglan M, Chao L, Chunxiang Q, Sitao Y, Jie L, Fengqing G, Fashui H. Rubisco Activase mRNA Expression in Spinach: Modulation by Nanoanatase Treatment. *Biological Trace Element Research* 2008, 122. 168-178.
- Liu K, Lin X, and Zhao J. Toxic effects of the interaction of titanium dioxide nanoparticles with chemicals or physical factors. *International Journal of Nanomedicine*. 2013, 8. 2509-2520.
- Ma CC, Gao YB, Guo HY, and Wang JL. Photosynthesis, Transpiration, and Water Use Efficiency of *Caragana microphylla*, *C. intermedia*, and *C. korshinskii*. *Photosynthetica*. 2004, 42:1. 65-70.

- Mahdavi S, Jalali M, Afkhami A. Heavy metals removal from aqueous solutions using TiO₂, MgO, and Al₂O₃ nanoparticles. *Chemical Engineering Communications* 2013, 200. 448-470.
- Mendoza-Cózatl DG, Jobe TO, Hauser F, and Schroeder JI. Long-distance transport, vacuolar sequestration, tolerance, and transcriptional responses induced by cadmium and arsenic. *Current Opinion in Plant Biology*. 2011, 14. 554-562.
- Nel A, Xia T, Madler L, Li N. Toxic Potential of Materials at the Nanolevel. *Science* 2006, 311. 622-627.
- Owolade OF, Ogunleti DO, and Adenekan MO. Titanium dioxide affects diseases, development, and yield of edible cowpea. *Electronic Journal of Environmental, Agricultural, and Food Chemistry*. 2008, 7:5. 2942-2947.
- Ridley MK. Characterization and surface-reactivity of nanocrystalline anatase in aqueous solutions. *Langmuir* 2006, 22. 10972-10982.
- Sablayrolles C, Gabrielle B, Montrejuad-Vignoles M. Life cycle assessment of biosolids land application and evaluation of the factors impacting human toxicity through plant uptake. *Journal of Industrial Ecology* 2010, 14. 231-241.
- Schrauzer GN, Guth TD. Nitrogen photoreduction on desert sands under sterile conditions. *Proceedings of the National Academy of the Sciences of the USA* 1983, 80. 3873-3876.
- Schrauzer GN, Guth TD. Photolysis of water and photoreduction of nitrogen on titanium dioxide. *Journal of American Chemical Society* 1977, 99. 7189-7193.
- Scientific Committee on Emerging and Newly Identified Health Risk. The appropriateness of the risk assessment methodology in accordance with the Technical Guidance Documents for

- new and existing substances for assessing the risks of nanomaterials. 2007, European Commissions, Brussels, Belgium.
- Simon-Deckers A, Loo S, Mayne-L'Hermitte M, Herlin-Boime N, Menguy N, Reynaud C, Gouget B, and Carriere M. Size-, composition- and shape-dependent toxicological impact of metal oxide nanoparticles and carbon nanotubes toward bacteria. *Environmental Science and Technology* 2009, 43. 8423-8429.
- Srivastava S, Suprasanna P, and Souza SFD. Mechanisms of arsenic tolerance and detoxification in plants and their application in transgenic technology: a critical appraisal. *International Journal of Phytoremediation*. 2012, 14. 506-517.
- Su M, Chao L, Chunxiang Q, Lei Z, Liang C, Hao H, Xiaoqing L, Xiao W, and Fashui H. Nano-Anatase Relieves the Inhibition of Electron Transport Caused by Linolenic Acid in Chloroplasts of Spinach. *Biological Trace Element Research* 2008, 122. 73-81.
- Su M, Fashui H, Chao L, Xiao W, Xiaoqing L, Liang C, Fengqing G, Fan Y, and Zhongrui L. Effects of Nano-anatase TiO₂ on Absorption, Distribution of Light, and Photoreduction Activities of Chloroplast Membrane of Spinach. *Biological Trace Element Research* 2007, 118. 120-130.
- Sun H, Zhang X, Niu Q, Chen Y, Crittenden JC. Enhanced accumulation of arsenate in carp in the presence of titanium dioxide nanoparticles. *Water, Air, and Soil Pollution* 2007, 178. 245-254.
- Sun H, Zhang X, Zhang Z, Chen Y, and Crittenden J. Influence of titanium dioxide nanoparticles on speciation and bioavailability of arsenite. *Environmental Pollution* 2009, 157. 1165-1170.

- Sun W, Ubierna N, Ma JY, Cousins AB. The influence of light quality on C4 photosynthesis under steady-state conditions in *Zea mays* and *Miscanthus x giganteus*: changes in rates of photosynthesis but not the efficiency of the CO₂ concentrating mechanism. *Plant, Cell & Environment* 2012, 35. 982-993.
- Tan C and Wang WX. Modification of metal bioaccumulation and toxicity in *Daphnia magna* by titanium dioxide nanoparticles. *Environmental Pollution*. 2014, 186. 36-42.
- Torre-Roche RDL, Hawthorne J, Deng Y, Xing B, Cai W, Newman LA, Wang C, Ma X, and White JC. Fullerene-enhanced Accumulation of p,p'-DDE in agricultural crop species. *Environmental Science and Technology*. 2012, 46. 9315-9323.
- Torre-Roche RDL, Hawthorne J, Deng Y, Xing B, Cai W, Newman LA, Wang Q, Ma X, Hamdi H, and White JC. Multiwalled carbon nanotubes and C₆₀ fullerenes differentially impact the accumulation of weathered pesticides in four agricultural plants. *Environmental Science and Technology*. 2013, 47. 12539-12547.
- Tourinho PS, Van Gestel CAM, Lofts S, Svendsen C, Soares AMVM, Lourereiro S. Metal-based nanoparticles in soil: fate, behavior, and effects on soil invertebrates. *Environmental Toxicology and Chemistry* 2012, 31(8). 1679-1692.
- USEPA, Method 3050b: Acid Digestion of Sediments, Sludges, and Soils In Test Methods for Evaluating Solid Waste Physical/Chemical Methods, SW-846 Environmental Protection Agency, Office of Solid Waste: 1996; 12.
- Verbruggen N, Hermans C, and Schat H. Mechanisms to cope with arsenic or cadmium excess in plants. *Current Opinion in Plant Biology*. 2009, 12. 364-372.
- Verbruggen N, Hermans C, and Schat H. Mechanisms to cope with arsenic or cadmium excess in plants. *Current Opinion in Plant Biology*. 2009, 12. 364-372.

- Xu Z and Meng X. Size effects of nanocrystalline TiO₂ on As(V) and As(III) adsorption and As(III) photooxidation. *Journal of Hazardous Materials* 2009, 168. 747-752.
- Yang F, Hong F, You W, Liu C, Gao F, Wu C, and Yang P. Influences of nano-anatase TiO₂ on the nitrogen metabolism of growing spinach. *Biological Trace Element Research* 2006, 110. 179-190.
- Yang F, Liu C, Gao F, Su M, Wu X, Zheng L, Hong F, and Yang P. The improvement of spinach growth by nano-anatase TiO₂ treatment is related to nitrogen photoreduction. *Biological Trace Element Research* 2007, 119. 77-88.
- Yang WW, Miao AJ, Yang LY. Cd²⁺ toxicity to a green alga *Chlamydomonas reinhardtii* as influenced by its adsorption on TiO₂ engineered nanoparticles. *PLoS ONE* 2012, 7(3): e32300. doi:10.1371/journal.pone.0032300.
- Ze Y, Liu C, Wang L, Hong M, and Hong F. The Regulation of TiO₂ Nanoparticles on the Expression of Light-Harvesting Complex II and Photosynthesis of Chloroplasts of *Arabidopsis thaliana*. *Biological Trace Element Research* 2011, 143. 1131-1141.
- Zhang X, Sun H, Zhang Z, Niu Q, Chen Y, Crittenden JC. Enhanced bioaccumulation of cadmium in carp in the presence of titanium dioxide nanoparticles. *Chemosphere* 2007, 67. 160-166.
- Zheng L, Hong F, Lu S, and Liu C. Effect of Nano-TiO₂ on Strength of Naturally Aged Seeds and Growth of Spinach. *Biological Trace Element Research* 2005, 104. 83-91.
- Zheng L, Mingyu S, Xiao W, Chao L, Chunxiang Q, Liang C, Hao H, Xiaoqing L, and Fashu H. Effects of Nano-anatase on Spectral Characteristics and Distribution of LHCII on the Thylakoid Membranes of Spinach. *Biological Trace Element Research* 2007, 120. 273-283.

Zheng L, Mingyu S, Xiao W, Chao L, Chunxiang Q, Liang C, Hao H, Xiaoqing L, and Fashui H.

Antioxidant Stress is Promoted by Nano-anatase in Spinach Chloroplasts Under UV-B

Radiation. *Biological Trace Element Research* 2008, 121. 69-79.

VITA

Graduate School

Southern Illinois University

Scott J. Bradfield

sbradfield3@gmail.com

University of Southern Illinois University Carbondale

Bachelor of Science, Plant Biology, May 2012

Thesis Title:

Influence of TiO₂ Engineered Nanoparticles on Photosynthetic Efficiency and Contaminant

Uptake

Major Professor: Stephen D. Ebbs